AD-A036 567

INVESTIGATION OF THE PROPAGATION MECHANISM OF PRESSURE FLUCTUATIONS IN TURBULENT FLOW

New York University

Westbury

December 1976
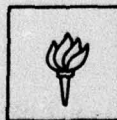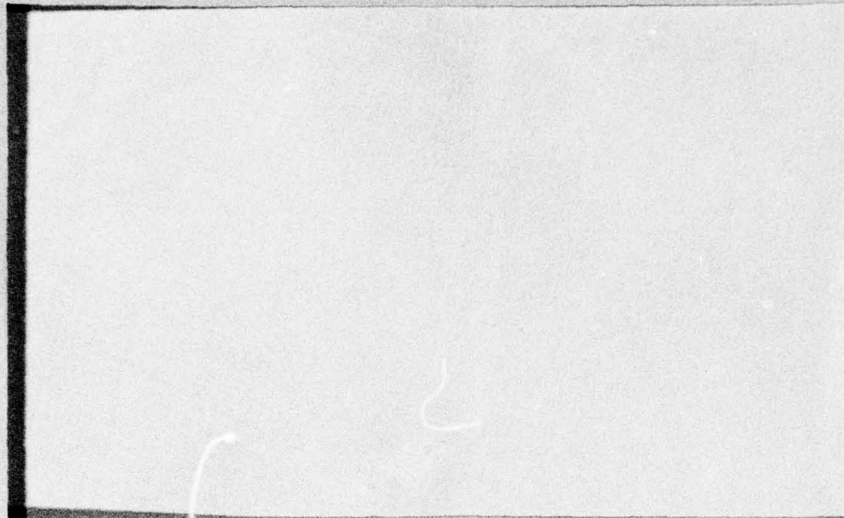
DDC
MAR 9 1977
C

NEW YORK UNIVERSITY

FACULTY OF ARTS AND SCIENCE
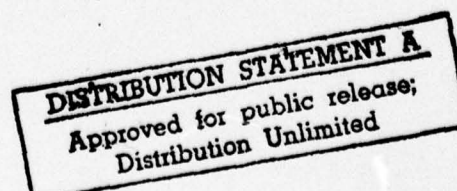
DEPARTMENT OF APPLIED SCIENCE

for public release;
distribution unlimited.

INVESTIGATION OF THE PROPAGATION MECHANISM
OF PRESSURE FLUCTUATIONS IN TURBULENT FLOW

Victor Zakkay
Vincent Barra
Chi R. Wang

NEW YORK UNIVERSITY

FACULTY OF ARTS AND SCIENCE
DEPARTMENT OF APPLIED SCIENCE

i.

INVESTIGATION OF THE PROPAGATION MECHANISM
OF PRESSURE FLUCTUATIONS IN TURBULENT FLOW

Victor Zakkay
Vincent Barra
Chi R. Wang

NEW YORK UNIVERSITY
DEPARTMENT OF APPLIED SCIENCE
AEROSPACE AND ENERGETICS LABORATORY
MERRICK AND STEWART AVENUE
WESTBURY, L.I.N.Y. 11590 NEW YORK

ACCESSION for

NTIS	White Section
DDC	Buff Section
UNANNOUNCED	
JUSTIFICATION	

BY
DISTRIBUTION/AVAILABILITY CODES

Dist.	AVAIL. and/or SPECIAL
A	

DECEMBER 1976

ia

PREFACE

This report represents research carried out from 1 September 1975
to 30 September 1976 under AFOSR Grant 76-2947, "Investigation of the
Propagation Mechanism of Pressure Fluctuations in Turbulent Flow". This
contract was technically monitored by Lt. Colonel R.C. Smith of the
Department of the Air Force, AFOSR, Bolling Air Force Base, Washington, D.C.

The authors wish to acknowledge the cooperation of Grumman Aerospace
Corporation for allowing us the use of their Ambilog 200 facility for
data conversion. We also wish to thank Mr. T. Keller for his guidance
and assistance in preparing the necessary programs.

ABSTRACT

A wind tunnel facility (M = 0.6 to 0.8) with extremely low noise levels $(u'/u_\infty = .08\%)$ has been designed, constructed, and tested at the New York University Aerospace and Energetics Laboratory. The facility is to be used for the purpose of investigating the propagation mechanism of pressure fluctuations in turbulent boundary layers. The facility was designed as an induction tunnel in order to minimize the influence of the downstream region of the wind tunnel on the flow field in the test section. This report presents a description of the facility and the flow quality obtained, and a discussion of the instrumentation and experimental procedures being used. The results obtained from the analysis of several measurements are also presented. This includes spectra of the velocity, wall-pressure and wall-shear fluctuations and the results of a digital processing scheme which conditionally samples the fluctuations to obtain a description of turbulent "bursts" in the boundary layer.

LIST OF FIGURES

iii

TABLE OF CONTENTS

I. INTRODUCTION

Turbulent flows have been investigated for several decades.
Technically speaking, almost every important fluid flow is turbulent,
and such flows have considerably higher surface drag than laminar flows.
Experience has shown that turbulent flow noise is radiated both directly
from the boundary layer and indirectly from the boundary walls which
are stimulated by the turbulent wall pressure fluctuations. There is a
relationship between turbulence production, the occurrence of turbulent
wall pressure fluctuations, and the so-called turbulent shear stress
(Reynolds-stress). By influencing the turbulent flows, it should be
possible to reduce drag and turbulent flow noise. Better knowledge of
the mechanism of turbulence production could show how it is possible to
influence a fully-developed turbulent flow, for example, by means of
suitably designed flexible walls, without using additional energy.

Before any research effort could be directed towards an understand-
ing of the mechanisms by which drag and noise reduction could be
accomplished, it would be necessary to examine carefully the structure
of the boundary layer turbulence under normal flow conditions. It is
the intention of the research reported here to primarily establish the
details of the structure of such a boundary layer.

It has been found in many experiments (Refs. 1-10) that large scale
disturbances that have substantial three-dimensional characteristics
called "bursts", appear in boundary layer flow. The "burst" is
described as a thick low-speed streak lifting up from the surface.
Such a profile is unstable, and the formation is probably connected with
some kind of instability triggered by small disturbances. A basic

1

objective of this investigation is to study the mechanism that triggers

such a "burst" and what effect it has on the structure of the boundary

layer. The necessity of producing real two-dimensional boundary con-

ditions is an important point of the experiment. Many so called two-

dimensional investigations are made on flat plates, or flat tunnel

walls. In these experiments the presence of ends or corners can have

substantial effects in determining some of the properties of turbulence.

It is for this reason that an axially symmetric configuration has been

chosen for this investigation.

Furthermore it has been determined that the frequency and amplitude

of the instabilities associated with the turbulent "bursts" can be

characterized as being uniformly distributed through the flow. These

instabilities have been shown to move downstream with a constant speed,

U_c, (i.e., the flow structure repeats itself in space and time). No

interaction occurs between neighboring "bursts" and U_c is greater than

the local flow velocity.

Black (Ref. 10) has tried to make an energy balance by choosing a

coordinate system based on one of the burst cells. By basing his energy

balance on the incoming and outgoing primary velocity profiles relative

to this system, he performed a mass, momentum, energy, and vorticity

balance to deduce the vortex flow pattern within the burst. Based on

this observation, the vortex pattern responsible for the eruption of

fluid from the sublayer to the outside flow could be calculated, and

its contribution to the additional shear stress within the boundary

layer found.

To the best of our knowledge the research which has been performed

up to now in investigating these "bursts", has involved measurements

2

made either at the wall (Ref. 6) or in the boundary layer (Refs. 16-18).
In this investigation simultaneous measurements will be made of the
pressure and shear at the wall and of the velocity in the boundary layer.
In this manner it will be feasible to get a relationship giving the
fluctuating shear stress at the wall in terms of the induced local pressure
fluctuations. The tests were performed in a one foot tunnel at $M_\infty = .64$.

Present day experimental research in turbulent flows relies heavily
on electronic measuring devices, and therefore any report which pertains
to this type of research is not complete unless a discussion of the in-
strumentation being used is included. It is for this reason that a
significant portion of this report is devoted to a detailed discussion of
the instrumentation and measurement techniques utilized in this investiga-
tion.

II. DESCRIPTION OF FACILITY

A.   WIND TUNNEL

1. Wind Tunnel Set-up

An induction wind tunnel was constructed for the present experiment.
It was built of heavy gauge steel material. The inlet section of the
tunnel consists of a circular cone 5 ft in diameter and has several meshed
screens. The cone is followed by a cylindrical section 3 ft in diameter in
which plastic tubes (1.5 inches in diameter) are arranged parallel to the
center line of the wind tunnel. These plastic tubes act as flow
straighteners. Several fine mesh screens were placed downstream of the
flow straighteners in order to further reduce the turbulence scale. A conical
section 3 ft in length connects the inlet to a pipe with an inside diameter
of 12 inches and a length of 30 ft This pipe is followed by a cylindrical
test section which is 5 ft long, has an inside diameter of 12 inches, and is
fitted with four rectangular windows. The inner surfaces of the windows were
contoured in order to match the test section inside diameter. The instru-
mentation for the measurements were mounted on these windows. A three degree
half angle conical diffuser was placed downstream of the test section to
reduce the flow velocity prior to the entrance to the vacuum sphere
$(40,000 \text{ ft}^3)$ The entire assembly was isolated from the supporting structure
and its vibrations were damped by putting thick rubber pads at the supports.
Sketches of the wind tunnel and test section are given in Figs. 1 and 2

In order to minimize the noise level of the wind tunnel, the flow
passing through it was generated by induction by connecting the downstream
end of the tunnel to the vacuum sphere. A 6° half angle cone was put

4

inside the tunnel immediately downstream of the test section to create a sonic throat. In this manner, the propagation of noise from sources downstream of the test section was eliminated at the throat.

To start the wind tunnel, the pressure in the vacuum tank was reduced to a very low pressure. A hydraulic valve located between the vacuum tank and the diffuser was opened and atmospheric air was induced into the wind tunnel. Steady flow was established within half a second after the tunnel was started. By moving the conical center body upstream and downstream with respect to the test section, the cross section of the sonic throat can be changed in order to vary the free stream velocity within the test section. For the present experiments, a Mach 0.64 free stream was established with a vacuum pressure of 8 psia and the smallest contraction ratio between the test section and the sonic throat.

2. Wind Tunnel Calibration

The flow in the test section was calibrated with a pitot probe and a hot-film probe utilizing a constant temperature anemometer. The free stream Mach number, boundary layer profiles of the mean velocity and turbulence intensity (u'/U) in the test region were measured. Details of the wind tunnel calibration are presented here.

Pressure orifices, 0.0312 inches in diameter, have been flush mounted in the streamwise direction along the inner surface of the test section to measure the surface static pressure. These measurements were used in order to insure that no appreciable axial pressure gradient exists during the test, and was monitored for all tests. With a wind tunnel total pressure of 14.7 psia, the streamwise surface pressure decreases from 11.13 psia to 10.97 psia in a distance of 3 ft. The free stream Mach numbers for these tests were between 0.64 and 0.66.

5

In order to determine the velocity boundary layer thickness, the static and total pressure distributions across the boundary layer at the test section were measured. A pitot probe was traversed in a distance of 6" normal to the tunnel inner surface. This pitot probe was connected to pressure transducers calibrated within a range of 0-15 psia to measure the local static pressure and total pressure. Based on these pressure distributions, the boundary layer Mach number profile and the corresponding velocity profile with the assumption of constant total temperature were calculated and shown in Fig. 3.

The boundary layer turbulent intensity profile has been measured with a cylindrical alumina coated hot film probe and constant temperature anemometer. The hot-film probe was also traversed across the boundary layer. The DC and RMS voltage outputs from the constant temperature anemometer were also measured at different locations normal to the wall. The local turbulent intensity was computed according to King's law. The boundary layer profile of the turbulent intensity is presented in Fig. 4. A free stream turbulent intensity of 0.008 was obtained and a maximum turbulent intensity of 0.08 has been found near the wall. The free stream turbulent intensity obtained for these tests were to the authors' knowledge, the lowest thus far obtained at these velocities.

3. Flow Quality

Based on the results of the wind tunnel calibration, the velocity boundary layer thickness, displacement thickness, and momentum thickness have been computed. The boundary layer velocity profile could also be described by a 1/7 power law. The parameters of the boundary layer flow in the test section are presented in the following table:

6

U_∞	675 ft/sec
δ	0.334 ft
δ^*	0.047 ft
θ	0.032 ft
Re_θ	1.06×10^5
u_τ^2/ν	1.61×10^6 1/sec
u'/U_∞	0.008

B. INSTRUMENTATION

It has been found in many experimental investigations that large scale quasi-ordered disturbances (called "bursts") having substantial three-dimensional characteristics appear in boundary layer flow. Because of the intermittent and coherent nature of the bursts, usual time and space averaged measurements tend to "smear out" their essential features. It has become necessary to utilize various visual (Refs. 12-15) and conditional sampling (Refs. 16-19) techniques in order to reveal more clearly the "bursting" characteristics of the turbulent boundary layer. However, the previous investigations involved measurements made either at the wall or in the boundary layer. To our knowledge, this will be the first time that simultaneous measurements of the fluctuating pressure and shear at the wall, and fluctuating velocity in the boundary layer are made in order to study the generation and structure of turbulent "bursts".

1. Data Acquisition

The general set-up of the data recording instrumentation is shown in Fig. 5. Basically, two systems are required - one for measuring and recording the velocity in the boundary layer and the fluctuating shear on the wall of the tunnel and another for measuring and recording the fluctuating pressure on the wall.

7

a. Velocity and Shear

The mean and fluctuating components of the streamwise velocity in the flow are measured with hot-film probes and constant temperature anemometers. Two types of probes are available, those with an alumina coated cylindrical sensor and one with an alumina coated wedge type sensor. In the former case, miniature probes (Thermo-Systems type TSI-1260) are available for use on a rake holding five probes (see Figs. 6 and 7). Two rakes have been constructed - one spanning a distance of 2 inches from the wall of the tunnel and the other 1 inch as shown in Fig. 6. The constant temperature anemometer systems (DISA and Thermo-Systems) used in conjunction with these probes all include a linearizer and signal conditioner (amplifier/filter). The DC components of the linearized signals from the hot-film probes are recorded on a 30 channel Honeywell 1612 visicorder and are monitored during each test on several meters. The visicorder is also used to record the static pressure along the wall of the test section to insure that the proper running condition is achieved in each test. The fluctuating component of each of the signals is amplified and filtered, and then recorded on one of 7 channels of a Phillips Ana-Log 7 magnetic tape recorder. The RMS levels of the fluctuating signals are also monitored during each test on in-line meters.

The fluctuating shear on the tunnel wall is measured with a flush mounted hot-film sensor (Thermo-Systems type TSI-1237) as shown in Fig. 6. This measurement is made by replacing one of the hot-film probes in Fig. 5 with this flush hot-film sensor since the instrumentation required is the same as that described in the previous paragraph for the hot-film probes.

8

b. Pressure

Flush-mounted piezoresistive pressure transducers (Kulite type MIC-080-5) are used to measure the pressure fluctuations on the tunnel wall. The diameter of the pressure sensitive area of the transducers is .040" and they are rated for a pressure differential of 5 psi. A natural frequency of 200 kHz is quoted by the manufacturer. Five such transducers are available and can be placed at various spacings in a cross-shaped pattern on a plug in the tunnel wall below the hot-film probes (see Figs. 6 and 7). (This plug is also used to mount the flush hot-film sensor). The signal from each of the transducers is put through an amplifier/filter and then recorded on one of 7 channels of a Honeywell 5600 tape recorder. In-line RMS meters allow the signal levels to be monitored during each test. The input power for the transducers is provided by batteries which can supply up to 9 volts DC.

The two magnetic tape recorders have the capability of recording both in FM or Direct mode at speeds as high as 60 ips. All the elements of the instrumentation have been chosen so as to allow sensing and recording of fluctuations at frequencies as high as 40,000 Hz ($\omega \delta^{*}/U_{\infty} \cong 18$). The synchronization of the data on the two recorders is accomplished by simultaneously recording two signals on each recorder, a 100 kHz sine and a pulse train with a period of from 1 to 3 sec. The sine wave is provided by a Hewlett-Packard 3310A function generator and the pulse train by a General Radio 1340 pulse generator (see Fig. 5.)

2. Data Analysis

The tape recorded data can be analyzed with the systems shown schematically in Fig. 8. Spectral analyses of the pressure, shear and velocity fluctuations are obtained using a General Radio model 1900 wave analyzer

9

and model 1521 graphic level recorder, while auto and cross-correlations are performed with a Saicor SAI-42 correlation and probability analyzer. A continuous display of 5 simultaneous data channels is provided by an ink plotter which by slowing down the tape recorder sufficiently on playback can yield a resolution of up to 3 msec/inch. The sixth channel of the plotter is used to display the recorded pulses which serve as reference time marks.

The most important aspect of the data analysis involves the digitization of the recorded fluctuations and the subsequent manipulation of this data on a large digital computer. To accomplish this an Ambilog 200 computer with an analog-to-digital converter is utilized to obtain discrete time sequences of the fluctuations. The digitization process is triggered by one of the recorded pulses (chosen depending on the portion of test to be analyzed); and the rate at which samples are taken can be established in one of two ways, either by a timing loop within the digitizing program itself or by using the recorded 100 kHz sine as a clock. When it is necessary to preserve the simultaneity of the data on two channels digitized at different times or of the data on the two tape recorders, the latter procedure is chosen. (The need for these procedures will be discussed in greater detail in the next section). With a sufficiently large ratio of record-to-playback speed, it is possible to achieve sampling rates as high as 200,000 samples/sec. Up to 24,000 samples can be made and stored during one pass through the digitizing program. All digital data is transferred to magnetic tape which serves as the input medium to a CDC 6600 computer where final numerical analysis of the data is performed.

The overall experimental set-up including the instrumented tunnel test section and data acquisition instrumentation, as well as some of the data analysis equipment are shown in Figs. 9 and 10.

10

III. EXPERIMENTAL PROCEDURES

A. CALIBRATION OF INSTRUMENTATION

1. Hot-Film Probes and Constant Temperature Anemometers

The principle of the hot-film probe and anemometer is based on the convective heat loss from an electrically heated film (or wire) caused by the flow of gas or liquid surrounding the wire. Normally, the finite thermal capacitance of the transducer will affect the sensitivity and the phase relation so that changes in flow velocity can be measured only up to a frequency of around 1000 Hz. The constant temperature anemometer employs a technique that minimizes the effect of thermal lag, thereby increasing the upper frequency limit by a factor of approximately 100. The hot-film probe uses a conducting film on a ceramic substance, or a quartz rod with a platinum film on the surface. The hot-film probe sensor has a large diameter and is particularly helpful in reducing the breakage of the sensor due to the impact of the flow. For the present experiment, TSI-1260 miniature hot-film probes with 0.002 inch diameter by 0.04 inch long cylindrical sensors were used. This probe was capable of measuring velocity up to 1000 ft/sec and was operated with an overheat ratio of 1.5.

A DISA type 55D41 calibration wind tunnel was used to calibrate the miniature probes. This tunnel gives a maximum velocity of 700 ft/sec with an optimum turbulent intensity of 0.003 at 300 ft/sec and 100 kHz bandwidth. The hot-film sensor was placed perpendicular to the mean flow direction and the mean flow velocity was measured by means of a pitot tube.

First the frequency response of the bridge output circuits of the anemometers was adjusted. A square wave generator and oscilloscope were

11

connected to the anemometer for accurate adjustment so that no damped oscillations occur on the output signal and an optimum probe time constant was obtained. The anemometers upper frequency limit, in conjunction with the probe being used, is determined by this time constant. An upper frequency limit of approximately 20 kHz was obtained for the miniature probes used in the present experiment.

After the anemometers frequency response has been adjusted, the bridge output was connected to a linearizer to obtain a linear relation between the mean velocity and DC voltage output. The linearizer output was also bypassed to an RMS meter to measure the root-mean-square value of the output signal in order to compute the turbulent intensity. These calibration procedures are the same as those described in detail in Ref. 20 where a full description of the characteristics of the flush hot-film sensor is also given.

2. Pressure Transducers

The Kulite transducers to be used for this investigation are checked with both a static and dynamic calibration. In the static calibration, the pressure differential between the transducer reference tube and the sensing face was varied from zero to the rated pressure and the output voltage noted at several points. The output voltage was found to vary linearly with the applied pressure and the applied voltage to the trans-ducer bridge circuit. The five MIC-080-5 transducers were found to have a sensitivity on the order of 0.60 mV/psi/V(input). One MIC-080-25 transducer which is available was also calibrated and its sensitivity was found to be 0.45 mV/psi/V.

12

The dynamic calibration consisted of utilizing a Bruel & Kjaer pistonphone which supplied an oscillating pressure having a frequency of approximately 250 Hz and a precise level of 124 dB. The RMS level of the output voltage from the transducer exposed to this pressure field was measured and yielded a sensitivity of 142 dB below 1V/μbar for the MIC-080-5 transducers and 145 dB below 1V/μbar for the MIC-080-25 transducer. Both figures are given for an input voltage of 9 volts DC and are equivalent to the static sensitivities listed above. The frequency response of the transducers was not checked, but the specified natural frequency of 200,000 Hz would insure a flat frequency response up to 40,000 Hz ($\omega\delta^*/U_\infty \cong 18$).

B. PROCEDURES FOR MEASUREMENT OF TURBULENT FLUCTUATIONS

After the various instrumentation systems were calibrated, preliminary recordings were made of the fluctuating pressure and shear on the tunnel wall and of the fluctuating velocity in the boundary layer. Recordings were made in both FM and Direct mode and at the highest speed possible on the two recorders so that a data bandwidth of at least DC-100,000 Hz was available. Except for the DC component which was filtered before recording, the amplifier bandpasses chosen were within this range. It was necessary to have a wide data bandwidth during these first tests so that a good indication could be obtained of the entire spectral range of the fluctuating quantities, in particular of their high frequency extent. Since recordings eventually had to be made in FM mode (to allow playback at lower speeds without distortion) it was necessary to know whether the limited high frequency response in the FM mode (i.e., up to 10 kHz on the Phillips recorder and 40 kHz on the Honeywell) would be sufficient to

13

include all the components of interest in the fluctuations. This information was also valuable in determining the rate at which the data would have to be digitized.

The recordings were analyzed to obtain the overall RMS level and spectral distributions of the fluctuations. RMS meter readings taken both during the recordings and then on playback were used in conjunction with calibration data to obtain the overall RMS levels of the various fluctuating quantities, while the wave analyzer system described in Section II was utilized to obtain the spectral distribution of the fluctuations. A bandwidth of 50 Hz was normally used for the spectral analyses, although a 10 Hz bandwidth was also employed for some low frequency analyses. The FM recordings were analyzed to give the spectra for low frequencies while the Direct recordings gave corresponding information at the high frequency end. These results were combined to yield the spectral distributions of the fluctuating quantities over a rather broad range.

These preliminary recordings were also displayed on a two channel storage oscilloscope to provide qualitative information on the time histories of the fluctuating quantities, and to verify the feasibility of syncronizing two data channels on different recorders. This was done for the entire range of playback speeds to insure that no distortion occurred to the recorded signals when played back at slower speeds. For signals recorded in FM mode no significant distortion was found even for ratios of record-to-playback speeds as high as 32 or 64. As was expected however, the Direct recordings did show increasing low frequency distortion with increasing ratios of record-to-playback speed. To help identify the importance of various frequency ranges on selected events in the time histories of the fluctuating quantities, the recorded fluctuations were

14

also passed through a bandpass filter before being displayed on the oscilloscope.

These time averaged analyses did not require that the various measurements be made simultaneously. But in order to obtain spatial as well as temporal resolution of the "bursts" in turbulent boundary layers it is necessary that simultaneous measurements be made at several points in the flow. The following capabilities have been developed for simultaneous measurements in this investigation: up to five wall pressure fluctuation measurements together with either five streamwise velocity measurements in the boundary layer or four velocity measurements and one shear fluctuation measurement on the tunnel wall.

Once the required set of transducers and probes are placed in position in the tunnel test section certain procedures are followed for each test. First the signal conditioning elements of the instrumentation are each checked with a test signal. The filter bandpasses on the signal conditioners are normally set at 2-20,000 Hz ($\omega\delta^*/U_\infty$ = .0009-9.) for the velocity and shear fluctuations and 30-30,000 Hz ($\omega\delta^*/U_\infty$ = .013-13.) for the pressure fluctuations. Just before flow is initiated by opening a valve to the vacuum sphere, the three recorders (the two magnetic tape recorders and the visicorder) are started and the anemometers switched to operating condition. At about the time when steady flow conditions are reached the pulse generator is turned on and begins to mark a channel on each tape recorder with a pulse every three seconds. A 100 kHz sine is also being simultaneously recorded on one channel of each recorder at all times. Up to ten fluctuating quantities (five on each tape recorder) and five DC anemometer outputs (on the visicorder) are recorded during any one test. During the test itself, meter readings are also taken of the DC anemometer outputs and the RMS levels

15

of the fluctuating quantities. An entire test lasts a total of approximately 40 seconds with steady flow conditions being maintained for about 15 seconds. The steady portion of the test is identified with the use of one of the visicorder traces which records the static pressure along the test section wall during the entire test.

To date, successful recordings have been made for the following test configurations:

- Four hot-film probes on the 1" rake and a pressure transducer flush mounted on the wall directly below the probes.

- Three hot-film probes on the 1" rake, a flush hot-film sensor directly below the probes, and a pressure transducer approximately .5" upstream.

- Five pressure transducers in a cross-shaped pattern (equally spaced .15" apart, see Fig. 6) without any rakes in the flow.

- Five hot-film probes on the 2" rake, and the five pressure transducers of the previous configuration centered directly below the probes.

Preparations for several other tests are in progress and the possibility of repeating some tests for a lower flow velocity ($U_\infty \approx 100$ ft/sec) is being considered.

The analysis of these tests requires the digitization of the recorded fluctuations into discrete time sequences. This is accomplished utilizing the Ambilog 200 facility described in Section II. The five data channels and the pulse channel from one of the recorders are first simultaneously displayed on a six channel ink-plotter. This is done for both tape re-

16

corders and for sections of recordings falling within the period of steady
flow conditions. The digitization itself required that a choice be made
among several possible procedures. This involved choosing the way in which
the data sampling was to be timed and whether only one or several data
channels would be sampled during a single execution of the digitizing pro-
gram. One of the first procedures to be tried consisted of sampling a
single data channel with the sampling interval being timed either by an
external clock or by a timing loop within the program itself. Although
initial synchronization between successively sampled data channels was
provided by having the same recorded pulse serve as a trigger for the
digitization process, it became apparent that because of the lack of
synchronization between the timing mechanism and the recorded data any
real time unsteadiness such as in tape speed would eventually result in
the loss of simultaneity between the data channels. One possible solution
to this problem was to have the program digitize all five data channels on
one recorder at the same time. But since a finite time interval was re-
quired by the program between sequential samples of each channel (result-
ing in a time skew between the data from the five channels) and because
the problem described above would still exist between data on separate
recorders, this procedure was not implemented.

It was finally decided that the most acceptable solution would be to
record a 100 kHz sine on each recorder to serve as a clock for timing the
sampling interval. Of course the key to this procedure is that the sine
wave, like the pulses which serve as coarse time marks, must be recorded
on both tape recorders at the same time the data is. In this way, it
provides an absolute tape-time reference for all ten data channels on the
two recorders. The data on any one channel can be digitized using this

17

clock in the following way. One data channel and the pulse and 100 kHz sine channels from a given recorder are fed into the analog-to-digital converter. The program in core begins by sampling the pulse channel and comparing the the sampled value to a pre-set threshold. When the threshold is exceeded the pulse has been reached and the program then begins to sample the 100 kHz sine. At every sampled zero crossing, or at any multiple number of zero crossings, of the sine wave the program jumps to the data channel, samples a value and stores it in a core, and then returns to sampling the sine wave. The program continues in this way for a pre-set number of samples of the data channel up to a maximum of 24,000. To obtain another set of samples of the same channel, the procedure is repeated with a delay in the program from the time the pulse is detected to when sampling of the data is begun. This is accomplished by counting an appropriate number of zero crossings of the sine wave before the first sample of data is taken. This entire procedure is then repeated for every data channel.

The pulse and sine wave channels are sampled at a rate determined solely by the time required to perform certain program operations. Since this time is much larger than the 10 μsec period of the sine wave, it is necessary in the above procedure to slow down the tape recorders sufficiently on playback to allow the required sampling resolution of the sine wave. For this reason, ratios of record-to-playback speeds as high as 32 or 64 must be used. A maximum data sampling rate of 200,000 samples/sec would be possible under these circumstances. This would provide five samples within one cycle of 40,000 Hz ($\omega \delta^*/U_\infty = 18$) components of the data.

Once the digital data is stored on magnetic tape, it can be read on a CDC 6600 computer, converted to CDC format, and numerically analyzed with Fortran programs. Basically, a conditional processing scheme similar

18

to one devised by Kaplan and Laufer (Ref. 21) is utilized to infer the occurrence of a "burst" in the data. This involves calculation of the variable interval time average (VITA) variance (see Ref. 17) defined as:

$$VAR_{u'}(t) = \frac{\hat{u}'^2(t) - [\hat{u}'(t)]^2}{\overline{u'^2}} \tag{1}$$

where

$$\hat{u}'(t) = \frac{1}{T} \int_{t-T/2}^{t+T/2} u'(\tau)d\tau$$

and

$$\overline{u'} = \frac{1}{T_t} \int_{o}^{T_t} u'(\tau)d\tau \qquad (T_t = \text{total data sample time})$$

From this a detector function is calculated according to:

$$IVAR_{u'}(t) = \begin{cases} 1 \text{ for } VAR_{u'}(t) > V_o \\ \\ 0 \text{ for } VAR_{u'}(t) < V_o \end{cases} \tag{2}$$

where V_o is a preselected threshold level. For a physically meaningfull average time, T, and threshold level, V_o, periods of non-zero IVAR should indicate the presence of "bursts" in the fluctuating quantity. The detector function could then be used to determine the mean period between bursts, and a correlation of the variance for several simultaneous pressure or streamwise velocity fluctuation measurements would yield an estimate of the speed of propagation of bursts along the boundary layer wall or normal to the wall. An analysis of instantaneous velocity, pressure and shear fluctuations during a burst could reveal useful information on the mechanism of burst generation and on the structure of bursts.

19

IV. RESULTS AND DISCUSSION

A. TIME AVERAGED ANALYSES

The recorded data from the various tests can be analyzed in two basic ways. Conventional time averaged analyses (RMS level, spectral density, auto and cross-correlation) can be performed for comparison with similar work done by other investigators. From this it can be determined if the proper instrumentation systems have been chosen for the measurements, if typical turbulent flow conditions have been established, and what the overall boundary layer turbulence characteristics are. To obtain any information about the quasi-ordered structure of the turbulence it is necessary to analyze the data in a way that will reveal any intermittency or coherence in the turbulent fluctuations. This required the application of new conditional sampling schemes to the data.

Preliminary recordings of the fluctuating pressure and shear on the tunnel wall and of the fluctuating velocity in the boundary layer have been analyzed to obtain overall RMS levels and spectral distributions. Typical power spectra for the velocity, shear and pressure fluctuations are shown in Figs. 11-14, 15 and 16, respectively. The similarity between the spectra for the shear and velocity fluctuations is evident, the energy falling-off after approximately $\omega\delta^*/U_\infty = .3$ at a rate of about 6 dB/octave. Some uncertainty exists in the accuracy of the spectra at high frequencies due to the difficulty in optimizing and matching the frequency response characteristics of the various anemometers. This is particularly evident for the spectrum of the velocity fluctuations at $y/\delta = .14$ (Fig. 12) which shows that the anemometer in this case did not provide as high a frequency response as the others. A comparison of these results for the u-fluctuation spectra

20

with those of Serafini (Ref. 11) shows good overall agreement.

The spectrum of Fig. 16 shows that the pressure fluctuations contain significantly more high frequency energy than either the velocity or shear fluctuations. Although the fall-off in energy is also at a rate of about 6 dB/octave, this does not occur until around $\omega\delta^*/U_\infty = 3$. It has been found by several investigators (Refs. 5, 6, and 11) that transducer size has a significant effect on the resolution of wall pressure fluctuations. A comparison of various measurements seems to indicate that if the transducer diameter is too large, a loss of resolution of small-scale pressure fluctuations will occur. This manifests itself as consistently lower measured spectral densities at high frequencies, that is, above $\omega\delta^*/U_\infty \approx 1$. Emmerling (Ref. 6) has summarized the available results in terms of the nondimensional parameter du_τ/ν, where d is the transducer diameter. For values of this parameter above approximately 150 the overall RMS level of the wall pressure fluctuations is always measured to be around $0.005q_\infty$ $(q_\infty = \frac{1}{2}\rho_\infty U_\infty^2)$. Below this value, the measured RMS level increases linearly as du_τ/ν is lowered - levels as high as $.01q_\infty$ have been measured for $du_\tau/\nu \cong 50$. This increase is attributed to the increased resolution of intense small-scale fluctuations, or equivalently of high frequency spectral components, by the smaller transducers.

For the present investigation the condition $du_\tau/\nu \cong 50$ would require a transducer diameter on the order of .007". Since a transducer this small could not be obtained, it was decided upon consideration of sensitivity and durability requirements to use Kulite MIC-080-5 transducers whose pressure sensitive area has a diameter of .040". Although this gives a value of du_τ/ν equal to approximately 300, it was planned that if resolution of the small-scale fluctuations was required to achieve the goals of this

21

investigation a pinhole surface port could be used to reduce the effective transducer diameter. The main obstacle to using a surface port is that the pinhole-transducer cavity system must be designed so that its resonant frequency is significantly higher than any frequency of interest for the pressure fluctuations. The feasibility of designing a system which meets this requirement for our flow conditions is being investigated. The results presented in Fig. 16 (as well as in the rest of this report) are for the transducer mounted flush with the tunnel wall. A comparison of this wall pressure spectrum with those reviewed by Willmarth (Ref. 5) shows that some resolution of high frequencies is being lost by our transducer. The relatively low RMS level of $.0058q_\infty$ also bears out this fact.

The spectral analyses showed that the FM mode on the Phillips tape recorder was adequate for recording velocity and shear fluctuations, and that the FM mode on the Honeywell tape recorder (with its wider bandwidth) would have to be used to record the wall pressure fluctuations. The spectral content of the data also indicated that the digitization would have to be done at a sampling rate of 50,000 samples/sec or greater in order to obtain an adequate resolution of the highest frequencies in the fluctuations.

B. CONDITIONAL SAMPLING ANALYSIS

The most important aspect of this investigation involves the conditional sampling of the turbulent fluctuations to obtain a description of turbulent "bursts". The value of the investigation lies not only in the fact that simultaneous measurements are made of the velocity, wall-pressure, and wall-shear fluctuations to aid in obtaining a better description, but also in the range of flow conditions studied. Table I lists two typical investigations: one by Blackwelder and Kaplan (Ref. 17) of conditionally sampled

22

turbulent velocity profiles and another by Emmerling (Ref. 6) of the instantaneous distribution of wall-pressure fluctuations under a turbulent boundary layer. In comparison, the present investigation is of a boundary layer with a much higher free stream velocity (U_∞ = 600-800 ft/sec) and Reynolds number ($R_\theta \approx 10^5$), thus extending the range over which the "bursty" character of turbulent boundary layers has been studied.

One characteristic of interest is the mean period between "bursts". Lu and Willmarth (Ref. 16) have found that a consistent estimate of the average time interval between relatively large "bursts" is $\bar{T}U_\infty/\delta^* \approx 32$ (or, equivalenty, $\bar{T}U_\infty/\delta \approx 5$ as expressed by Laufer and Badri Narayanan (Ref. 22)). One column of Table I presents the ratio of this period to the data sampling interval and shows that for the sampling rates possible in the present study an accurate temporal resolution of the "bursts" would be obtained.

To date, the data from one of the test configurations listed in Section III-B have been completely digitized and analyzed. This was the case of four streamwise velocity measurements within a distance of 1" from the tunnel wall and one pressure fluctuation measurement on the tunnel wall directly below the velocity measurements. The positions of the velocity measurements and the mean velocity and overall RMS level of fluctuations measured at each point were as follows:

y/δ	.025	.08	.14	.25
U/U_∞	.62	.71	.76	.82
$\sqrt{\dfrac{\overline{u'^2}}{U}}$	.073	.053	.044	.033

The velocity fluctuations were measured within the frequency range 2-10,000 Hz ($\omega\delta^*/U_\infty$ = .009-4.5) and the pressure fluctuations within the

23

range 30-30,000 Hz($\omega\delta^*/U_\infty$ = .013-13). The overall RMS level of the

pressure fluctuations was approximately $\sqrt{\overline{p'^2}}/(\frac{1}{2}\rho_\infty U_\infty^2)$ = .006.

A short sample of the traces obtained on the ink plotter directly

from the tape recorder is shown in Figs. 17a and b (the two figures

actually represent six simultaneous traces). The duration of the sample

is approximately 250 msec. Since the pressure fluctuations were recorded

on both tape recorders for this test, the five data traces shown are from

one recorder. The sixth trace is of the pulse channel and shows one of

the pulses used as reference time marks. Qualitatively there is a great

degree of correlation in the time histories of the four velocity fluctua-

tion measurements, while correlation between the pressure and velocity

is not clearly discernible. Once data is available from the five simulta-

neous pressure fluctuation measurements and from the shear fluctuation

measurement at the wall, any correlation between characteristic events in

the velocity fluctuations and changes occurring at the wall (e.g., in the

pressure gradient fluctuations) will be more readily apparent.

The recorded data was digitized with a sampling interval Δt = 25 μsec

($\Delta t U_\infty/\delta^*$ = .357 or $\Delta t\, u_\tau^2/\nu$ = 40). Approximately 16,000 samples (400 msec)

were taken of each data channel. Two sections of the digitized data are

plotted in Figs. 18a-h. (Note: the first four figures are from tU_∞/δ^* = 0

to 1000 and the last four from tU_∞/δ^* = 4700 to 5700). The plots were

made on the CDC computer once the fluctuating quantities were normalized

with respect to their maximum value. For the velocity fluctuations at

y/δ = .025, .08, and .14, the vertical scales are about the same with $\pm$ 1

representing approximately $\pm$ 110 ft/sec. For y/δ = .25, $\pm$ 1 represents

$\pm$ 75 ft/sec. The scale for the pressure fluctuations is such that $\pm$ 1 is

equivalent to $\pm$ .075 psi.

The results obtained from the digital processing analysis are shown in

Fig. 19-23. Each figure consists of eight plots, the first four (a-d) are
for the time interval $5 < tU_\infty/\delta^* < 1005$ and the last four (e-h) for
$4705 < tU_\infty/\delta^* < 5705$. The results have been presented for these two time
intervals because they are representative of those obtained for the entire
test. The uppermost trace in each figure is of the fluctuating quantity
which has been normalized with respect to its maximum value over the entire
16,000 samples. Below this is shown the variable interval time average
variance (VAR) of the fluctuating quantity as defined by Eq. 1 of Section
III-B. This too has been normalized with respect to its maximum value so
that its amplitude varies between zero and + 1. The averaging time, T, in
Eq. 1 was chosen to be $TU_\infty/\delta^* = 3.57$ for the results presented here.
Several other values were tried before it was decided that this averaging
time gave the most consistent results for the variance. The lowermost
trace is of the detector function (IVAR) associated with the VITA variance
through the relationship expressed in Eq. 2 of Section III-B.

It can be seen that large values of VAR(t) indicate steep changes in
the fluctuating quantity, that is, strong streamwise accelerations in the
case of the velocity fluctuations (Figs. 19-22) and high temporal pressure
gradients for the wall-pressure fluctuations (Fig. 23). Since various
studies have reported that large and rapidly changing velocity and pressure
fluctuations are associated with turbulent "bursts", it is commonly
assumed that a period of large amplitude for VAR(t) indicates the presence
of a "burst" in the fluctuating quantity. Once a reasonable decision is
made as to what constitutes a large amplitude (that is, once a threshold
level, V_o, is chosen), a detector function can be defined as in Eq.2.
This function then serves to mark the time when a "burst" is deemed to
occur. For the results presented in Figs. 19-23 the threshold was chosen
so as to yield the best correlation between the detector function of the

25

five fluctuating quantities.

The detector function can be used to obtain the mean period between "bursts" for each of the fluctuating quantities. For the wall pressure fluctuations this period was found to be approximately $\bar{T}U_\infty/\delta^* = 32.5$, while for the velocity fluctuations the period ranged between $\bar{T}U_\infty/\delta^* = 34$ at $y/\delta = .025$ and $\bar{T}U_\infty/\delta^* = 36$ at $y/\delta = .25$. These results are in good agreement with those reported by other investigators. For example, Emmerling (Ref. 6) has found a mean period of $\bar{T}U_\infty/\delta^* = 27$ for the "occurrence of characteristic wall pressure structures", and Lu and Willmarth (Ref. 16) have reported a mean period of $\bar{T}U_\infty/\delta^* \cong 32$ for relatively large "bursts" in their velocity fluctuation measurements.

Although it is evident that a significant correlation exists between the "bursting" events detected in the four velocity fluctuation measurements, a thorough description of the propagation and structure of the "bursts" cannot be attempted until the analysis of other measurements included in the full test schedule (see Section III-B) is completed. This will include, of course, a test with five simultaneous wall pressure fluctuation measurements and another where the wall shear fluctuations are also measured. These measurements will be invaluable in determining the correlation between the "bursts" found in the velocity fluctuations along the boundary layer and those detected on the wall. The simultaneous pressure measurements will also allow the gradient of the wall pressure fluctuations to be included in the analysis.

In addition to the completion of the full test schedule and digital analysis of the collected data, the following investigations are in progress. Several of the tests will be repeated at a significantly lower free stream velocity ($U_\infty \approx 100\,\text{ft/sec}$) to determine how any observed

26

characteristics of the "bursts" scale with velocity. This will also serve
to check any inadequacies (e.g., at high frequencies) of the instrumenta-
tion. Along these lines, the possibility of designing a pinhole surface
port to decrease the effective diameter of the pressure transducers is
being investigated. Since it is critical for the analyses being performed
that the simultaneity of the measured fluctuations be preserved, it was
necessary to determine if the phase characteristics of the individual in-
strumentation systems were the same. All the elements, except for the
anemometers, were checked and found to have no relative phase shift. The
phase characteristics of the anemometers are in the process of being
investigated using a procedure described in Ref. 23.

The results presented in this report are preliminary in nature but
clearly demonstrate that the capability has been established for examining
the structure of the turbulent boundary layer under consideration. The
flow has been made truly two-dimensional and the free-stream turbulence
has been reduced to a relatively low level. The elaborate instrumentation
systems required have been set-up, calibrated and shown to give an
acceptable representation of the turbulent fluctuations. Most importantly,
the procedures and programs necessary to perform the critical conditional
sampling analyses on a digital computer have been established and ex-
ercised. Once the full test schedule is completed and all the acquired
data analyzed with these programs, the structure of the turbulent "bursts"
can be better described and their generating mechanism more clearly
understood. With this information about the boundary layer turbulence
characteristics clearly established, it will then be possible to proceed
with the next step in the investigation which will be to attempt to in-
fluence the characteristics by imposing external disturbances.

V. CONCLUSIONS

A wind tunnel facility (M = 0.6 to 0.8) with extremely low noise levels (u'/u_∞ = .08%) has been completed and tested. This facility is to be used for the investigation of the propagation mechanism of pressure fluctuations in turbulent flow. Results of the calibration of the facility are included in the report and indicate the excellent applicability of the facility to this investigation. A successful instrumentation package has been developed and tested for the measurements of the velocity, shear and pressure fluctuations in the turbulent boundary layer. Procedures have also been developed to produce discrete time sequences of the fluctuations which are conditionally sampled to obtain the frequency, amplitude and structure of the instabilities associated with turbulent "bursts".

Initial tests have been performed at M_∞ = 0.64 and indicate that the spectra of the turbulent fluctuations and the mean period between "bursts" is in agreement with results obtained by other investigations at lower free stream velocities. These previous results were obtained from measurements made either at the wall or in the boundary layer. Our conclusions are based on simultaneous measurements of the pressure at the wall and the velocity in the boundary layer. Additional tests have been completed and an analysis of the data is in progress.

REFERENCES

1. Willmarth, W.W., "Structure of Turbulence in Boundary Layers," Advances in Applied Mechanics, Vol. 15, p. 159, 1975.

2. Offen, G.R. and Kline, S.J., "A Proposed Model of the Bursting Process in Turbulent Boundary Layers," J. Fluid Mech., 70:209, 1975.

3. Bark, F.H., "On the Wave Structure of the Wall Region of a Turbulent Boundary Layer," J. Fluid Mech., 70:229, 1975.

4. Laufer, J., "New Trends in Experimental Turbulence Research," Annual Review of Fluid Mechanics, p. 307, 1975.

5. Willmarth, W.W., "Pressure Fluctuations Beneath Turbulent Boundary Layers," Annual Review of Fluid Mechanics, p. 13, 1975.

6. Emmerling, R., "The Instantaneous Structure of the Wall Pressure Under a Turbulent Boundary Layer," Max-Planch-Institut fur Stromungschung Rep. No. 9, 1973.

7. Frenkiel, F.N. and Klebanoff, P.S., "Probability Distributions and Correlations in the Turbulent Boundary Layer," Phys. Fluids, 16:725, 1973.

8. Landahl, M.T., "Wave Mechanics of Breakdown," J. Fluid Mech., 56:775, 1972.

9. Landahl, M.T., "Drag Reduction of Polymer Addition," Proceedings XIII International Congress of Theoretical and Applied Mechanics, Moscow, 1972.

REFERENCES CONT'D

10. Black, T.J., "A New Model of the Shear Stress Mechanism in Wall Turbulence," AIAA, 1968.

11. Serafini, J.S., "Wall-Pressure Fluctuations and Pressure Velocity Correlations in Turbulent Boundary Layers," AGARD Report 454, 1963.

12. Offen, G.R. and Kline, S.J., "Combined Dye-Streak and Hydrogen Bubble Visual Observations of a Turbulent Boundary Layer," J. Fluid Mech., 62:223, 1974.

13. Kim, H.T., Kline, S.J., and Reynolds, W.C., "The Production of Turbulence Near a Smooth Wall in a Turbulent Boundary Layer," J. Fluid Mech., 50:133, 1971.

14. Corrino, E.R. and Brodkey, R.S., "A Visual Investigation of the Wall Region in Turbulent Flow," J. Fluid Mech., 37:1, 1969.

15. Kline, S.J., Reynolds, W.C., Schraub, F.A., and Runstadler, P.W., "The Structure of Turbulence," J. Fluid Mech., 30:741, 1967.

16. Lu, S.S. and Willmarth, W.W., "Measurements of the Structure of the Reynolds Stress in a Turbulent Boundary Layer," J. Fluid Mech., 60:481, 1973.

17. Blackwelder, R.F. and Kaplan, R.E., "The Intermittent Structure of the Wall Region of the Turbulent Boundary Layer," U. Southern California A.E. Report No. 1-22, 1972.

REFERENCES CONT'D

18. Antonia, R.A., "Conditionally Sampled Measurements Near the Outer Edge of a Turbulent Boundary Layer," J. Fluid Mech., 56:1, 1972.

19. Rao, K.N., Narasismha, R., and Badri Narayanon, M.A., "The Bursting Phenomenon in a Turbulent Boundary Layer," J. Fluid Mech., 48:339, 1971.

20. Zakkay, V. and Wang, C.R., "Skin Friction Reduction by Slot Injection at Mach 0.8," NASA Contractor Report CR-2694, 1976.

21. Kaplan, R.E. and Laufer, J., "The Intermittently Turbulent Region of the Boundary Layer," 12th Proc. Int. Congr. Mech., p. 236, 1969.

22. Laufer, J. and Badri Narayanan, M.A., "Mean Period of the Production Mechanism in a Boundary Layer," Phys. Fluid, 14:182, 1971.

23. Nielsen, P.E. and Rasmussen, C.G., "Measurement of Amplitude and Phase Characteristics," DISA Information, No. 4, December 1966.

	U_∞ (ft/sec)	δ^* (in)	Re_θ	u_τ^2/ν (sec^{-1})	$\dfrac{\Delta t\, U_\infty}{\delta^*}$	$\dfrac{\Delta t\, u_\tau^2}{\nu}$	$\dfrac{\bar{T}}{\Delta t}$
Blackwelder & Kaplan (Ref. 17) (Velocity)	14	.42	2550	1.33×10^3	.31	1.02	100
Emmerling (Ref. 6) (Wall-Pressure)	25	.18	2000	7.6×10^3	.23	1.06	140
Present Study (Velocity, Wall-Pressure and Wall-Shear)	675	.57	108,000	1.6×10^6	.07 - .35	8-40	450-90

Δt = Data Sampling Interval

$\bar{T}$ = Mean Period Between Bursts as Calculated from
$\bar{T} U_\infty/\delta^* \approx 32$ (Ref. 16)

Table 1 Test Conditions and Data Sampling Densities for Two Typical Investigations and the Present Study

Fig. 1 Wind Tunnel

33<

TUNNEL WINDOW

HOT FILM PROBE

12"D

PRESSURE TAP

FLUSH MOUNTED HOT FILM PROBE

KULITE MIC-080-5 MICROPHONE

FLOW

Fig. 2 Test Section

34<
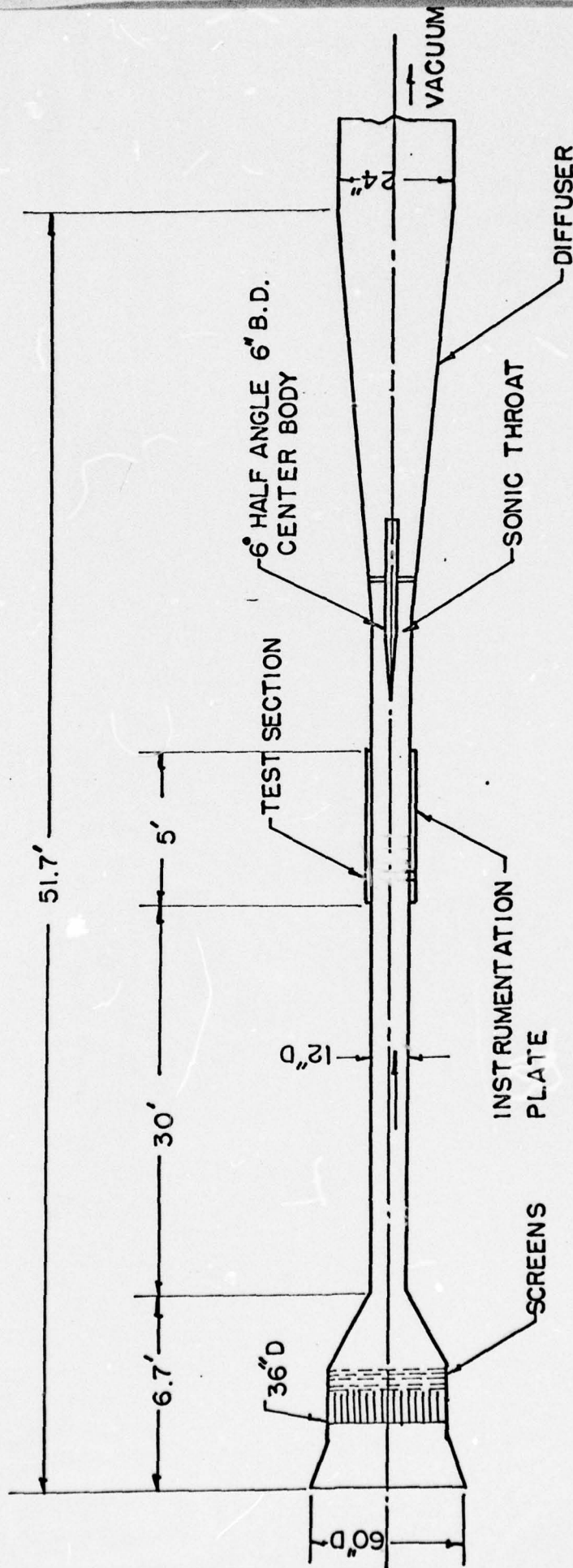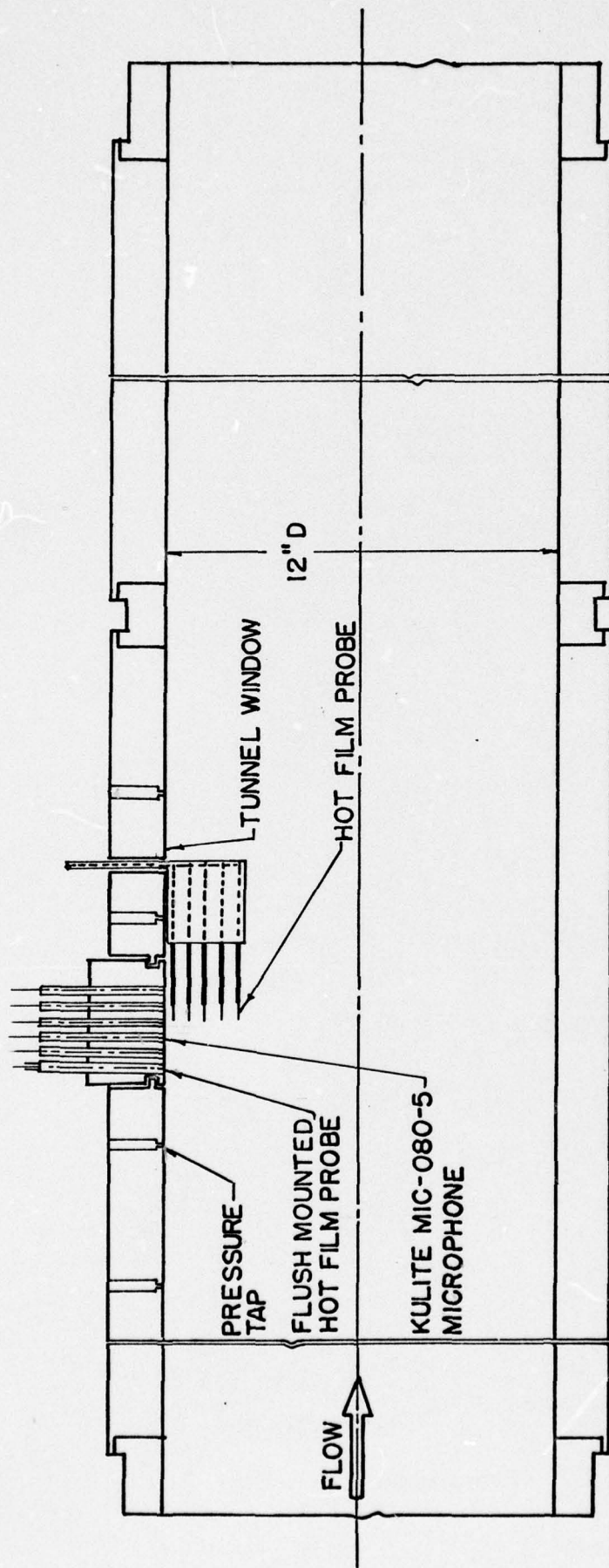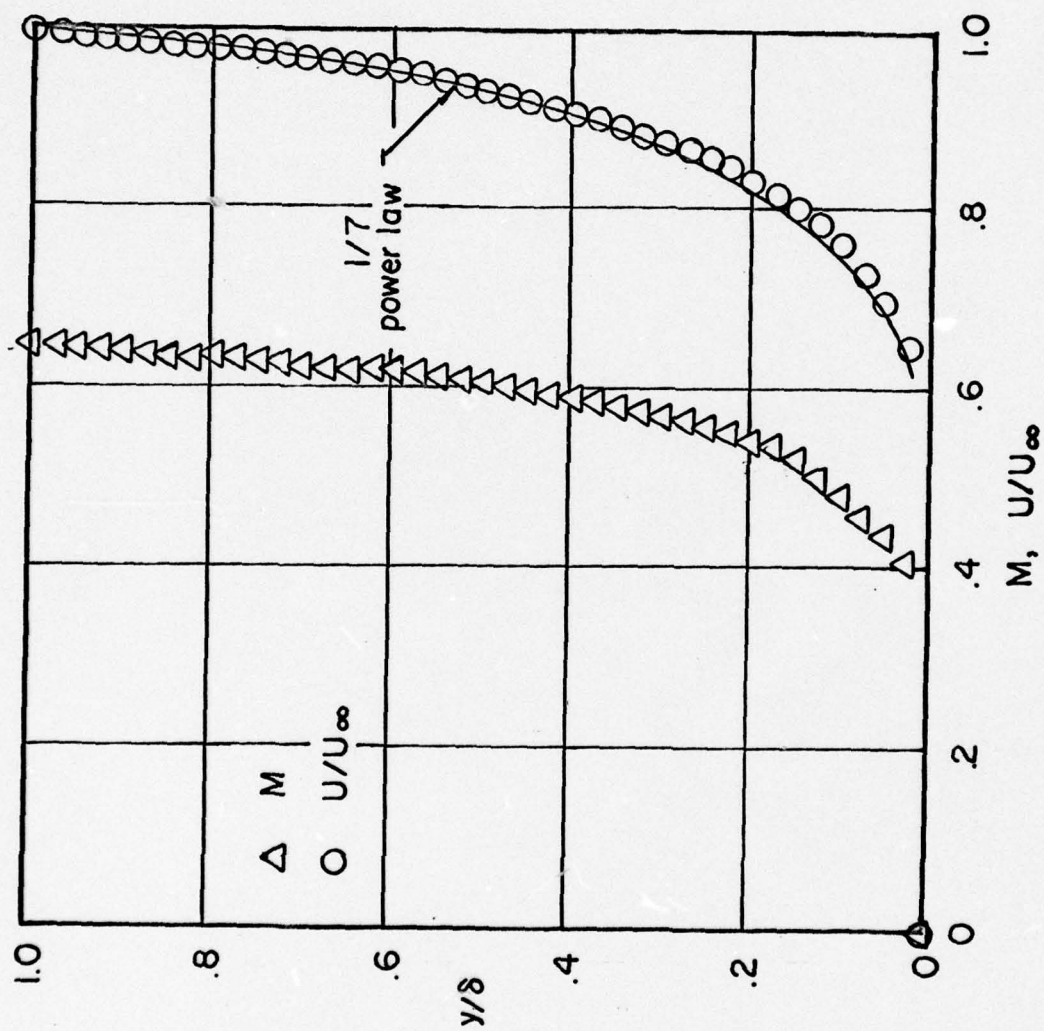
Fig. 3 . Boundary Layer Mach Number and Velocity Profiles
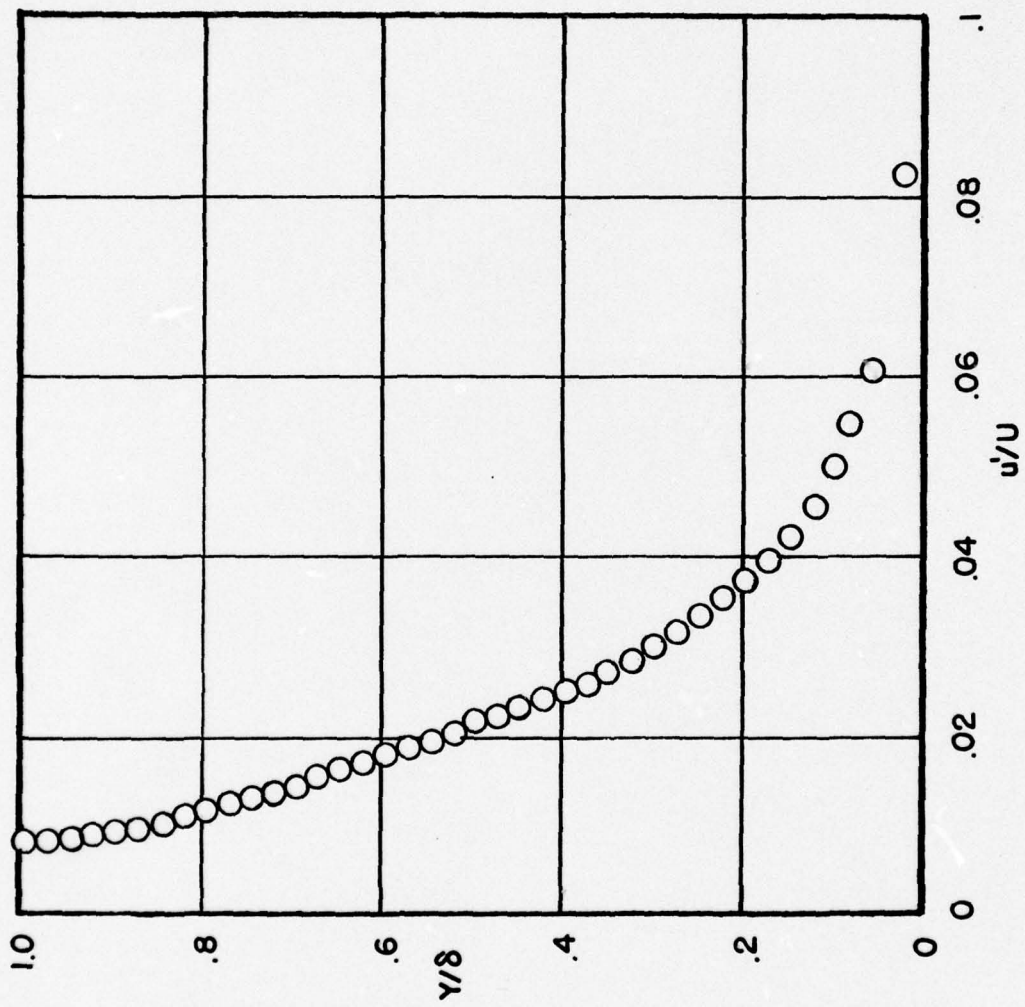
35<

Fig. 4 Turbulent Intensity Profile
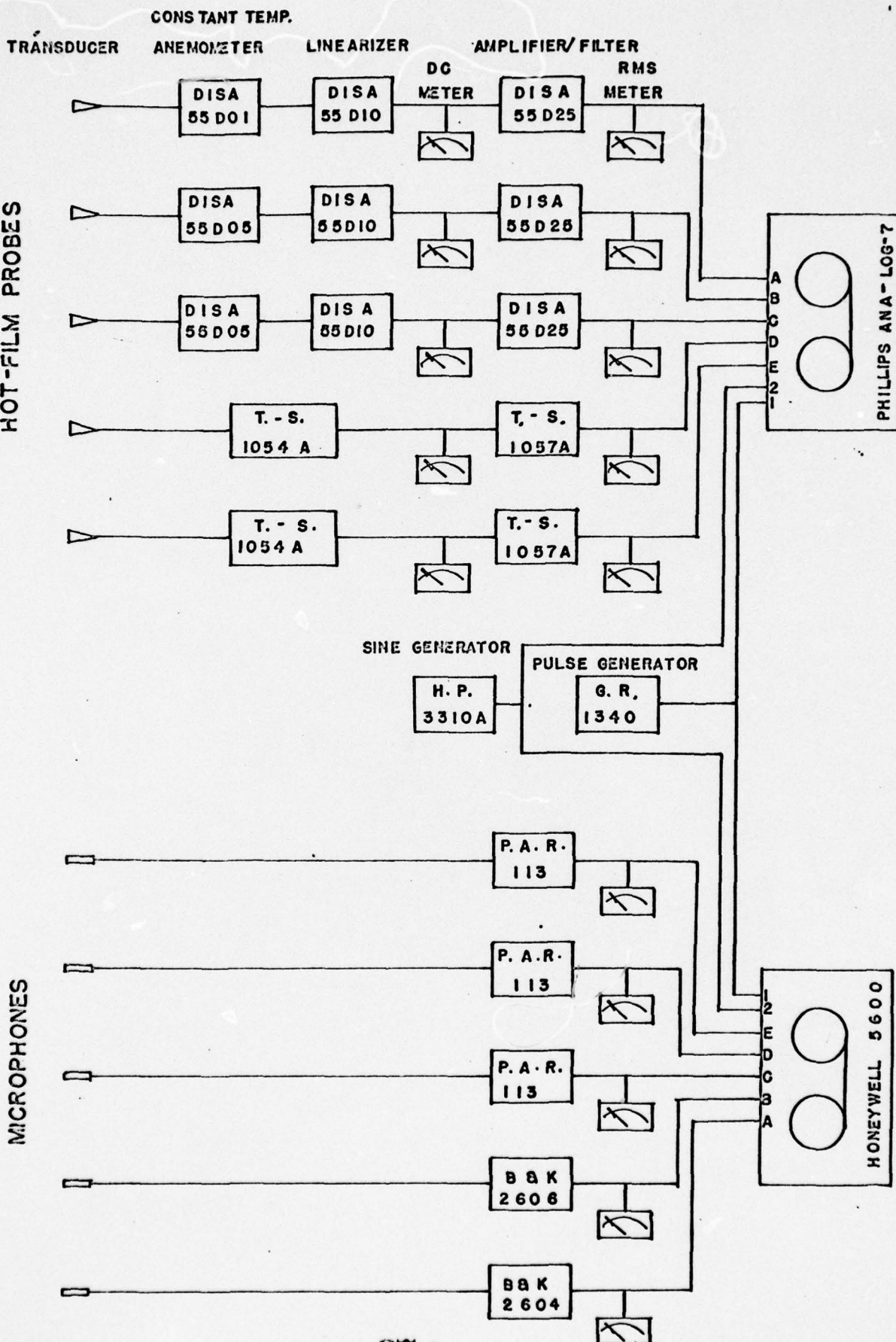
Fig. 5 Data Acquisition System
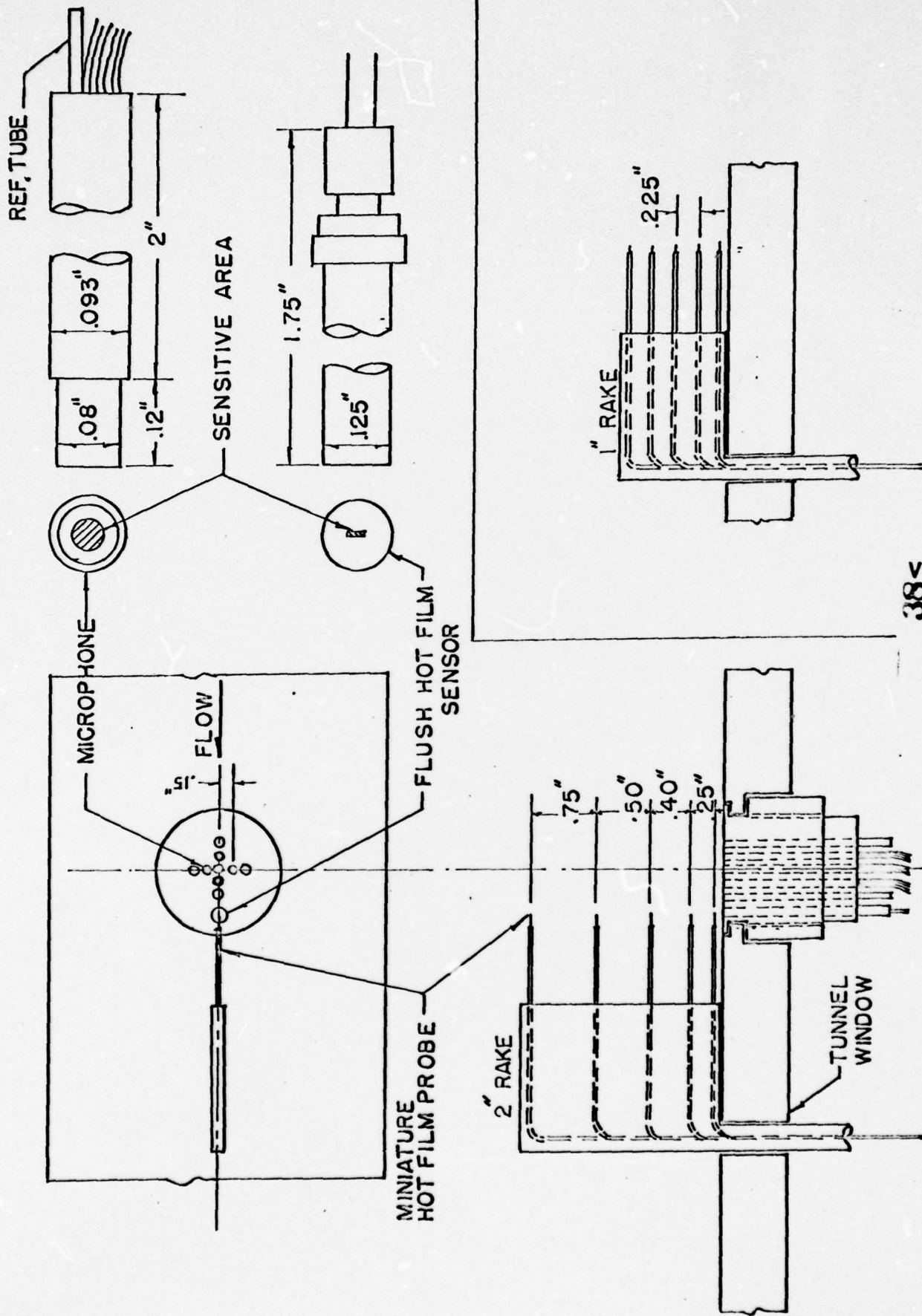
Fig. 6 Details of Instrumentation Set-Up
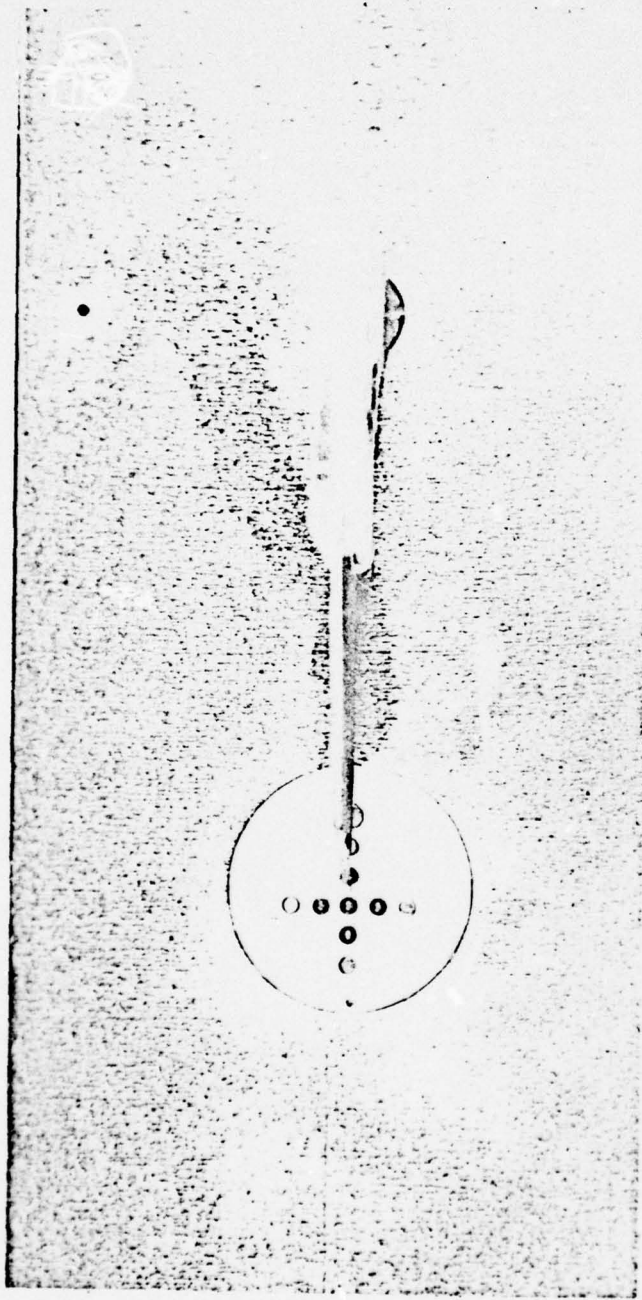
Fig. 7 Photograph of Pressure Transducers and Hot-Film Probes in the Tunnel

39
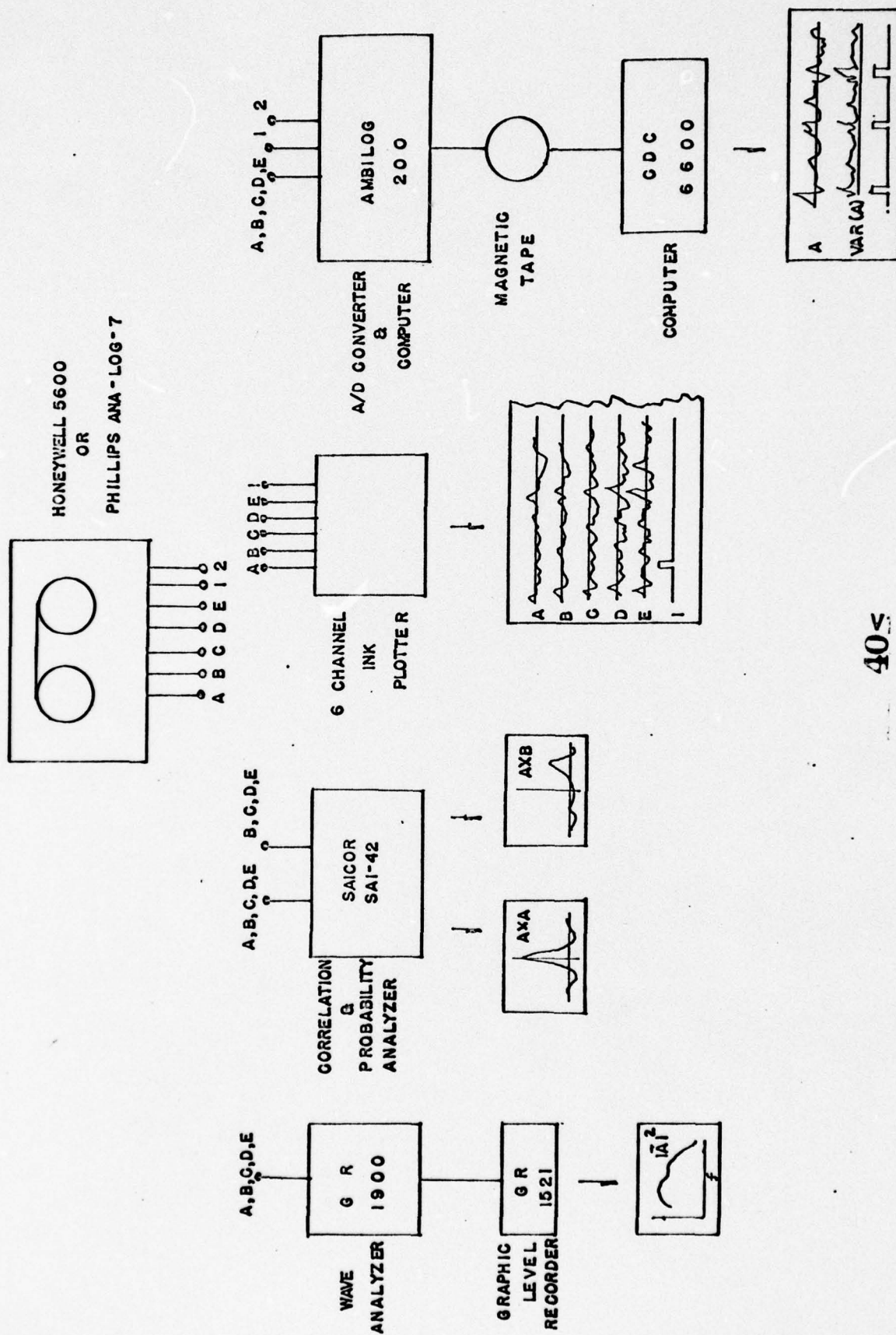
Fig. 8 Data Analysis Systems

Fig. 9 Photograph of Experimental Set-Up and Instrumentation

41<
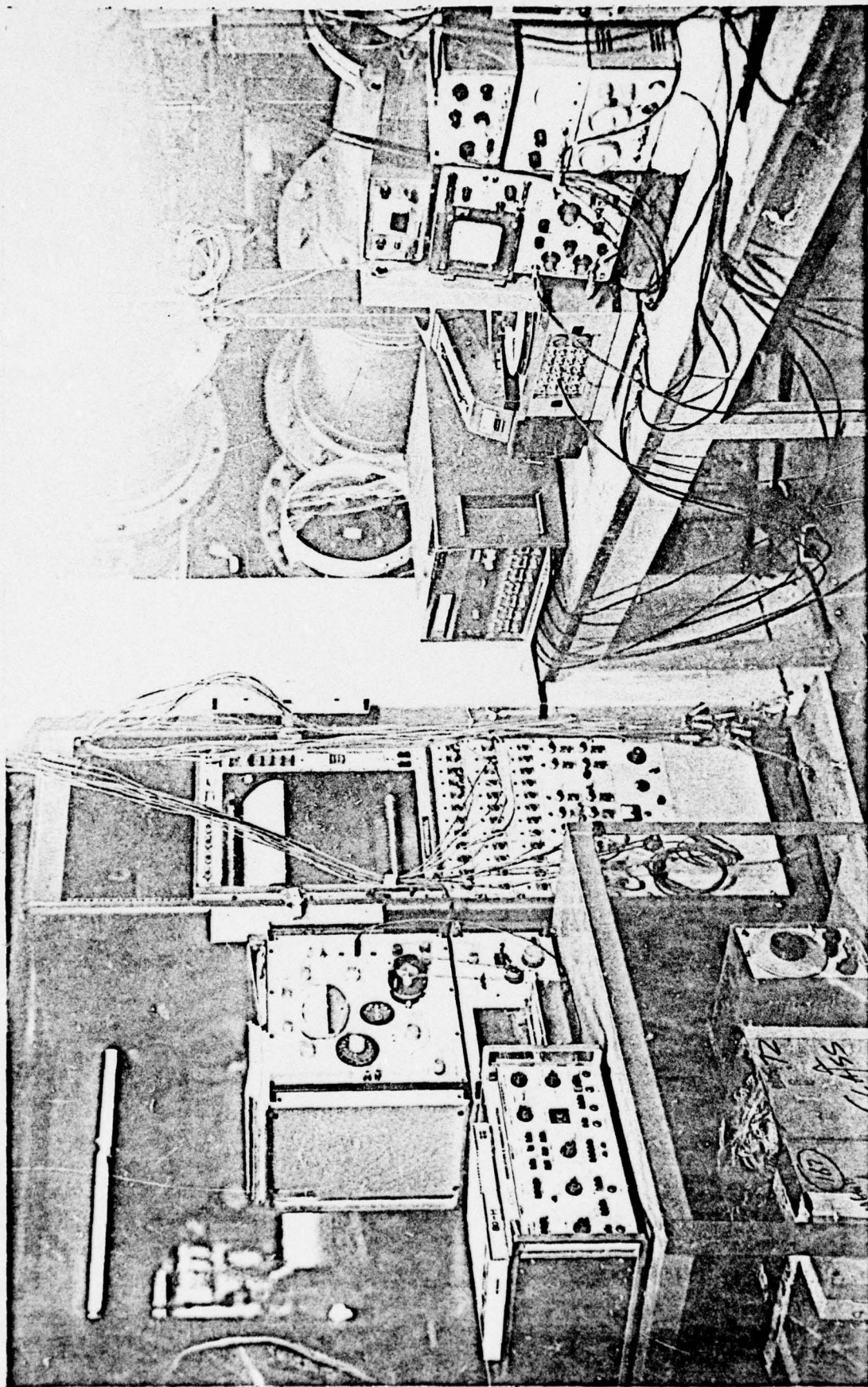
Fig 10   Photograph of Instrumentation and Some Data Analysis Equipment
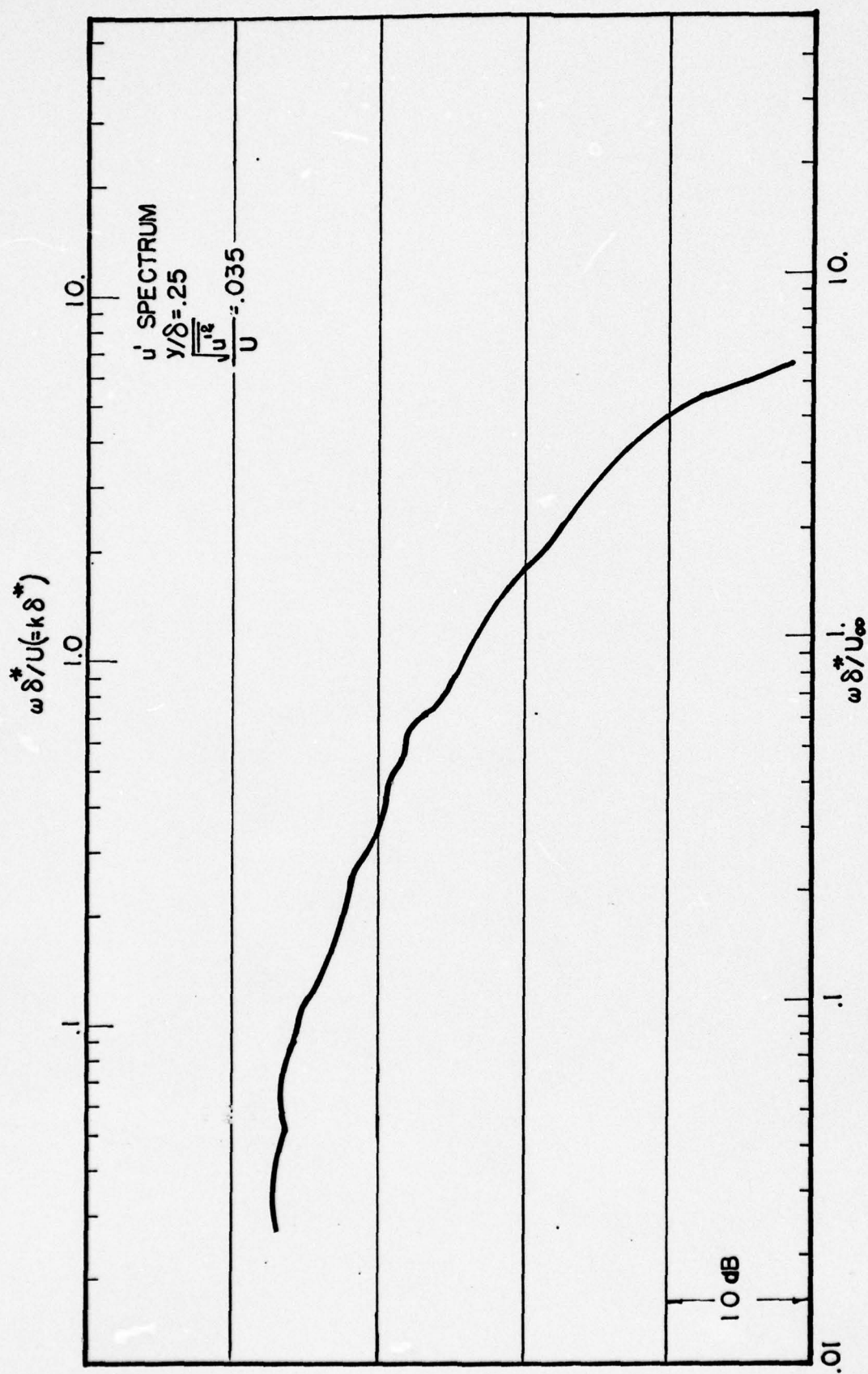
Fig. 11 Spectral Distribution of the Velocity Fluctuations at y/δ = .25

- 43<
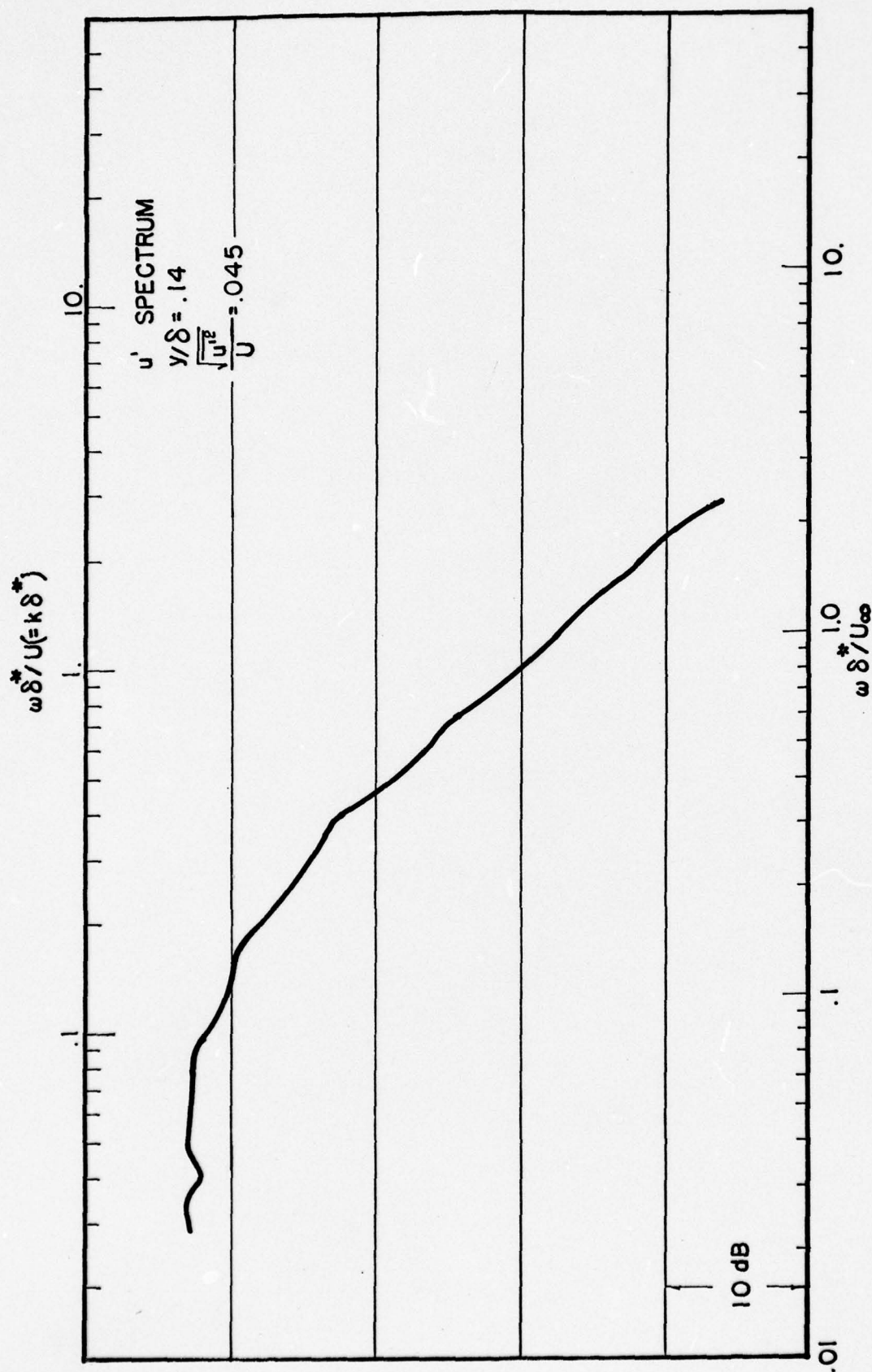
Fig. 12 Spectral Distribution of the Velocity Fluctuations at y/δ = .14

44<
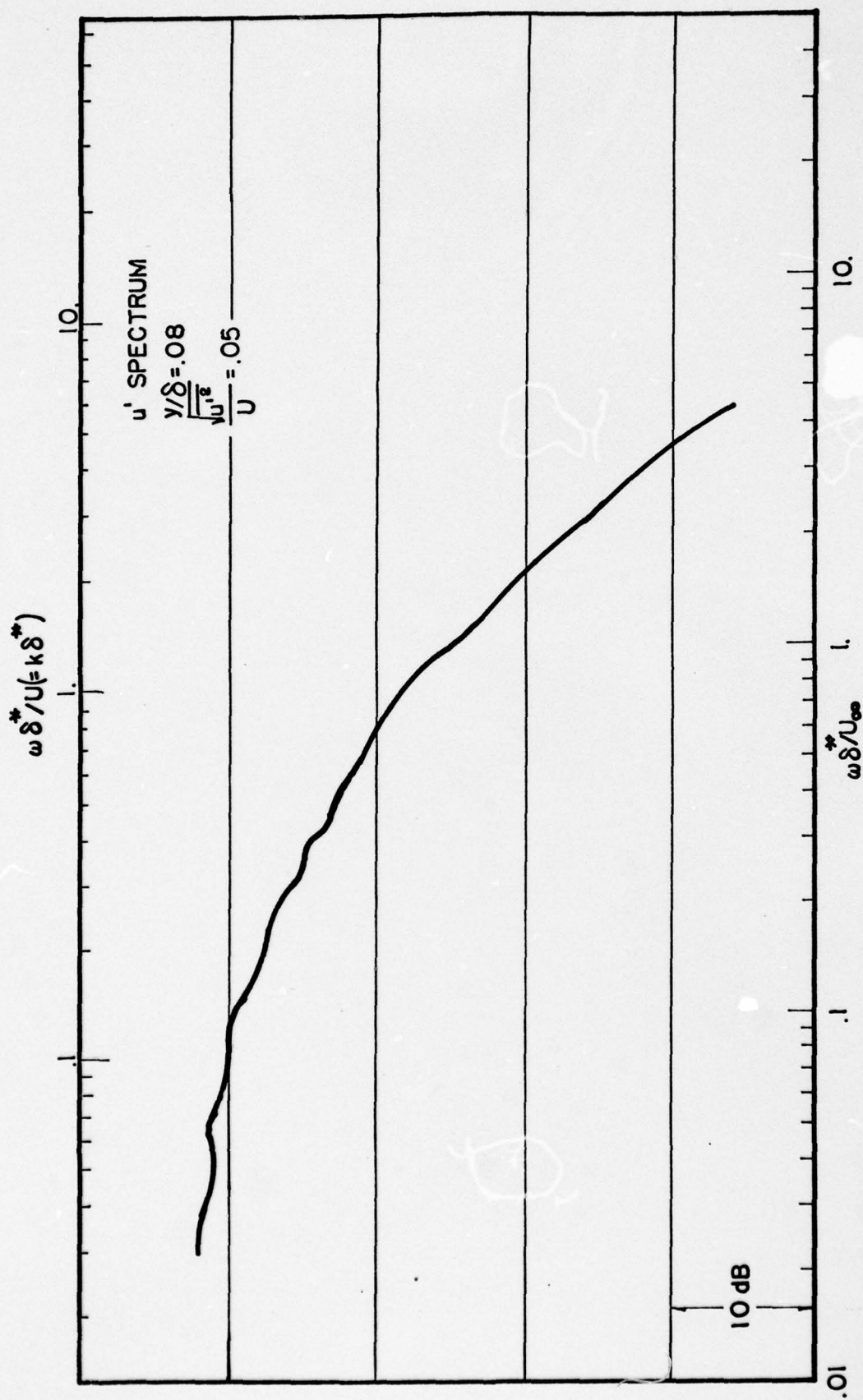
Fig. 13 Spectral Distribution of the Velocity Fluctuations at $y/\delta = .08$

—— 45<
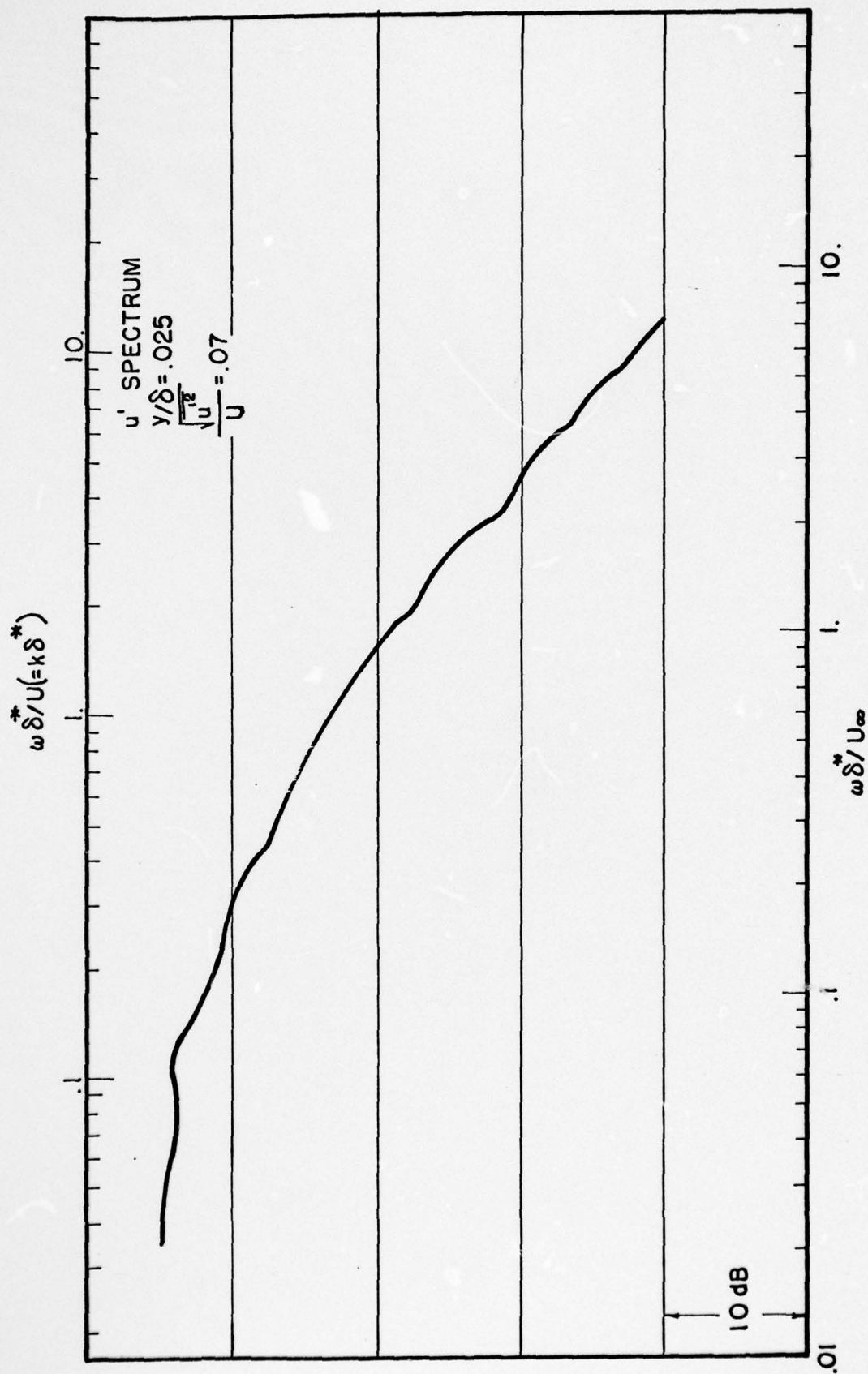
Fig. 14 Spectral Distribution of the Velocity Fluctuations at y/δ = .025

$-46<$
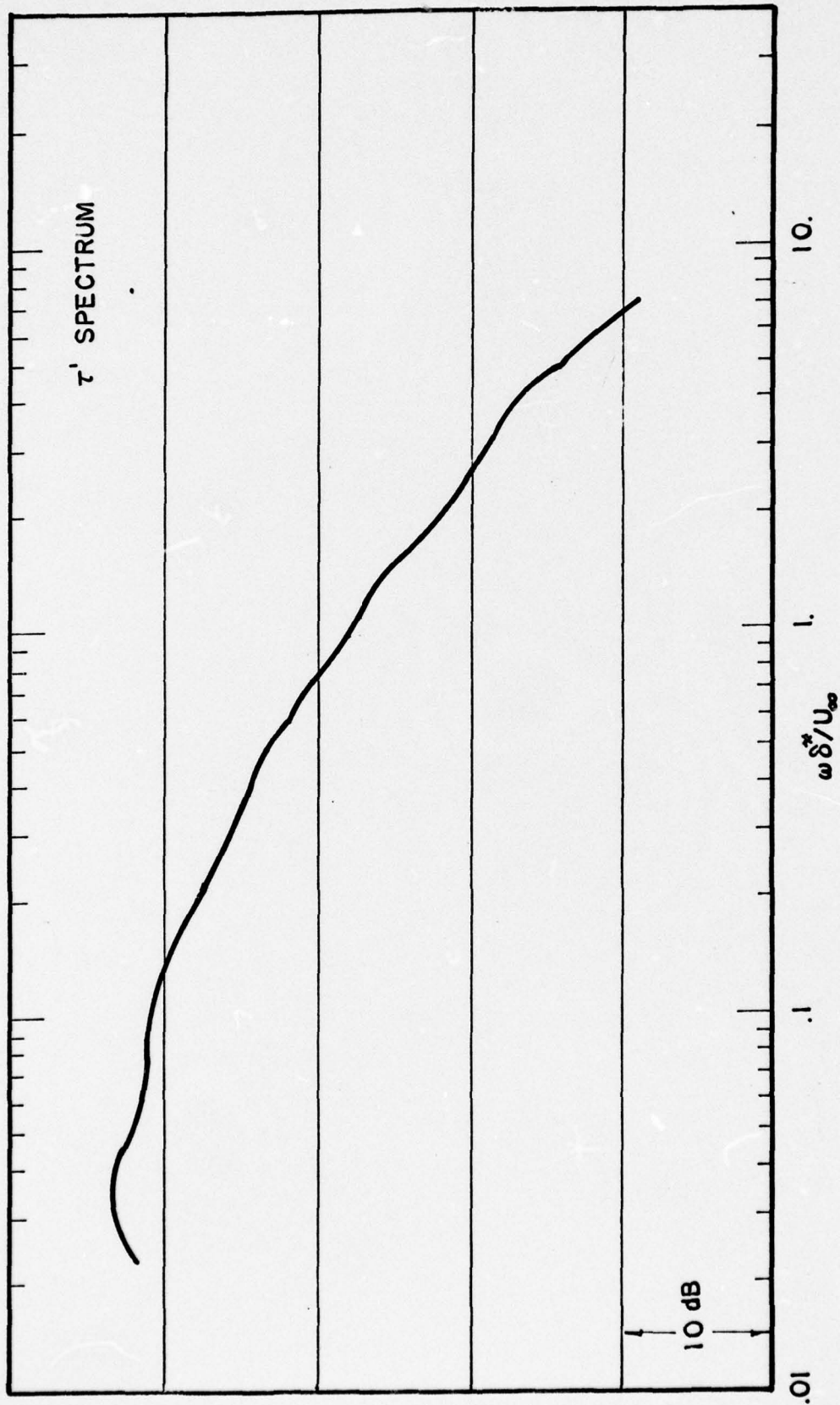
Fig. 15 Typical Spectral Distribution of Wall Shear Fluctuations
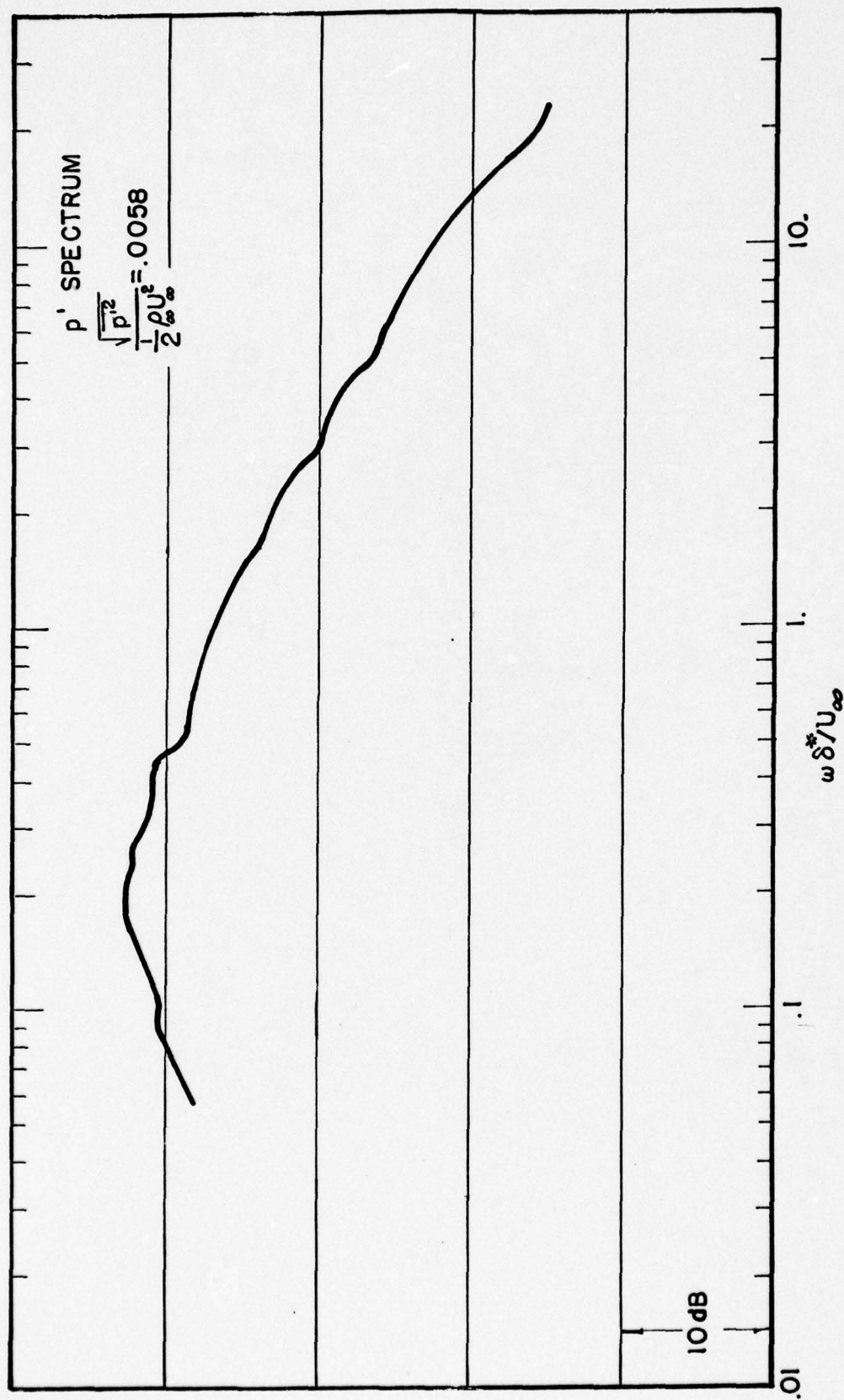
Fig. 16 Typical Spectral Distribution of Wall Pressure Fluctuations

48<
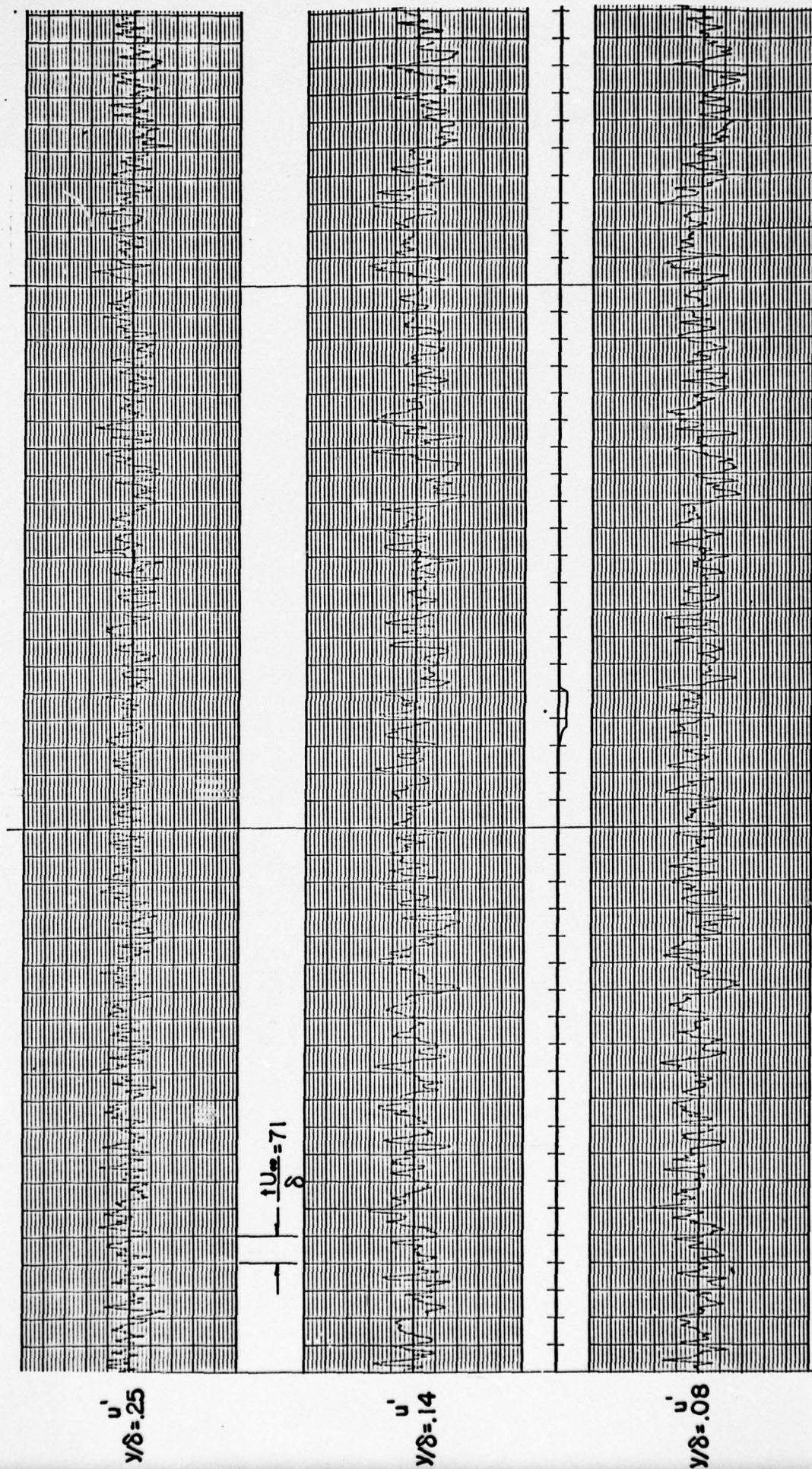
Fig. 17a Simultaneous Traces of Velocity and Wall Pressure Fluctuations Obtained from Analog Recording

49<
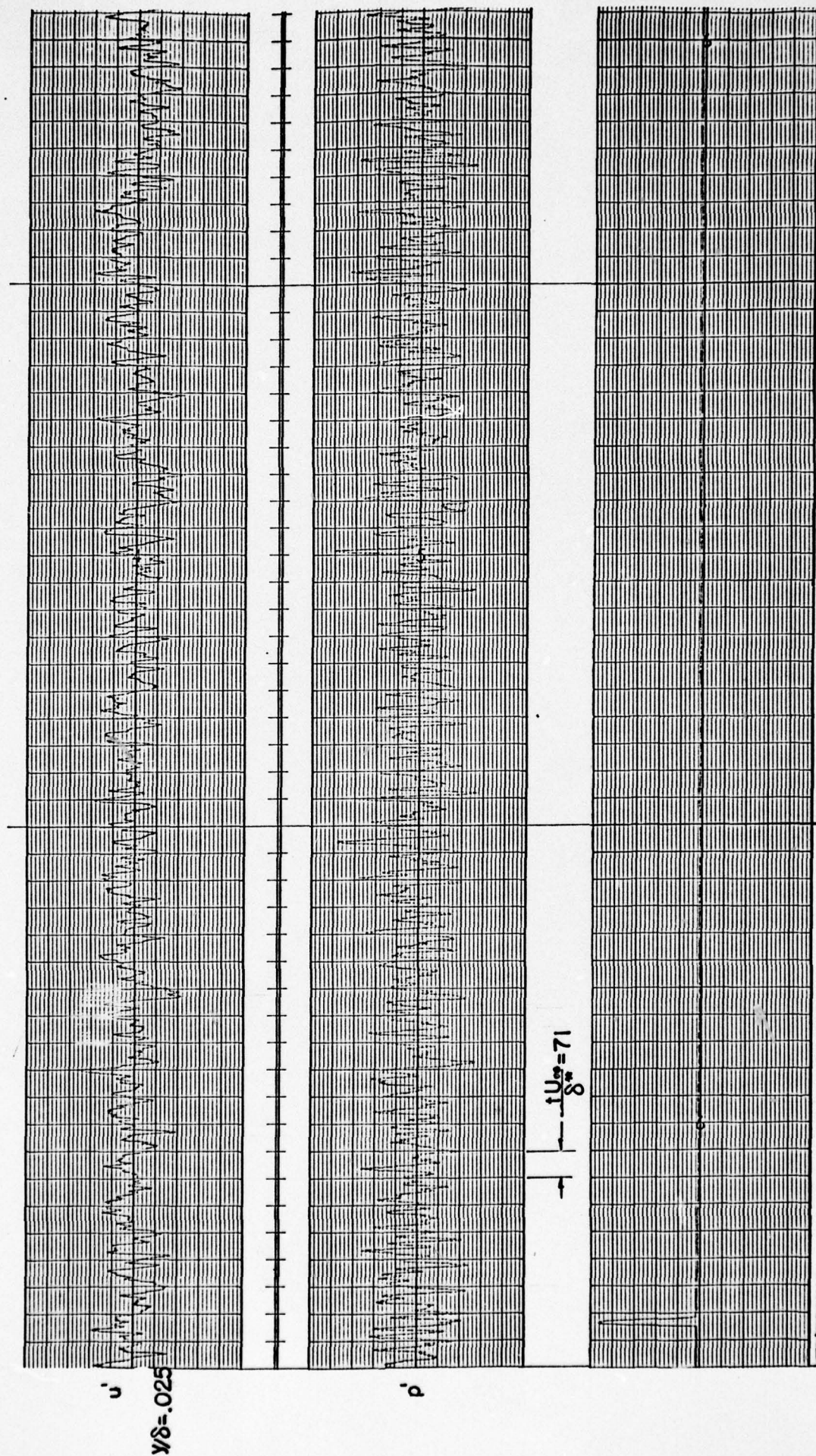
Fig. 17b Simultaneous Traces of Velocity and Wall Pressure Fluctuations Obtained from Analog Recording

50<
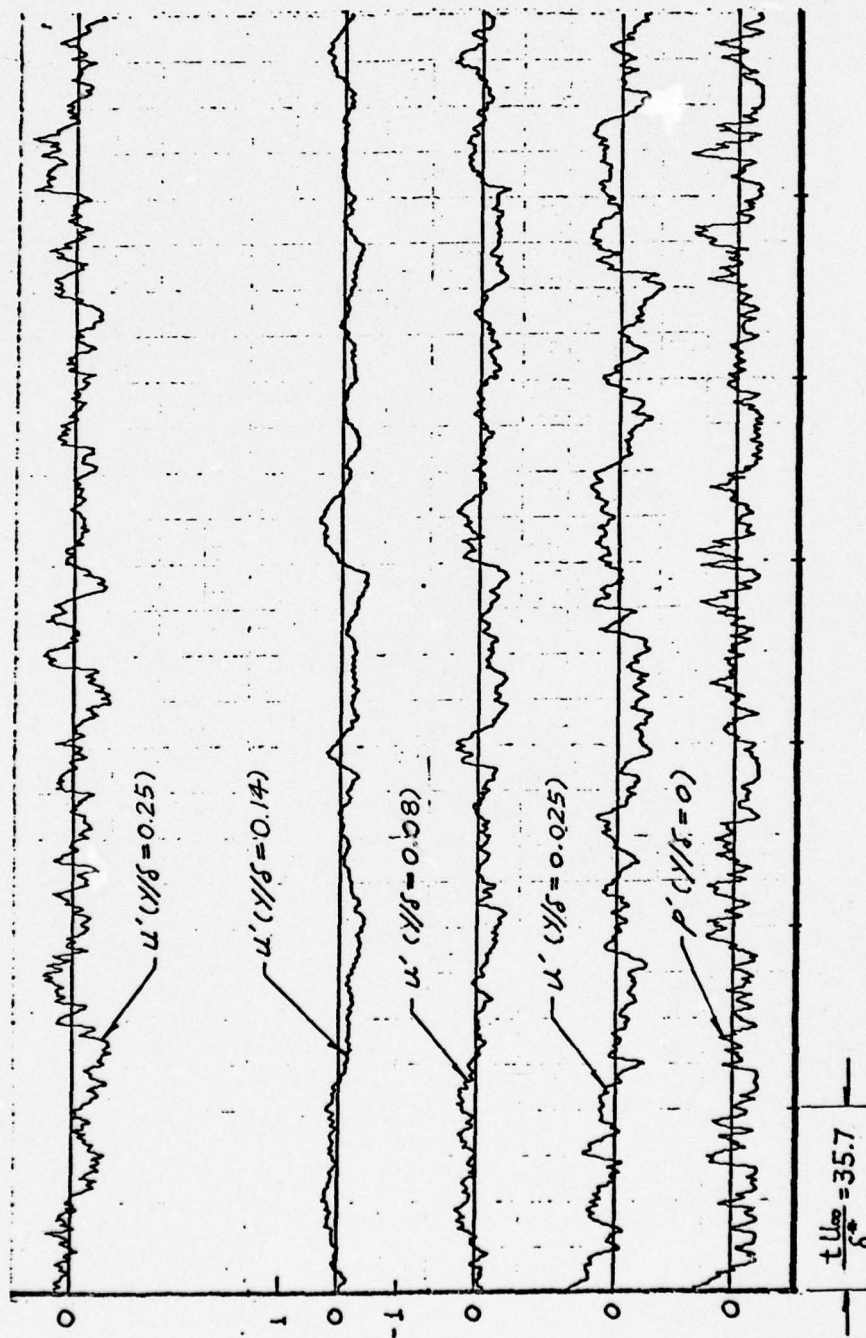
Fig. 18a Plot of Digitized Velocity and Wall Pressure Fluctuations $(0 < \frac{tU_\infty}{\delta^*} < 250)$
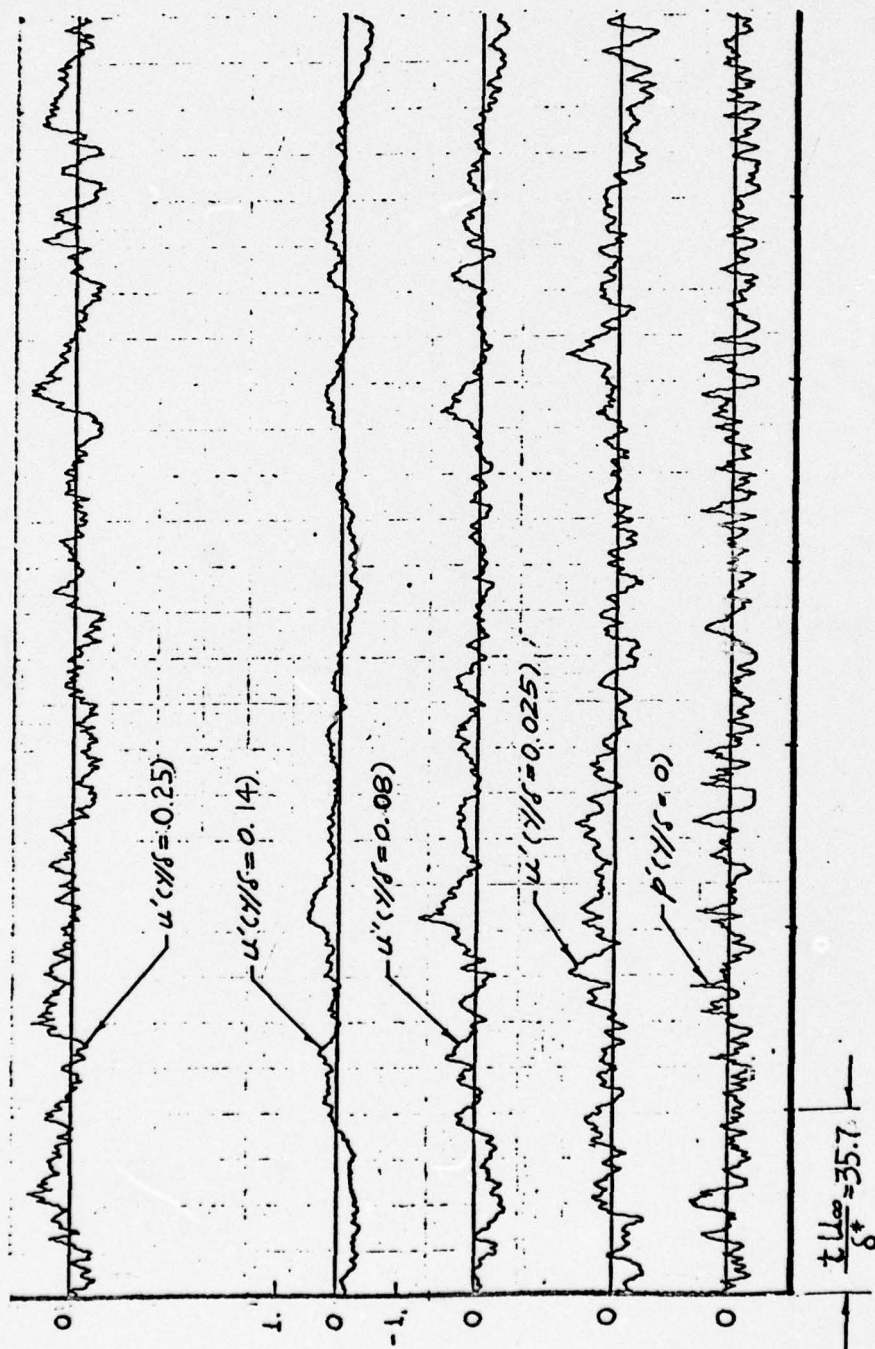
Fig. 18b Plot of Digitized Velocity and Wall Pressure Fluctuations ($250 < \frac{tU_\infty}{\delta^*} < 500$)

52<
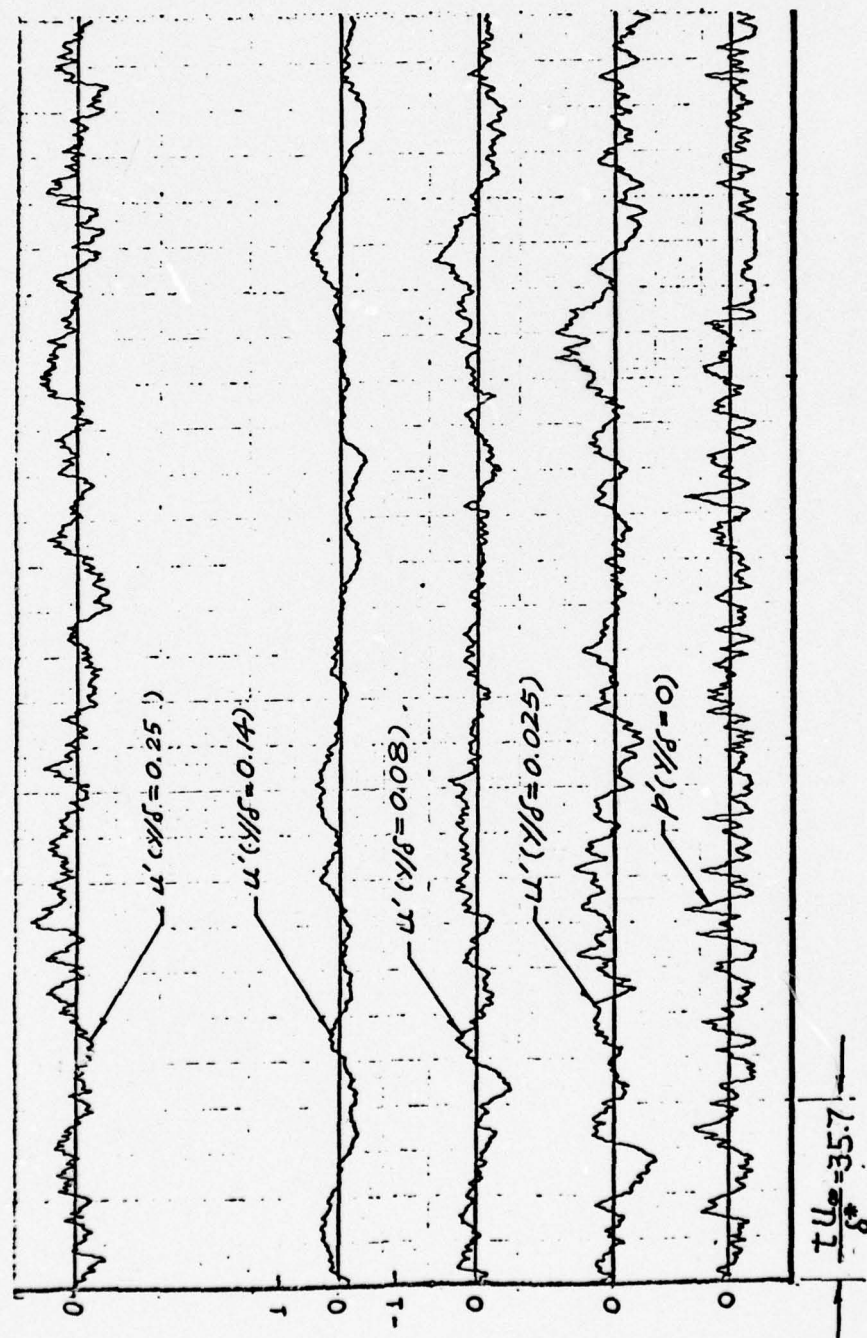
Fig. 18c Plot of Digitized Velocity and Wall Pressure Fluctuations ($500 < \frac{tU_\infty}{\delta^*} < 750$).
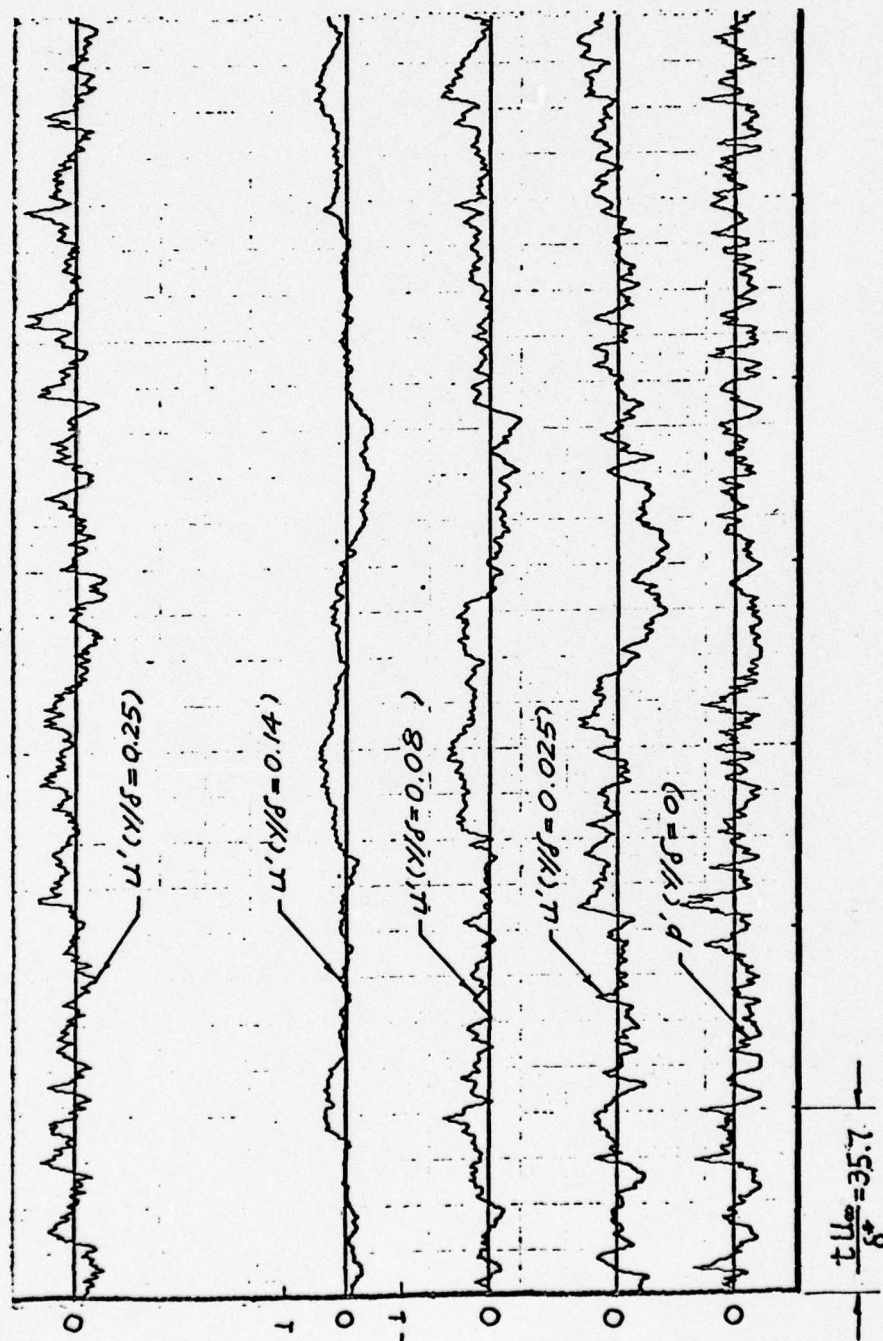
Fig. 18d Plot of Digitized Velocity and Wall Pressure Fluctuations (750 < $\frac{tU_\infty}{\delta^*}$ < 1000)

$\frac{tU_\infty}{\delta^*} = 35.7$

> 54 <
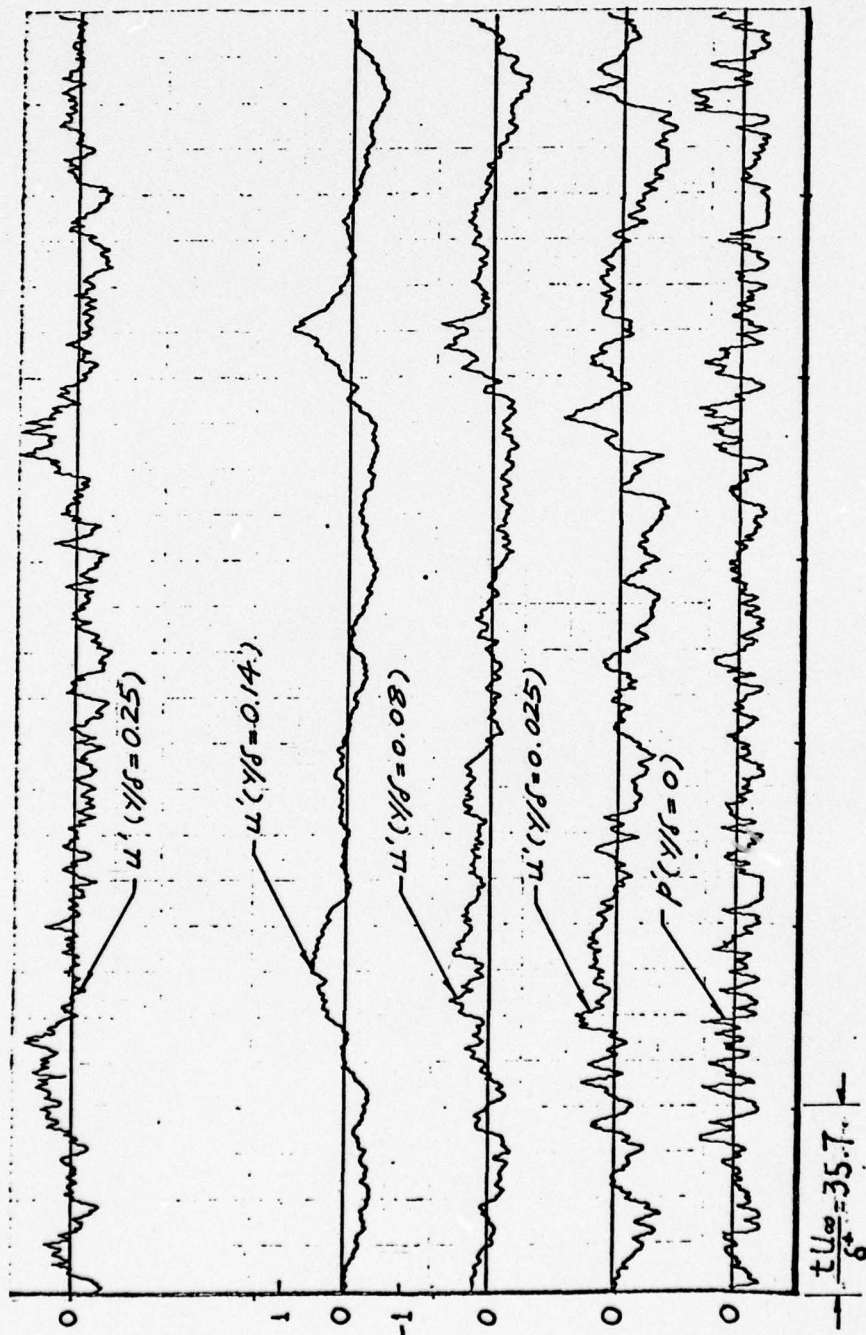
Fig. 18e Plot of Digitized Velocity and Wall Pressure Fluctuations (4700 < $\frac{tU_\infty}{\delta^*}$ < 4950)
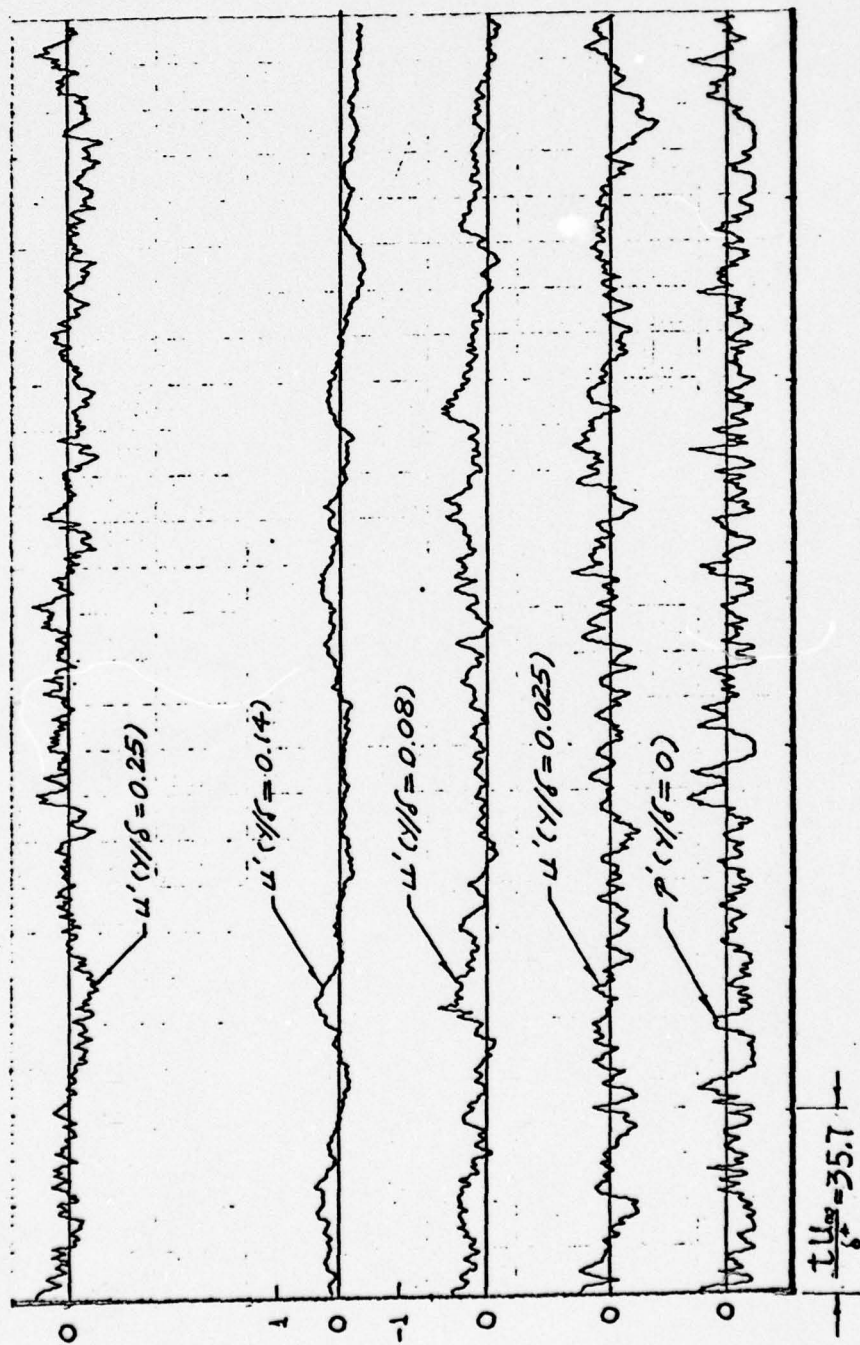
Fig. 18f Plot of Digitized Velocity and Wall Pressure Fluctuations ($4950 < \frac{tU_\infty}{\delta^*} < 5200$)

56
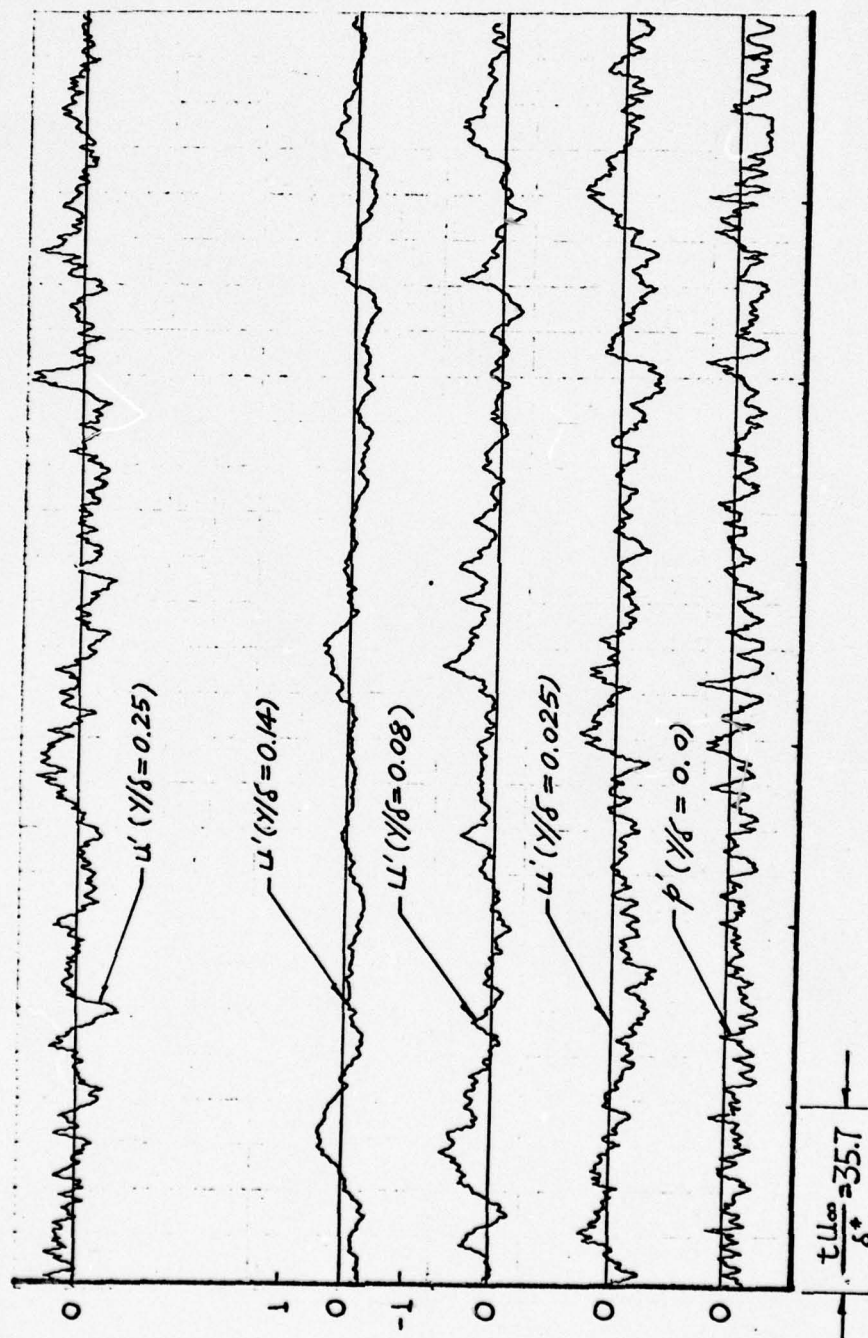
Fig. 18g Plot of Digitized Velocity and Wall Pressure Fluctuations (5200 < $\frac{tU_\infty}{\delta^*}$ < 5450)

$\frac{tU_\infty}{\delta^*}$ ≈ 35.7

57<

$u' \, (Y/\delta = 0.25)$

$u' \, (Y/\delta = 0.14)$

$u' \, (Y/\delta = 0.08)$

$u' \, (Y/\delta = 0.035)$

$p' \, (Y/\delta = 0)$

$\dfrac{t \, U_\infty}{\delta^*} = 35.7$

$\dfrac{tU_\infty}{\delta^*}$
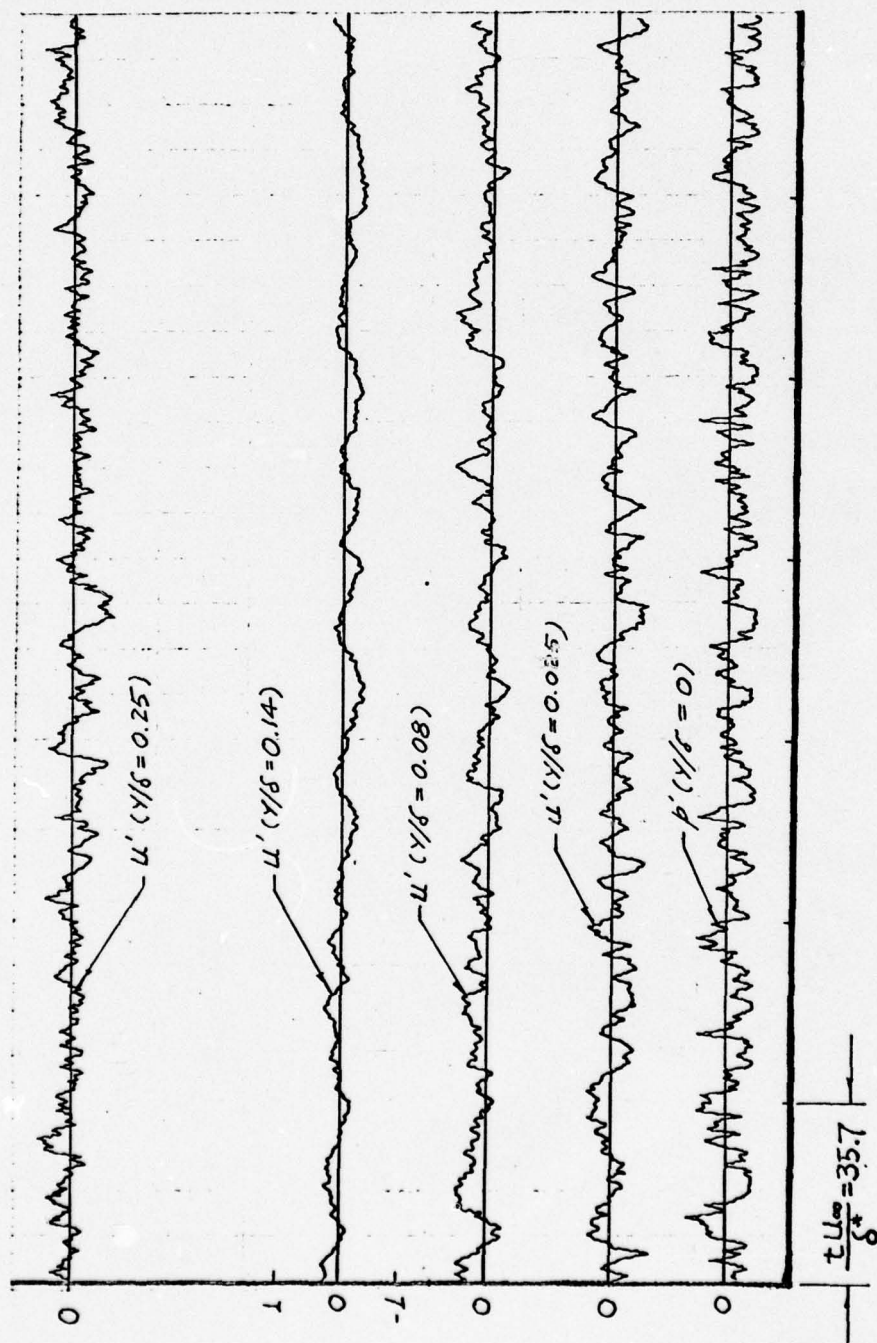
Fig. 18h Plot of Digitized Velocity and Wall Pressure Fluctuations ($5450 < \frac{tU_\infty}{\delta^*} < 5700$)
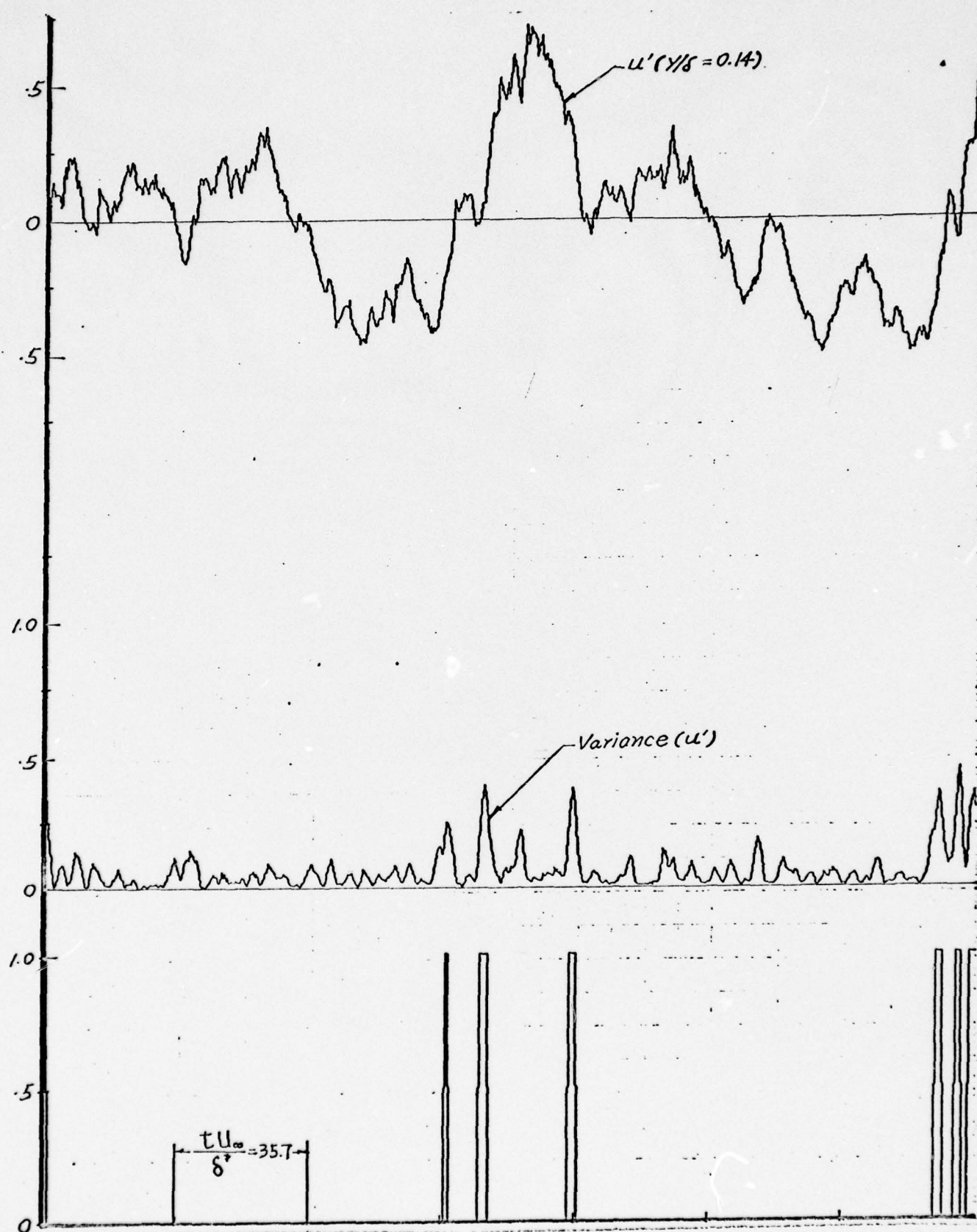
58<
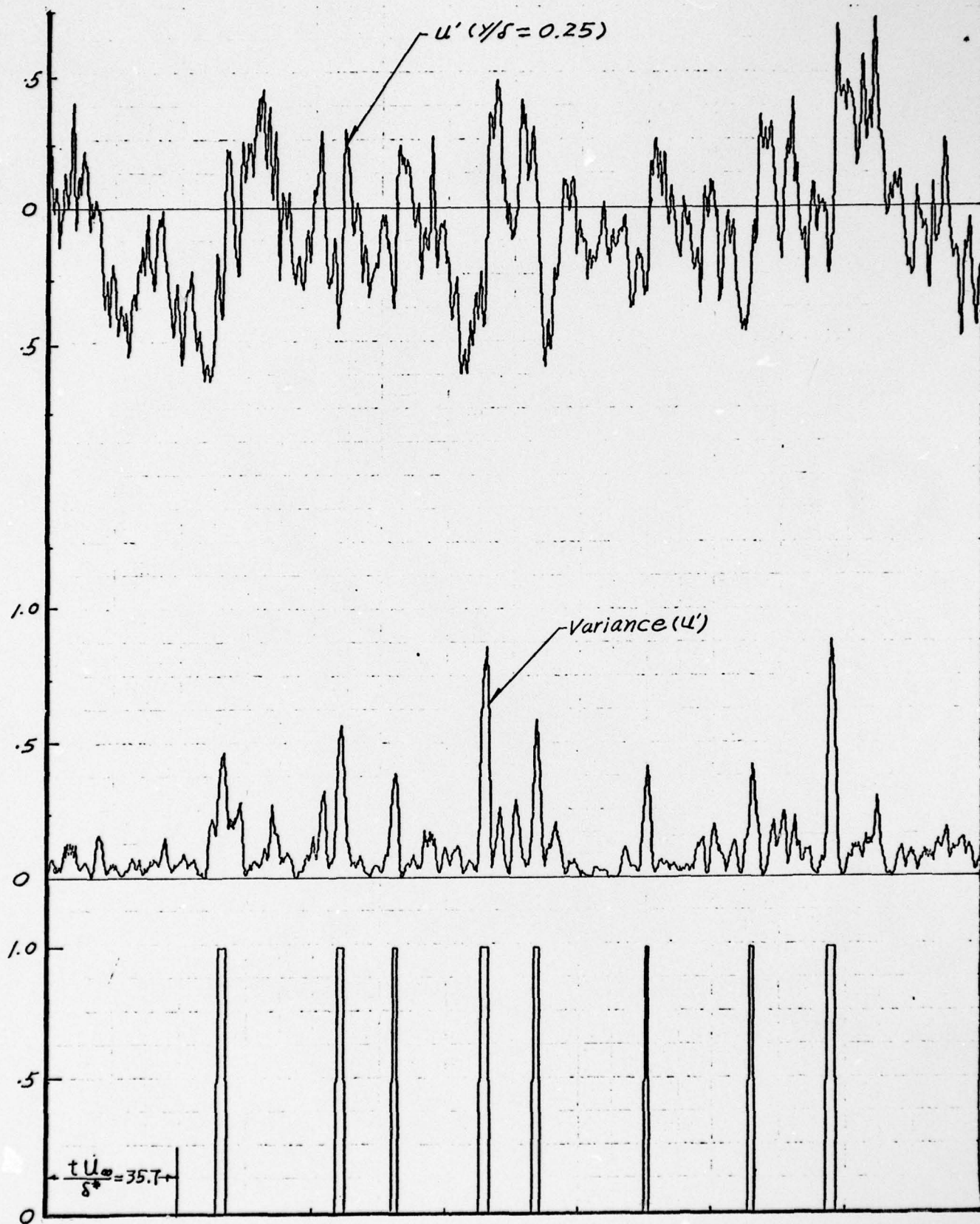
Fig. 19a Output of Digital Processing Scheme Showing the Fluctuating Velocity at $y/\delta = .25$, its VITA Variance and the Associated Detector Function $(5 < \frac{tU_\infty}{\delta^*} < 255)$
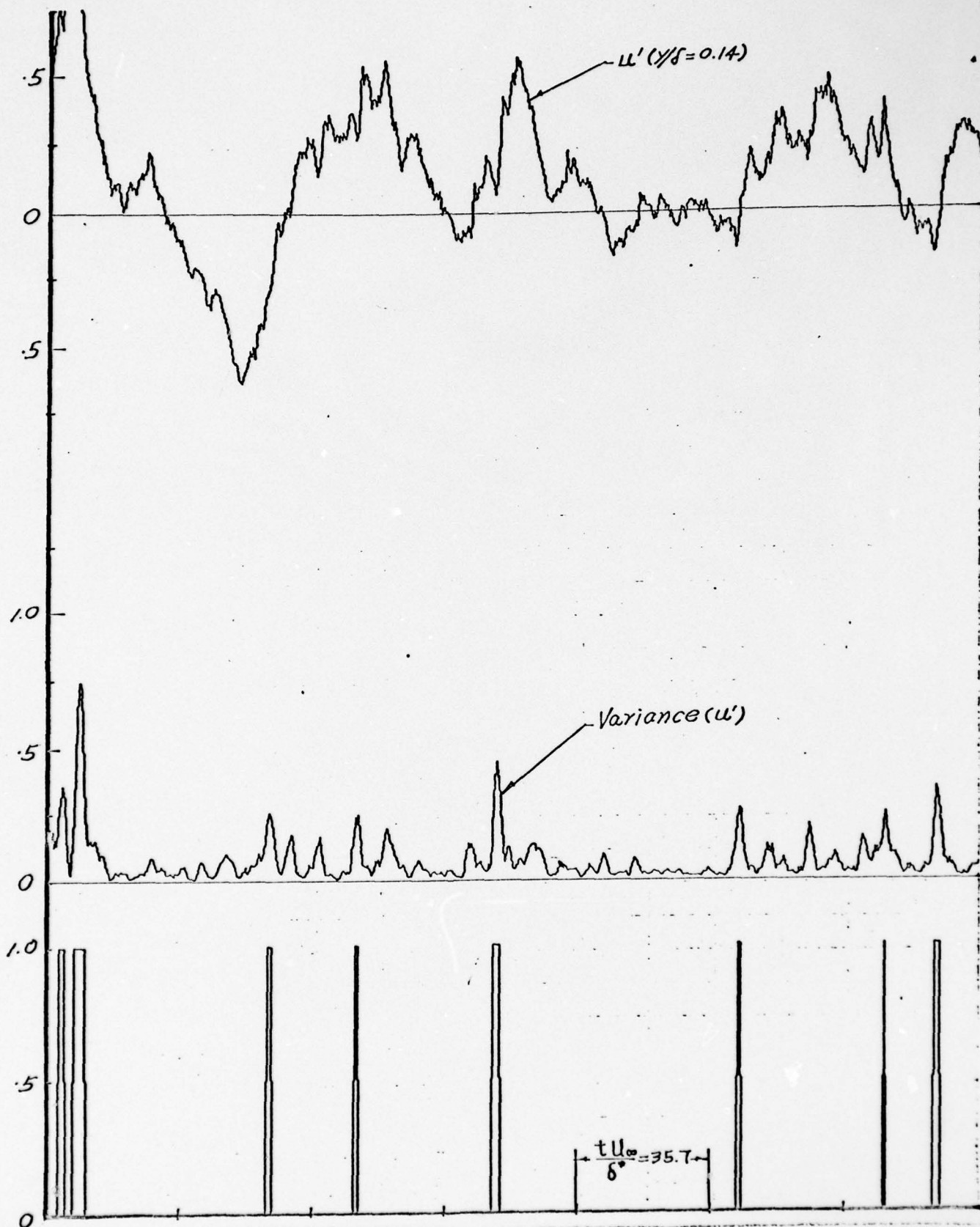
59<
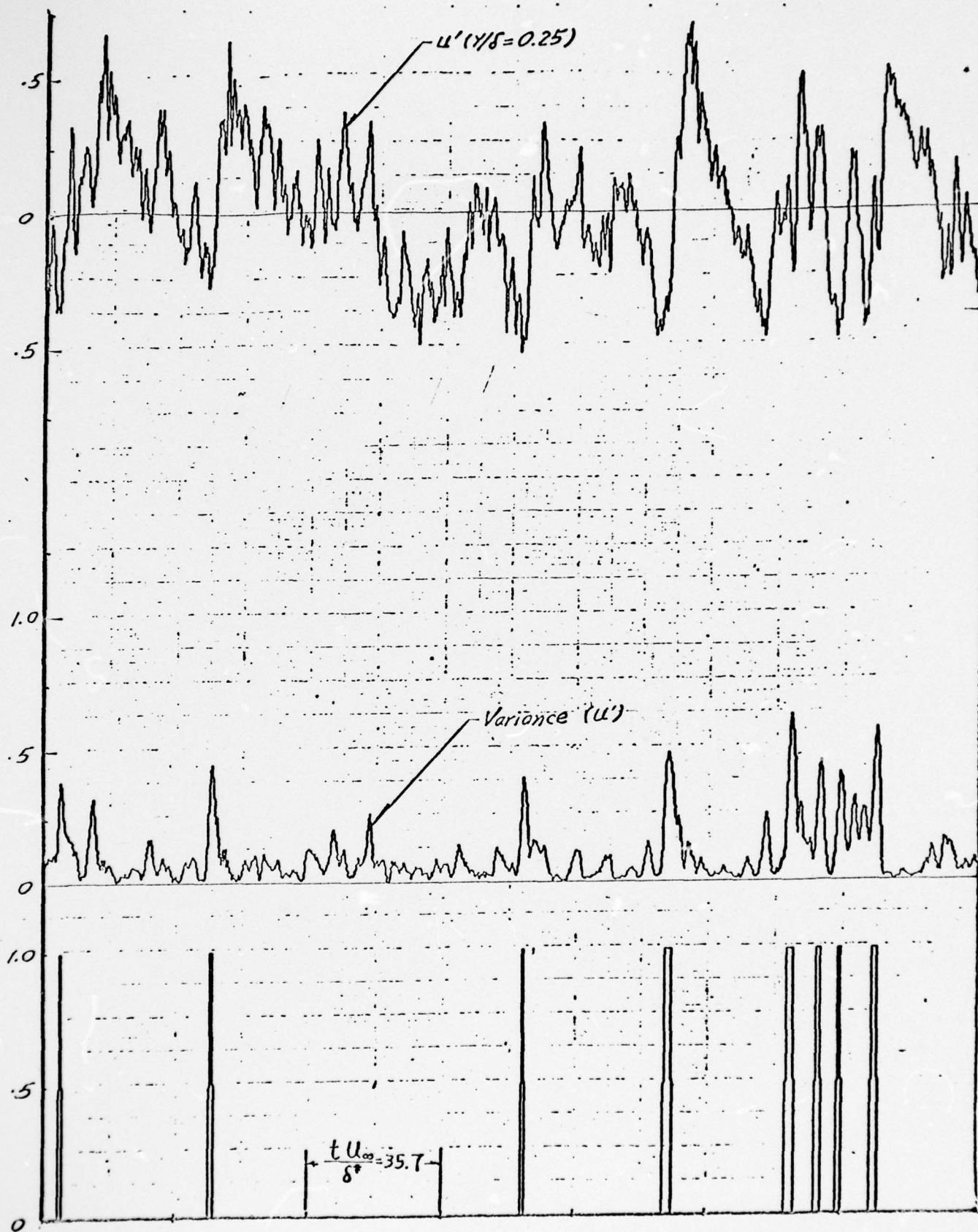
Fig. 19b Output of Digital Processing Scheme Showing the Fluctuating Velocity at y/δ = .25, its VITA Variance, and the Associated Detector Function $(255 < \frac{tU_\infty}{\delta^*} < 505)$

60<
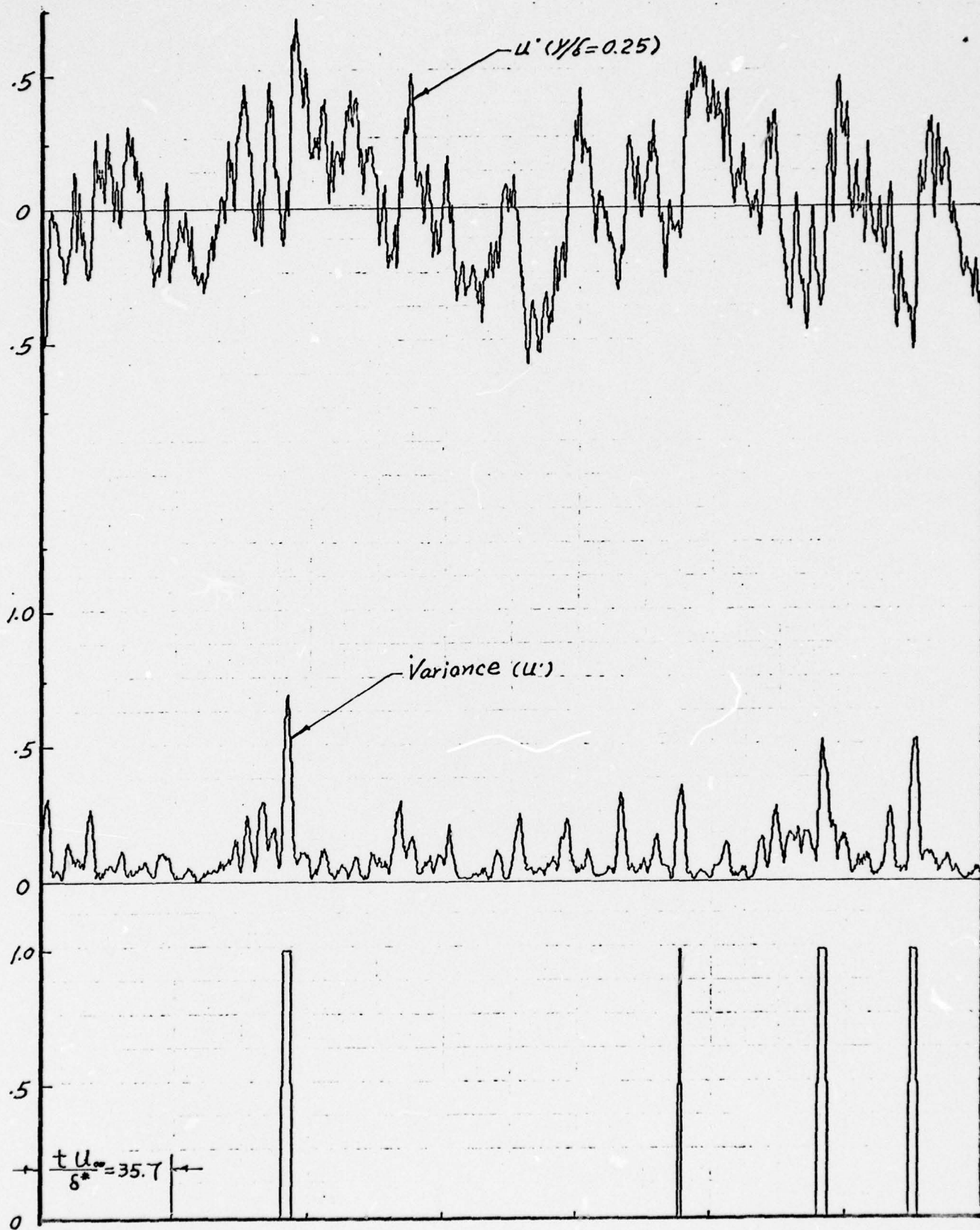
Fig. 19c Output of Digital Processing Scheme Showing the Fluctuating Velocity at
y/δ = .25, its VITA Variance, and the Associated Detector Function

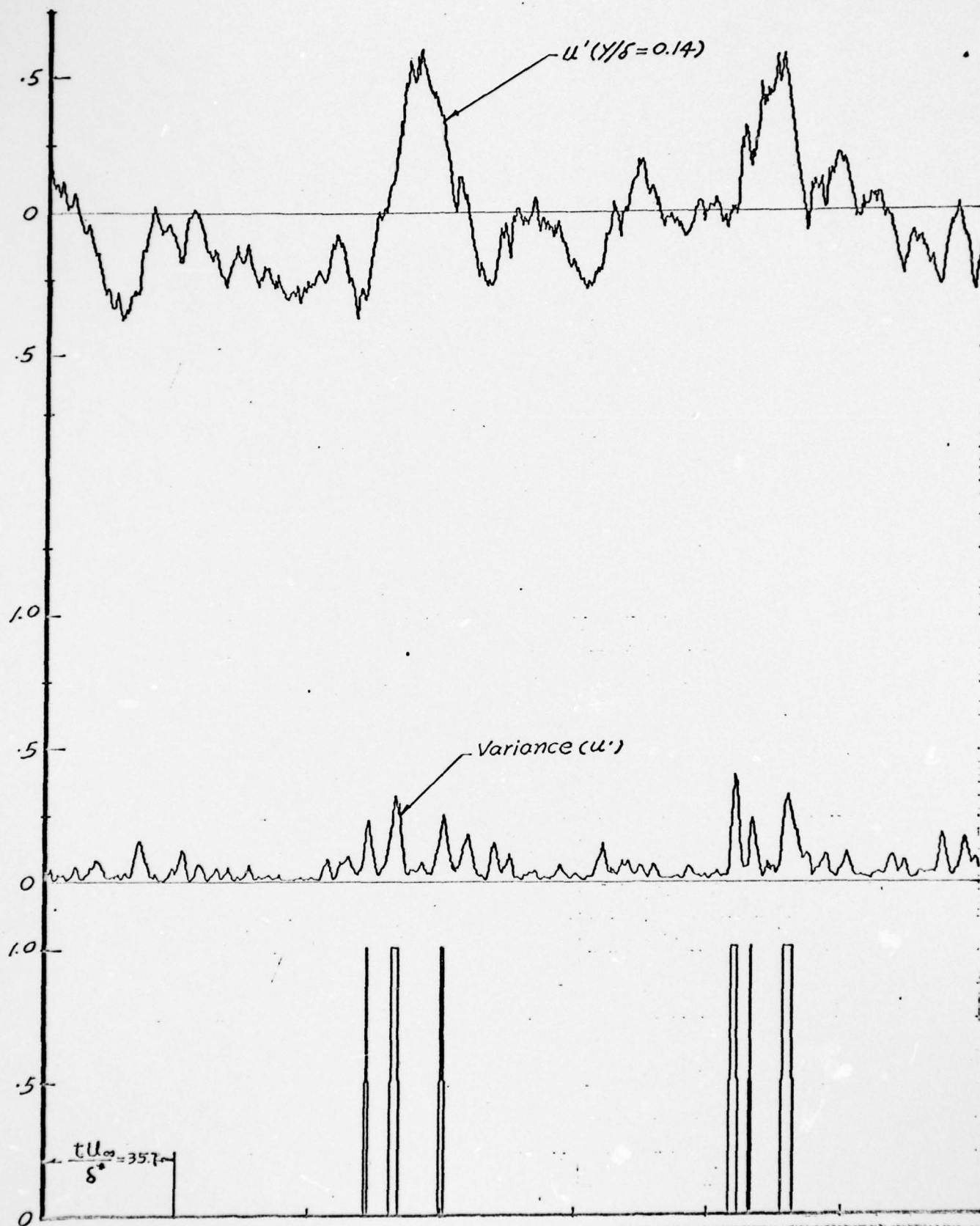$$\left(505 < \frac{tU_\infty}{\delta^*} < 755\right)$$

61<
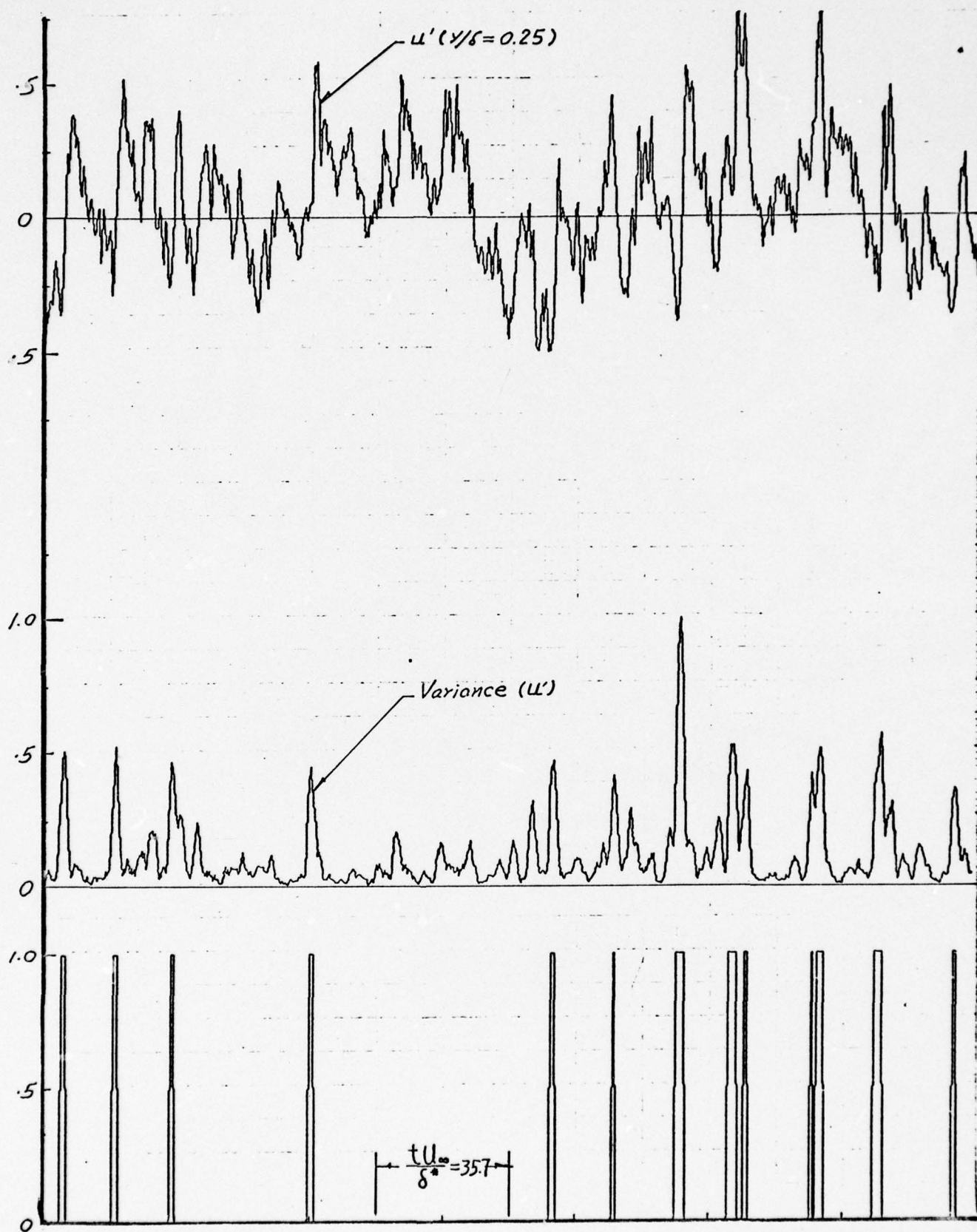
Fig. 19d Output of Digital Processing Scheme Showing the Fluctuating Velocity at
$y/\delta = .25$, its VITA Variance, and the Associated Detector Function
$(755 < \frac{tU_\infty}{\delta^*} < 1005)$

62<
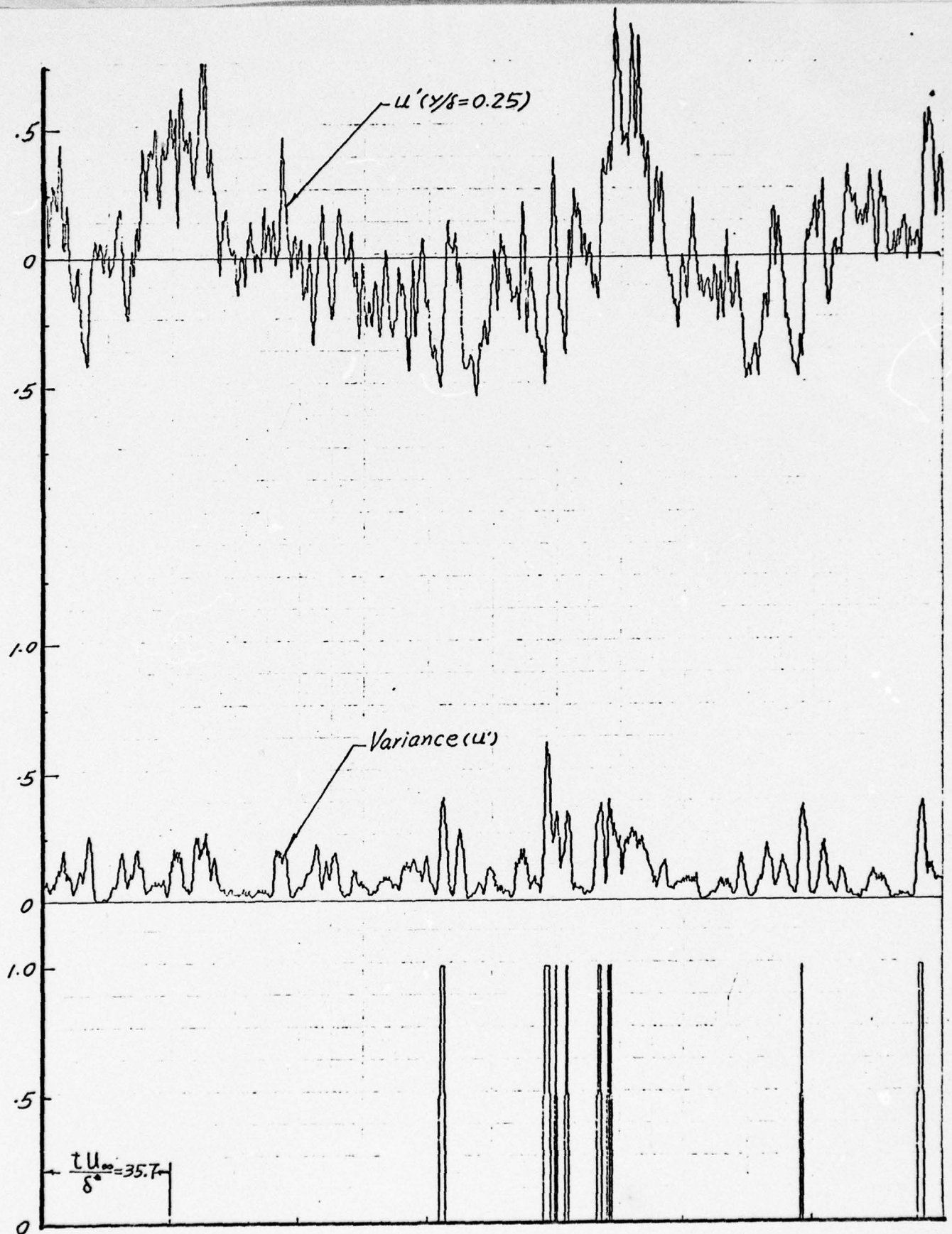
Fig. 19e Output of Digital Processing Scheme Showing the Fluctuating Velocity at
y/δ = .25, its VITA Variance, and the Associated Detector Function
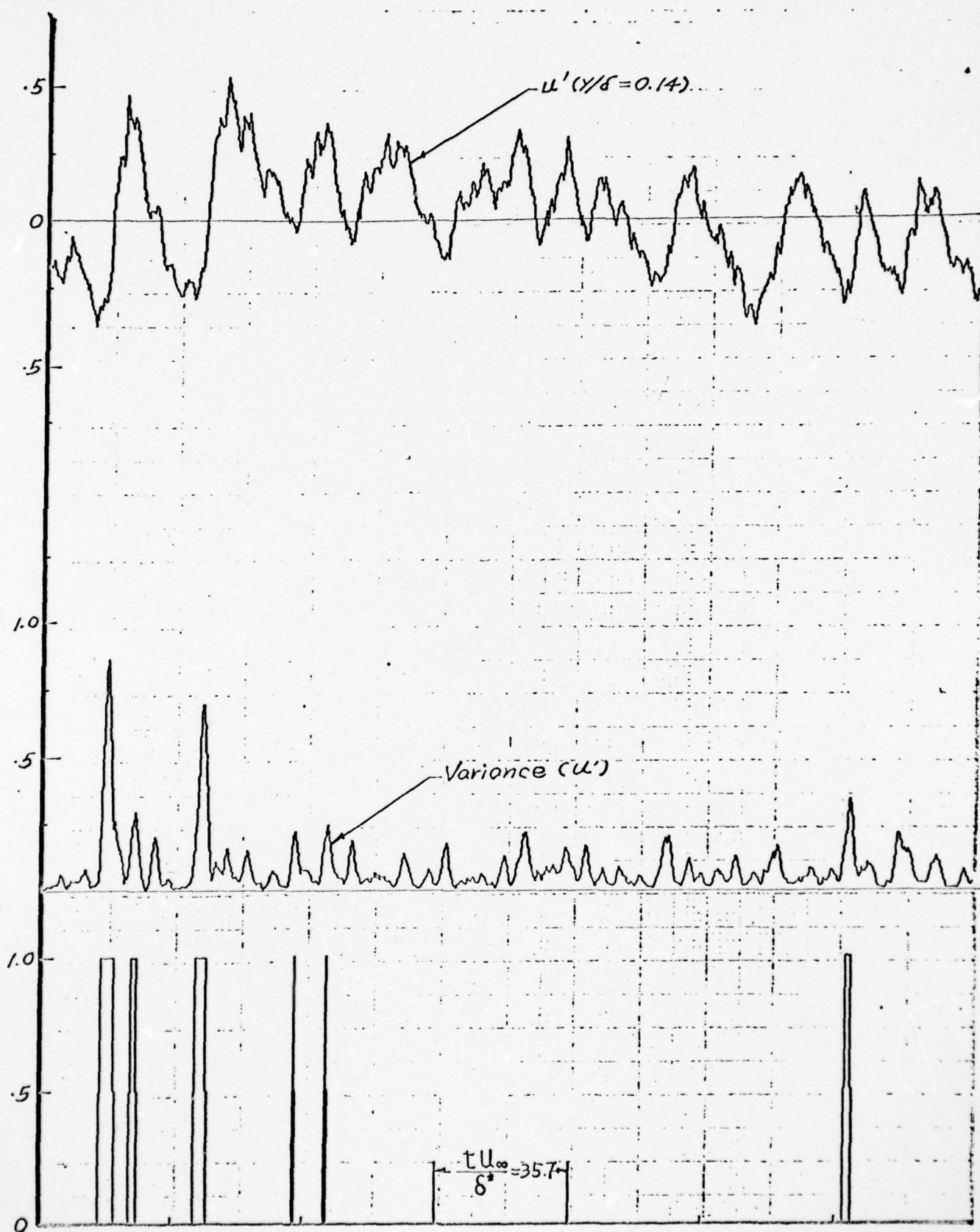$(4705 < \frac{tU_\infty}{\delta^*} < 4955)$
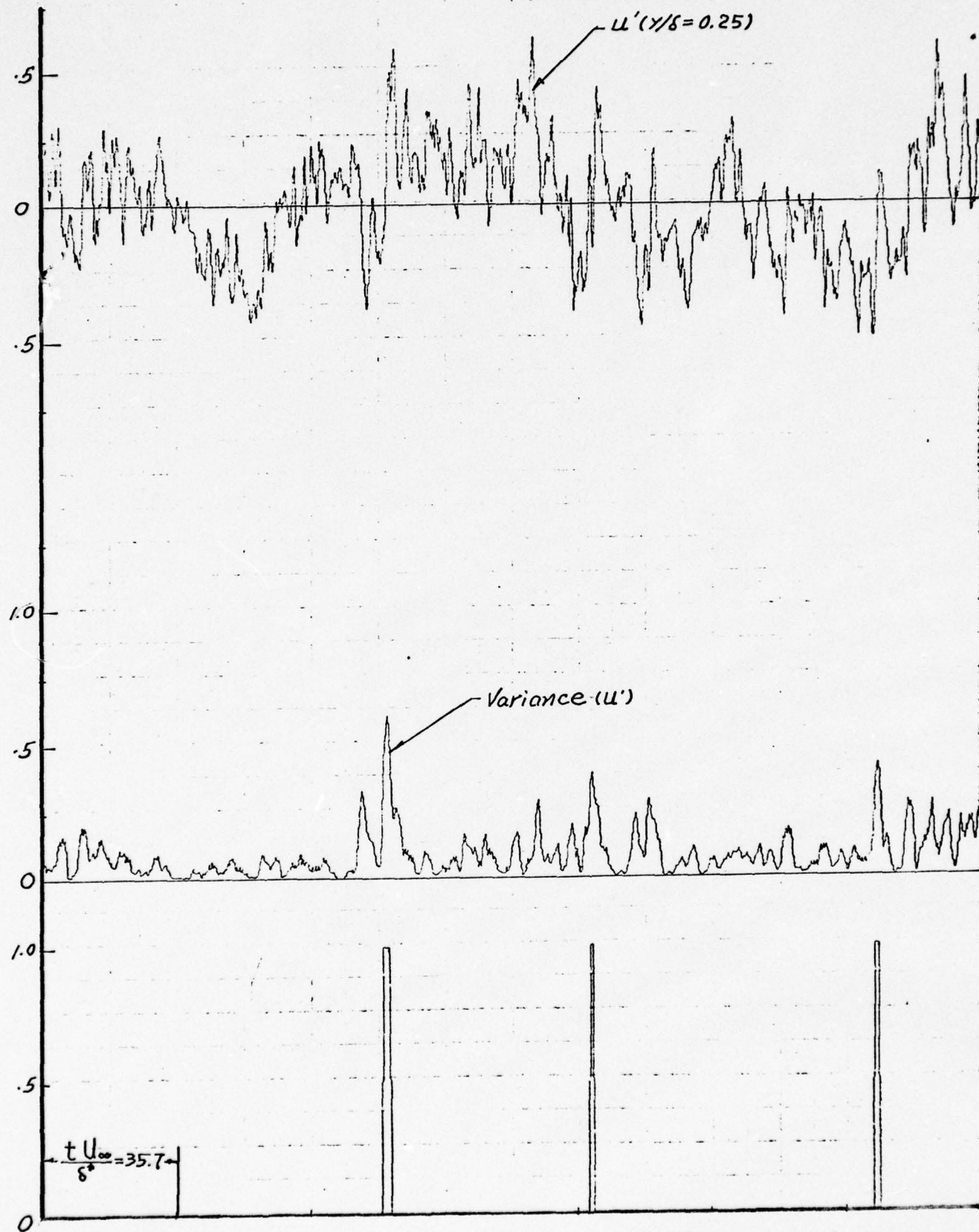
Fig. 19f Output of Digital Processing Scheme Showing the Fluctuating Velocity at
$y/\delta = .25$, its VITA Variance, and the Associated Detector Function
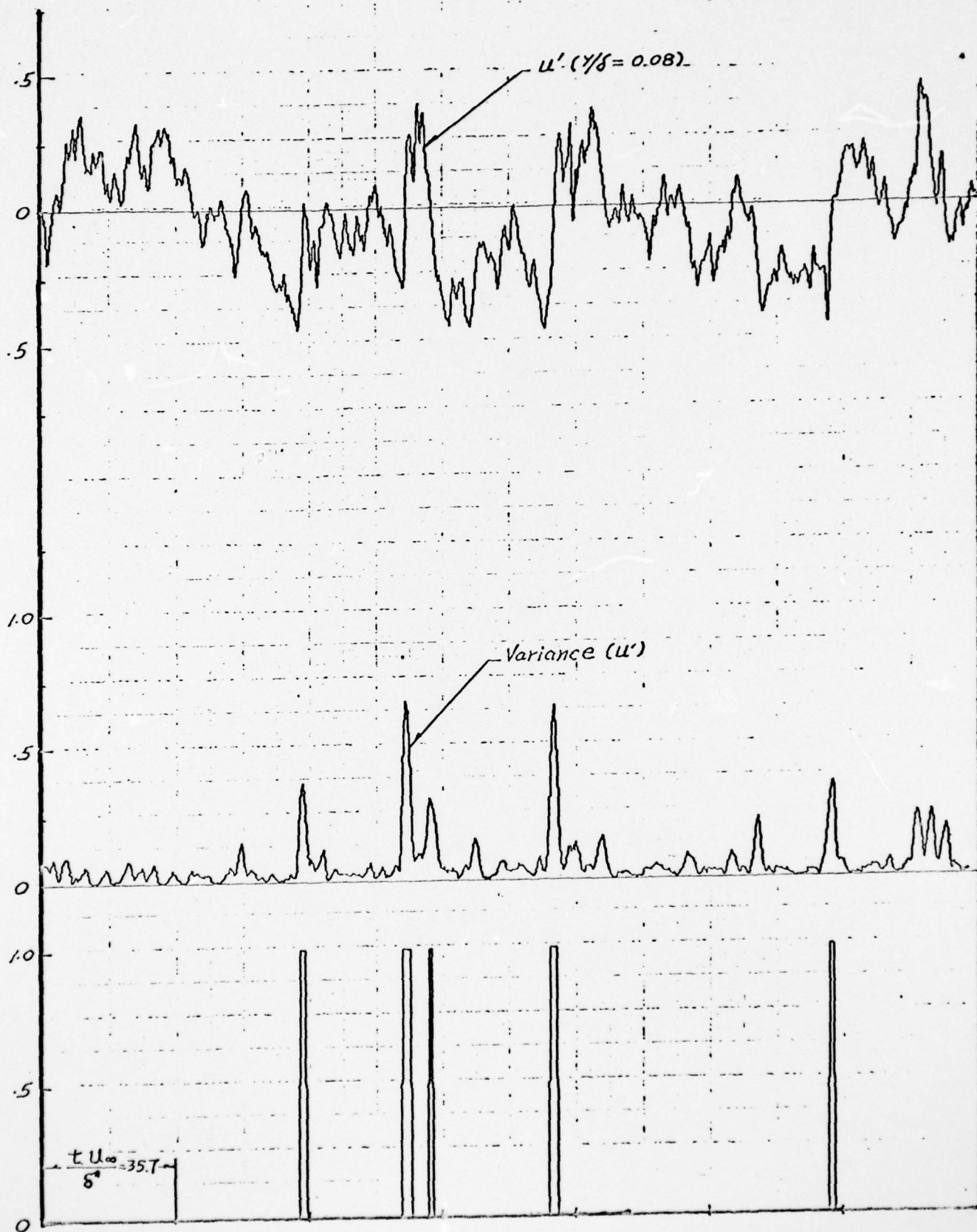$(4955 < \frac{tU_\infty}{\delta^*} < 5205)$

64<
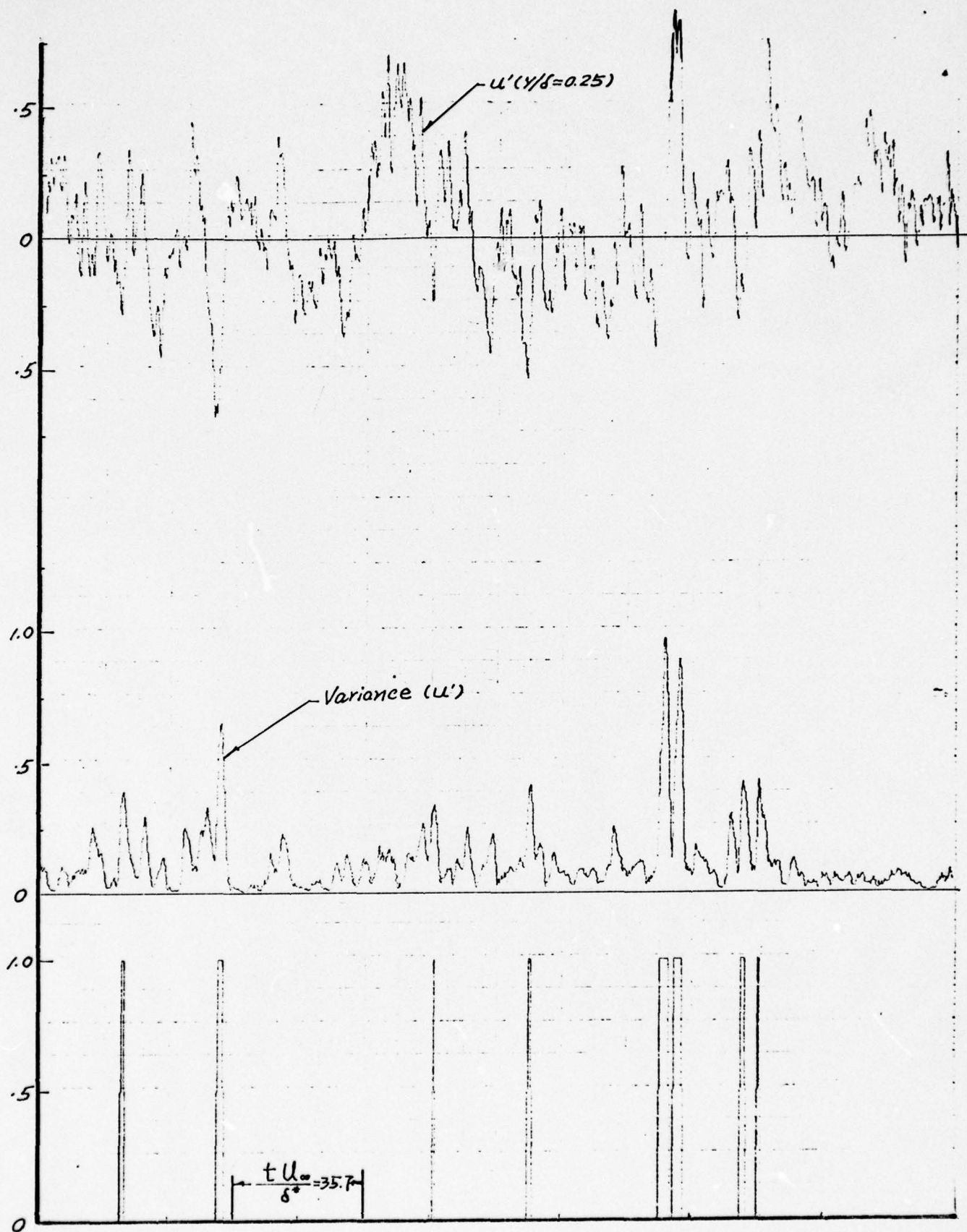
Fig. 19g Output of Digital Processing Scheme Showing the Fluctuating Velocity at $y/\delta = .25$, its VITA Variance, and the Associated Detector Function

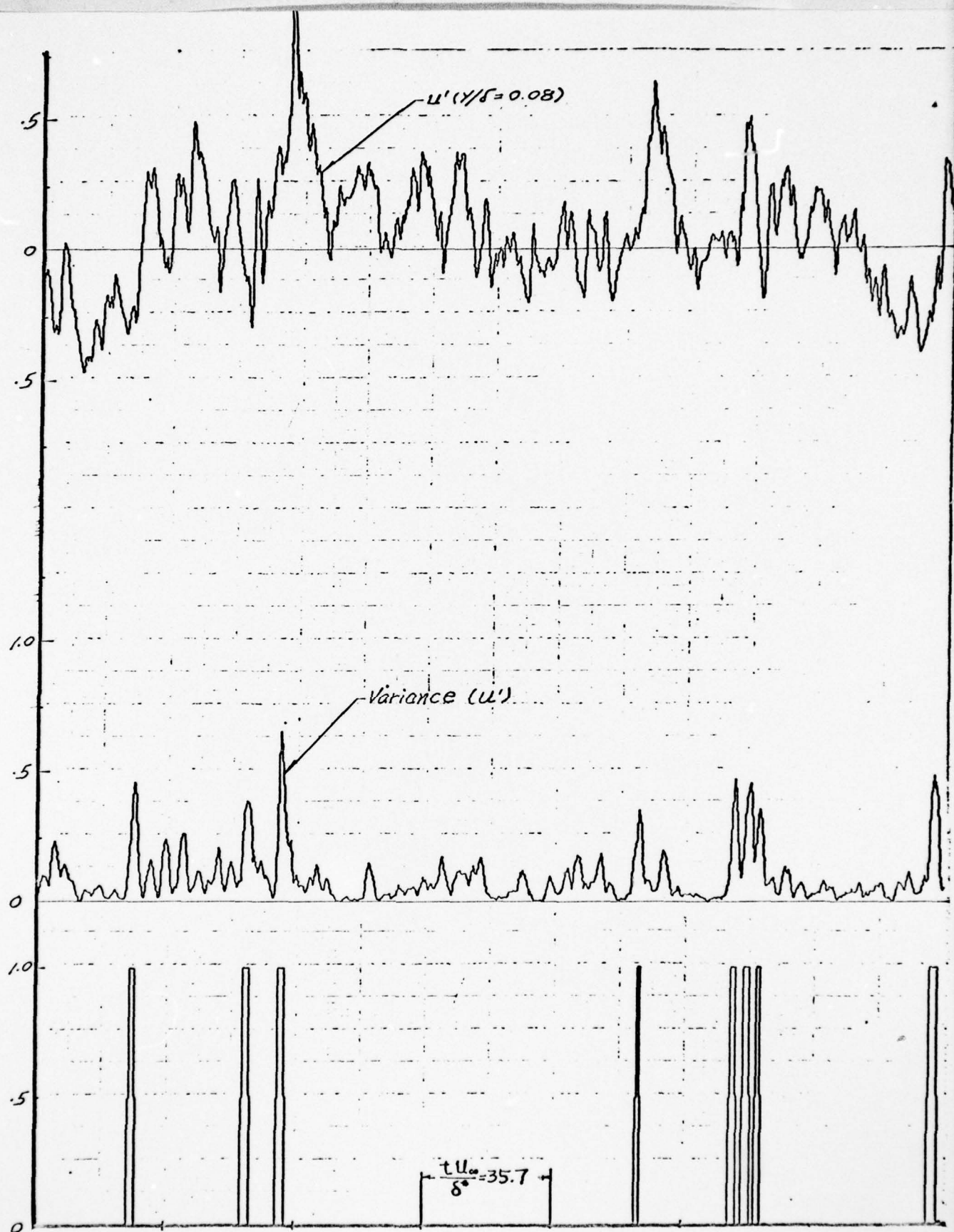$$(5205 < \frac{t U_\infty}{\delta^*} < 5455)$$
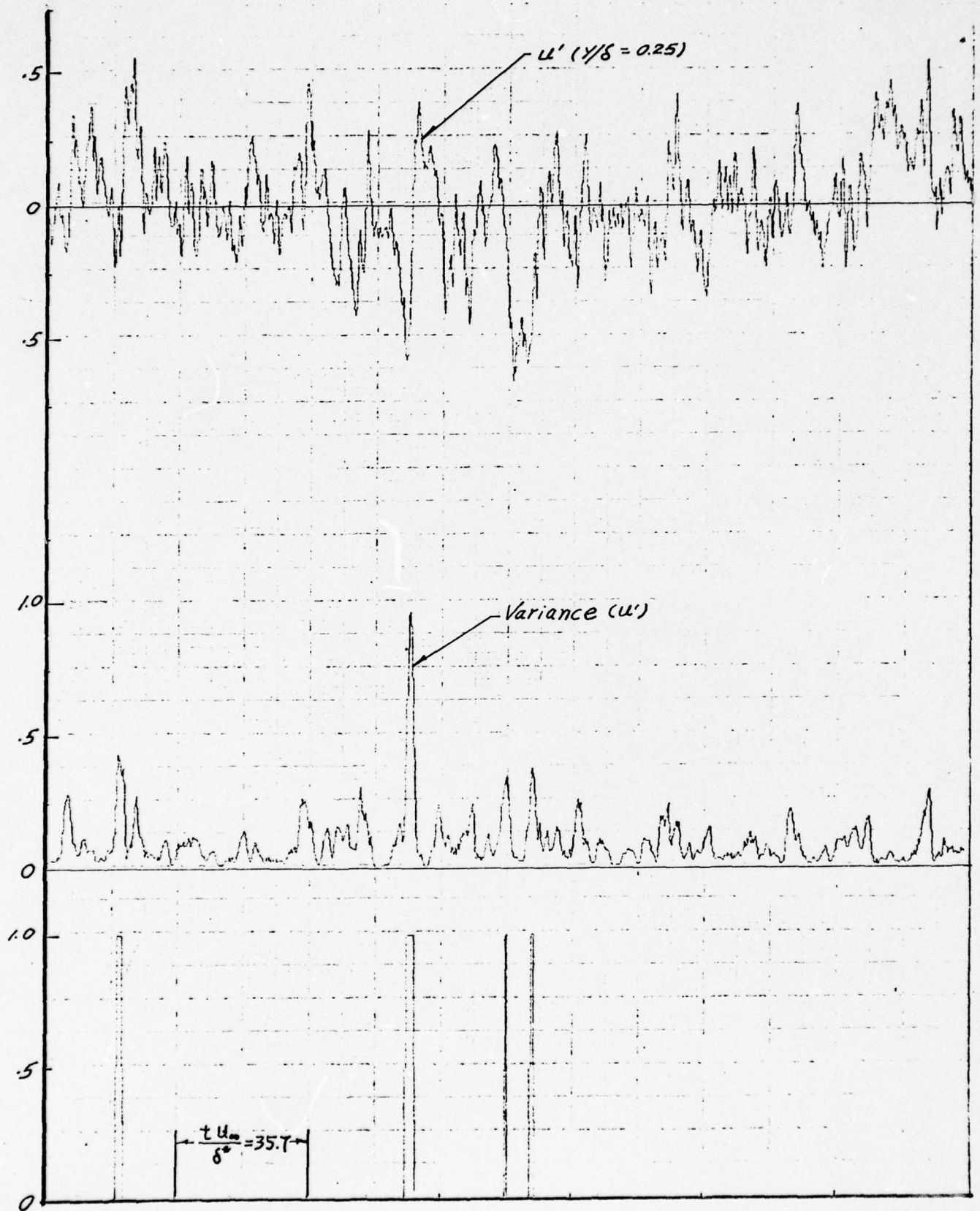
Fig. 19h Output of Digital Processing Scheme Showing the Fluctuating Velocity at $y/\delta = .25$, its VITA Variance, and the Associated Detector Function $(5455 < \frac{t\dot{U}_\infty}{\delta^*} < 5705)$

Fig. 19h Output of Digital Processing Scheme Showing the Fluctuating Velocity at
$y/\delta = .25$, its VITA Variance, and the Associated Detector Function
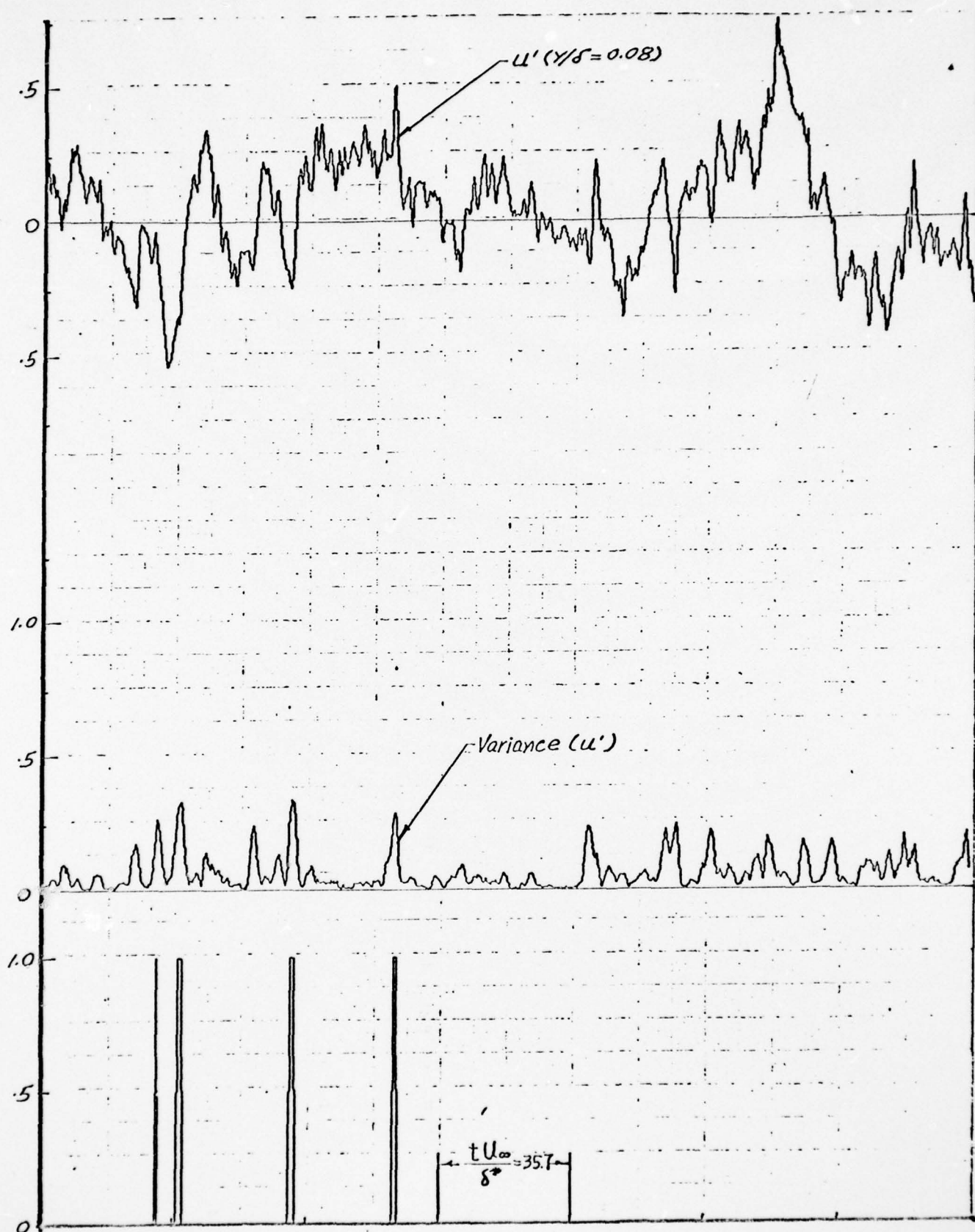$$(5455 < \frac{tU_\infty}{\delta^*} < 5705)$$

66<
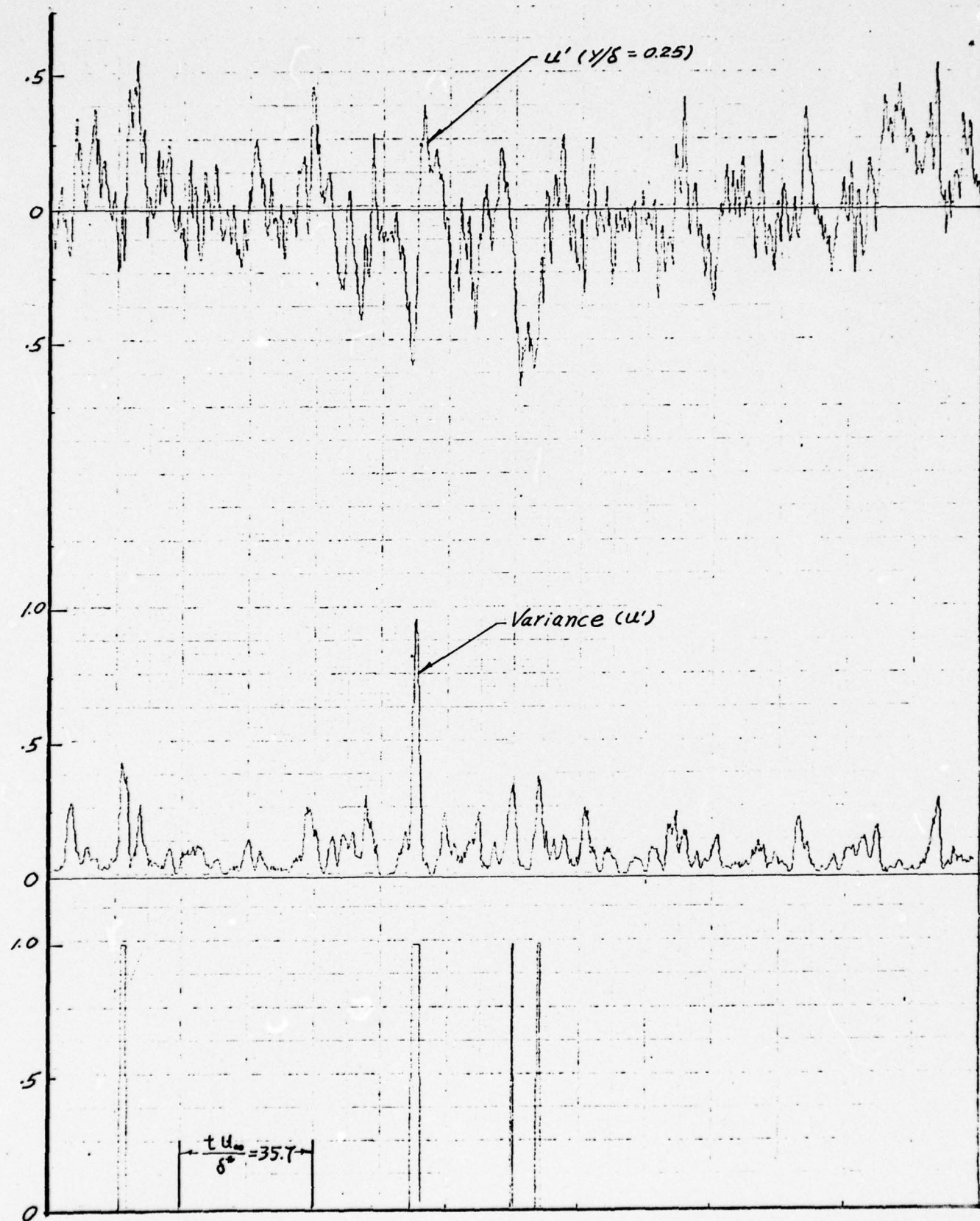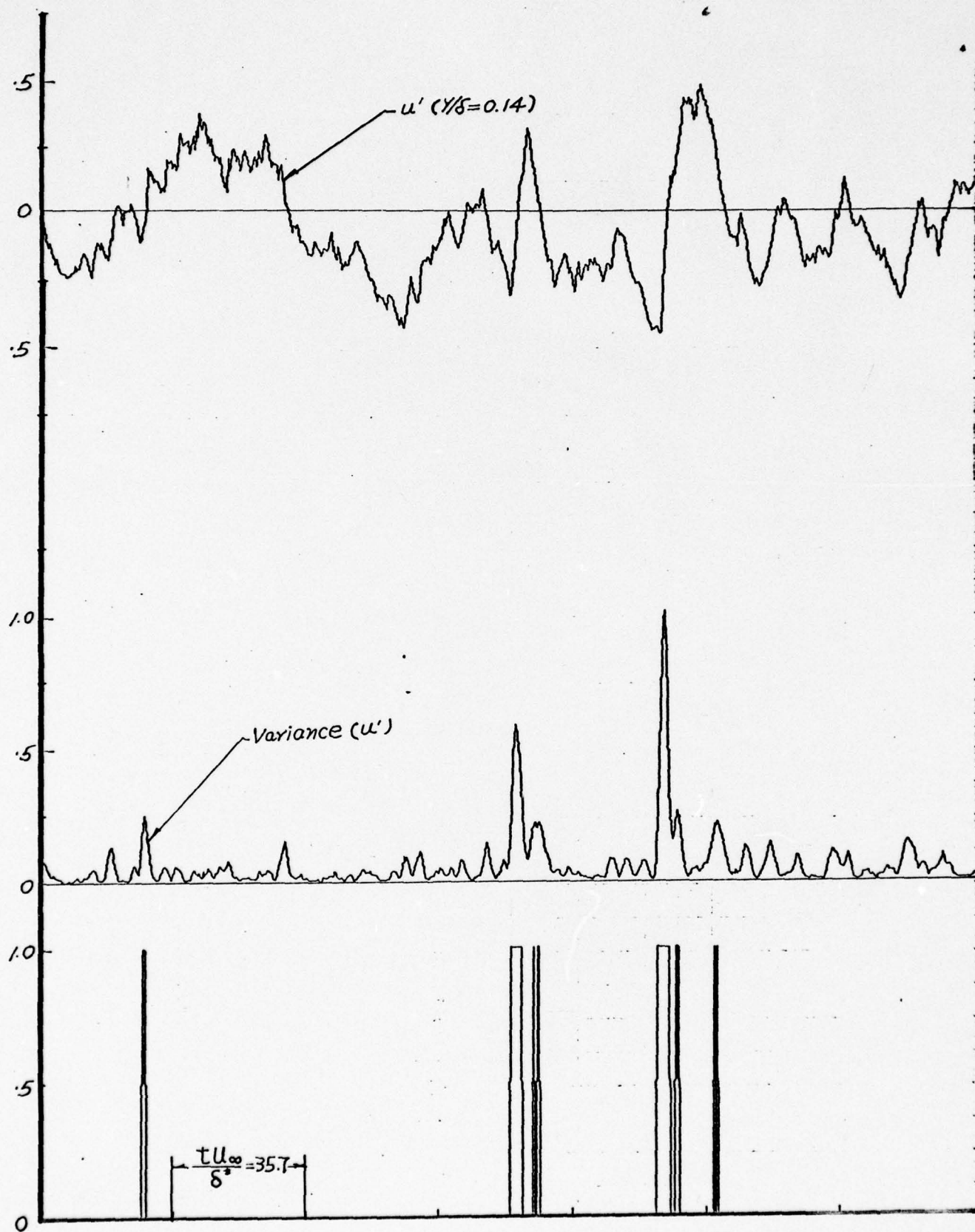
Fig. 20a Output of Digital Processing Scheme Showing the Fluctuating Velocity at $y/\delta = .14$, its VITA Variance, and the Associated Detector Function $(5 < \frac{t U_\infty}{\delta^*} < 255)$
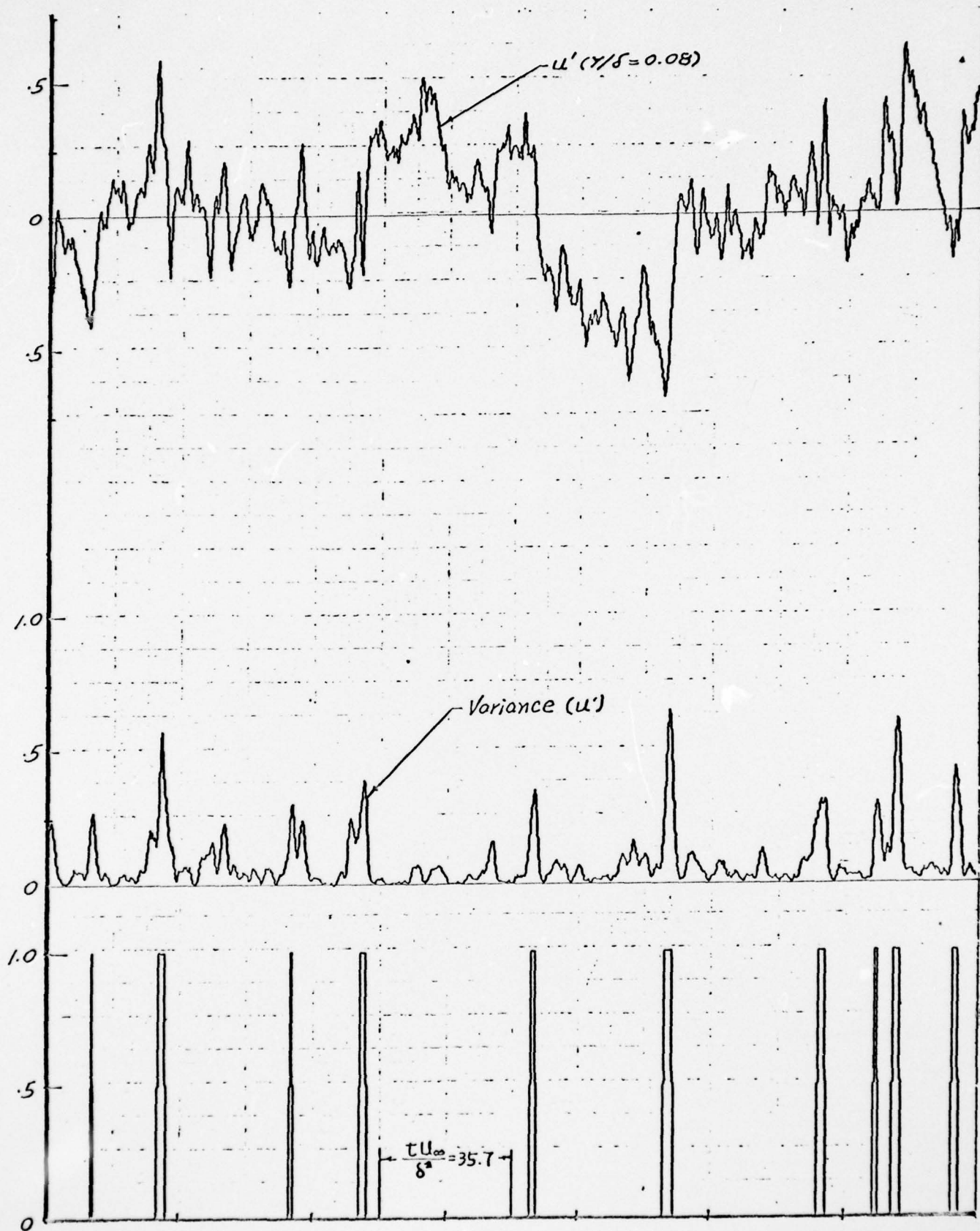
67<
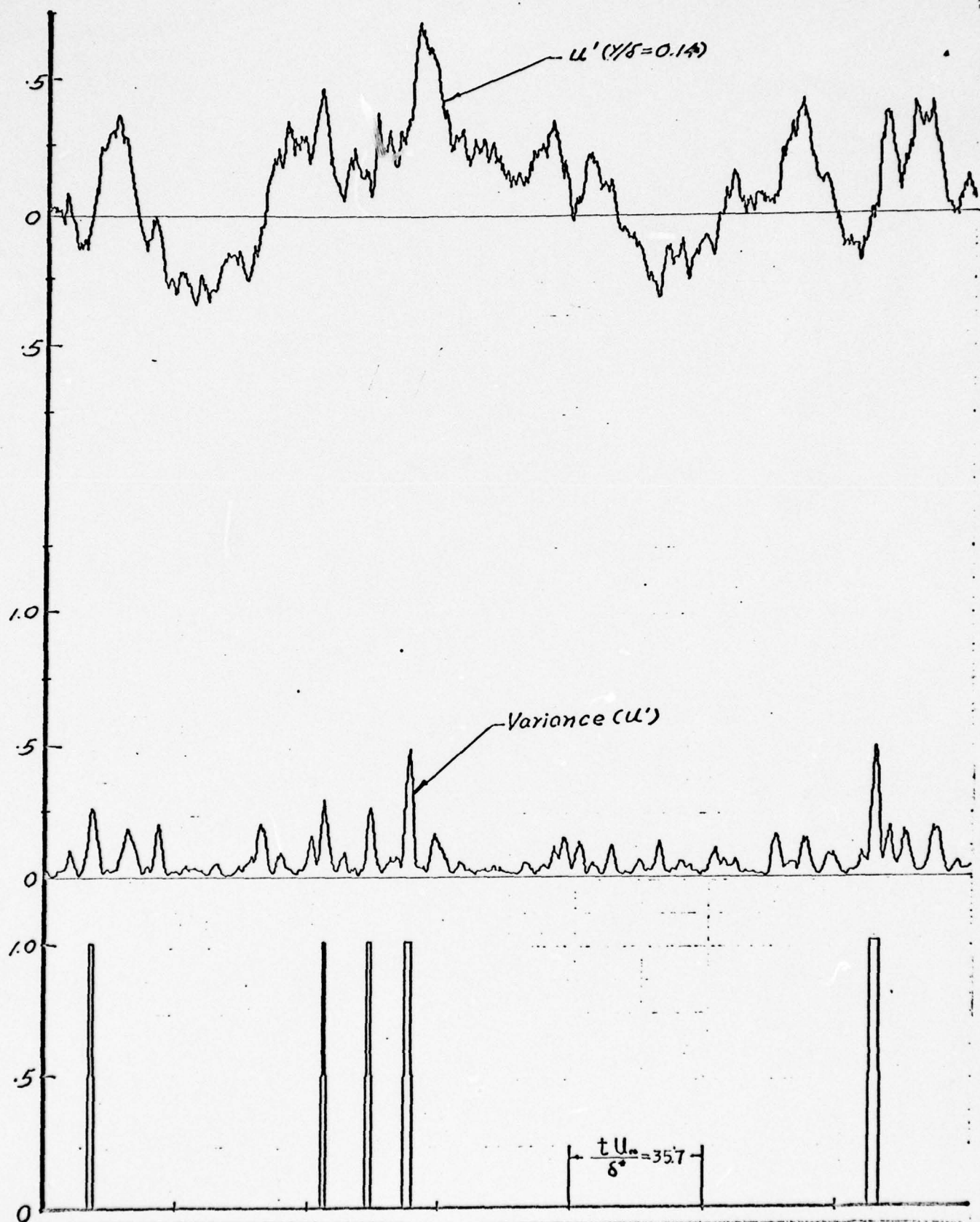
Fig. 20b Output of Digital Processing Scheme Showing the Fluctuating Velocity at
$y/\delta = .14$, its VITA Variance, and the Associated Detector Function
$(255 < \frac{tU_\infty}{\delta^*} < 505)$

68<
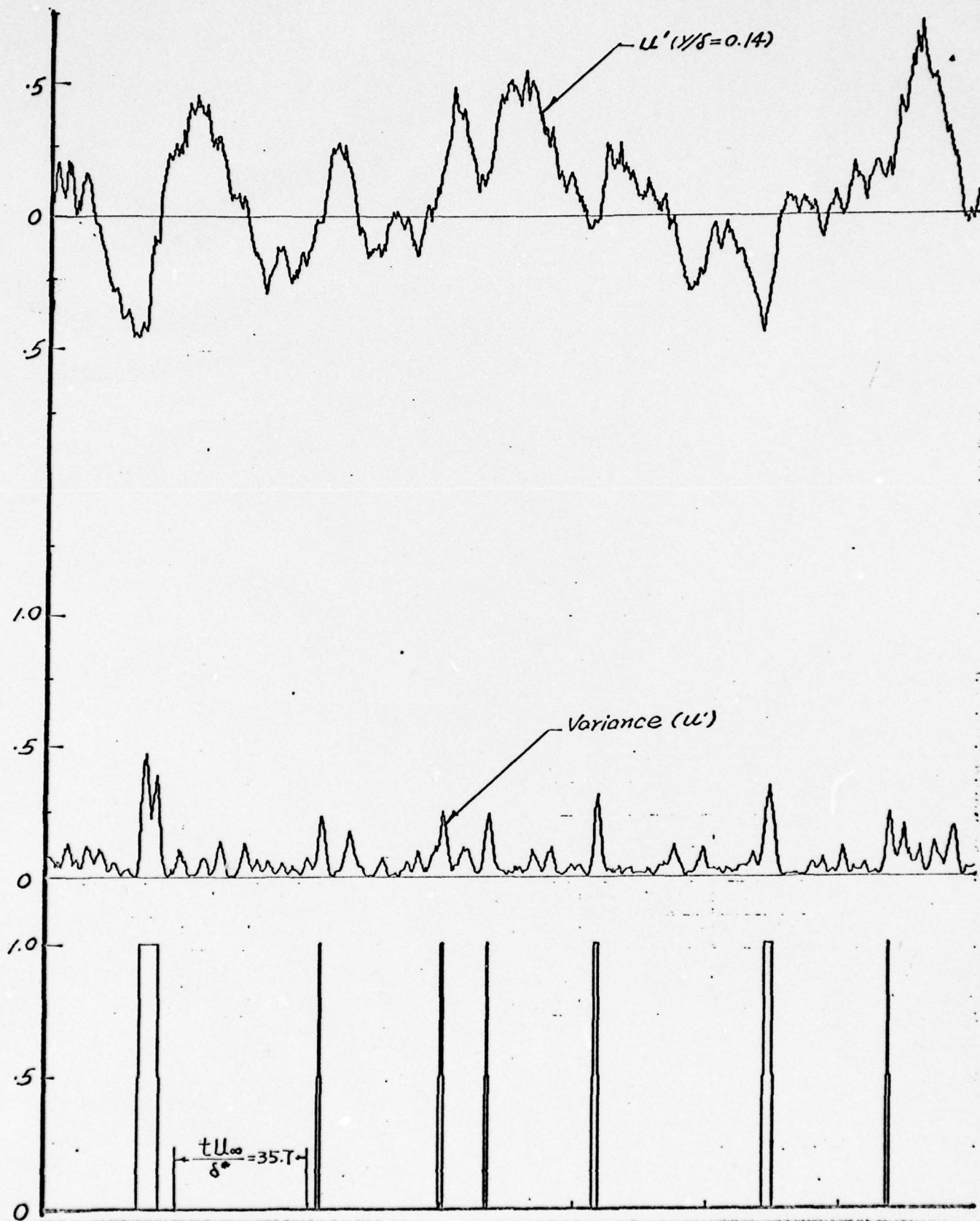
Fig. 20c Output of Digital Processing Scheme Showing the Fluctuating Velocity at $y/\delta = .14$, its VITA Variance, and the Associated Detector Function $(505 < \frac{tU_\infty}{\delta^*} < 755)$
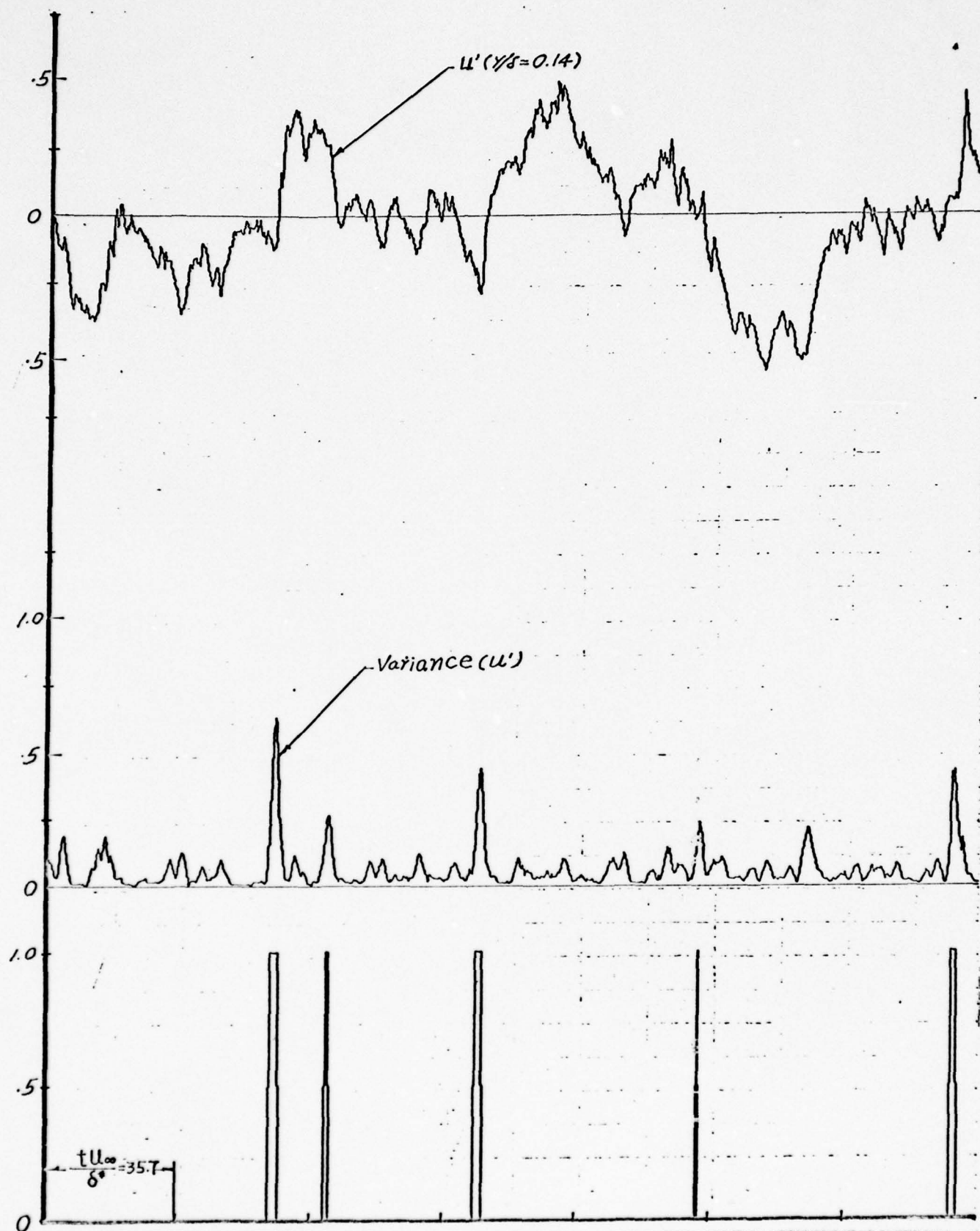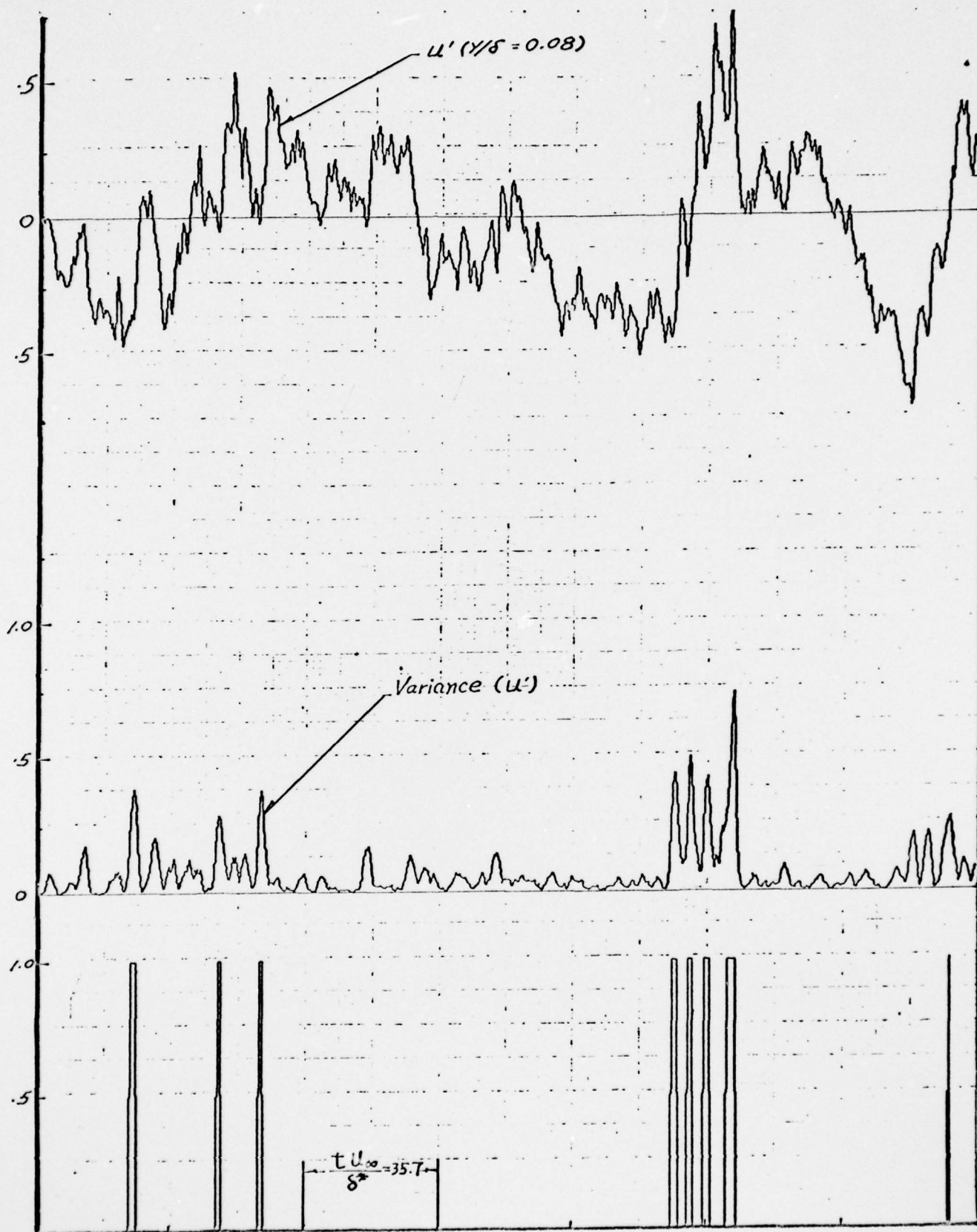
Fig. 20ᵈ Output of Digital Processing Scheme Showing the Fluctuating Velocity at
y/δ = .14, its VITA Variance, and the Associated Detector Function
$(755 < \frac{tU_\infty}{\delta^*} < 1005)$

70<

Fig. 20e Output of Digital Processing Scheme Showing the Fluctuating Velocity at
y/δ = .14, its VITA Variance, and the Associated Detector Function

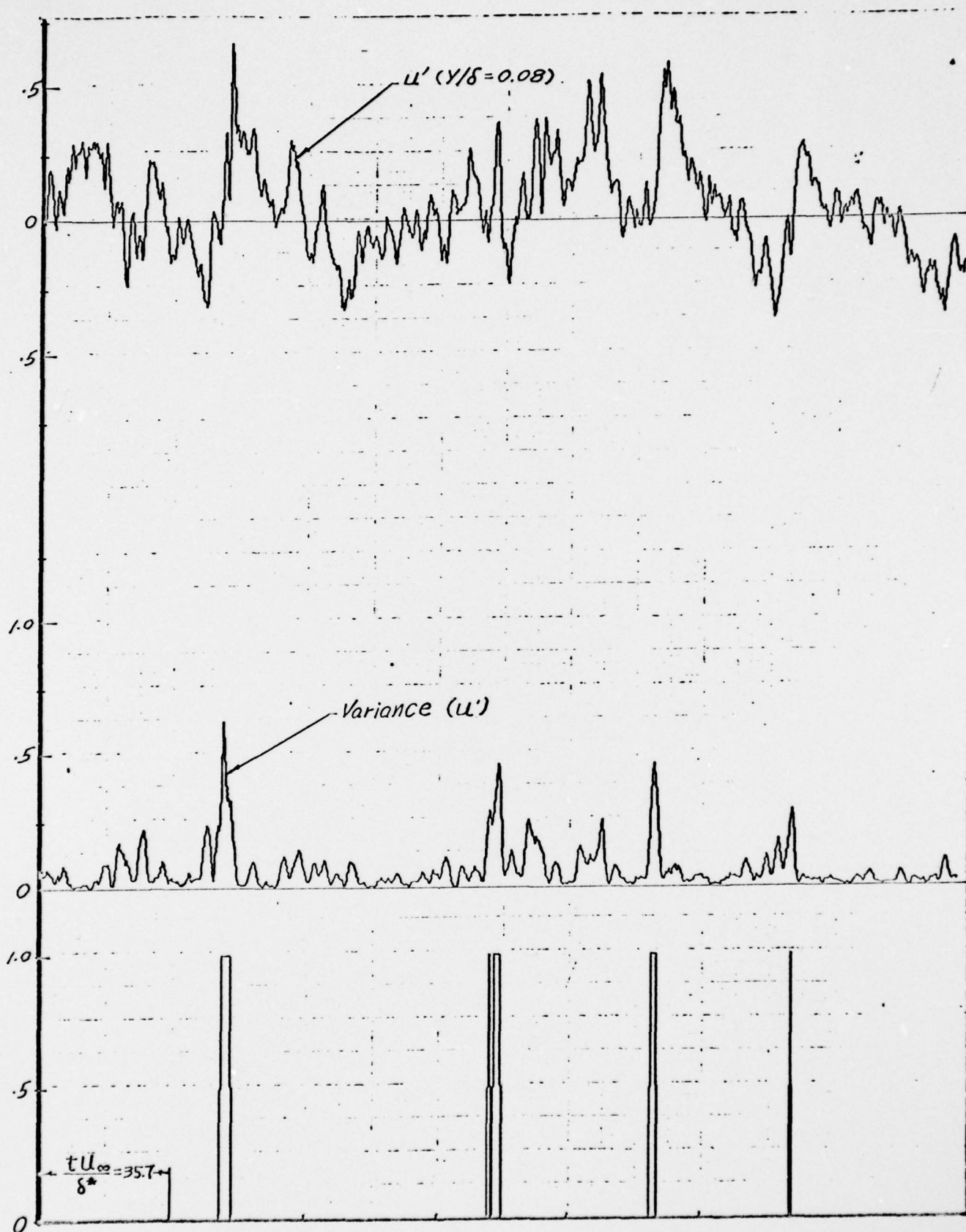$$\left(4705 < \frac{tU_\infty}{\delta^*} < 4955\right)$$

71<

Fig. 20 f Output of Digital Processing Scheme Showing the Fluctuating Velocity at $y/\delta = .14$, its VITA Variance, and the Associated Detector Function

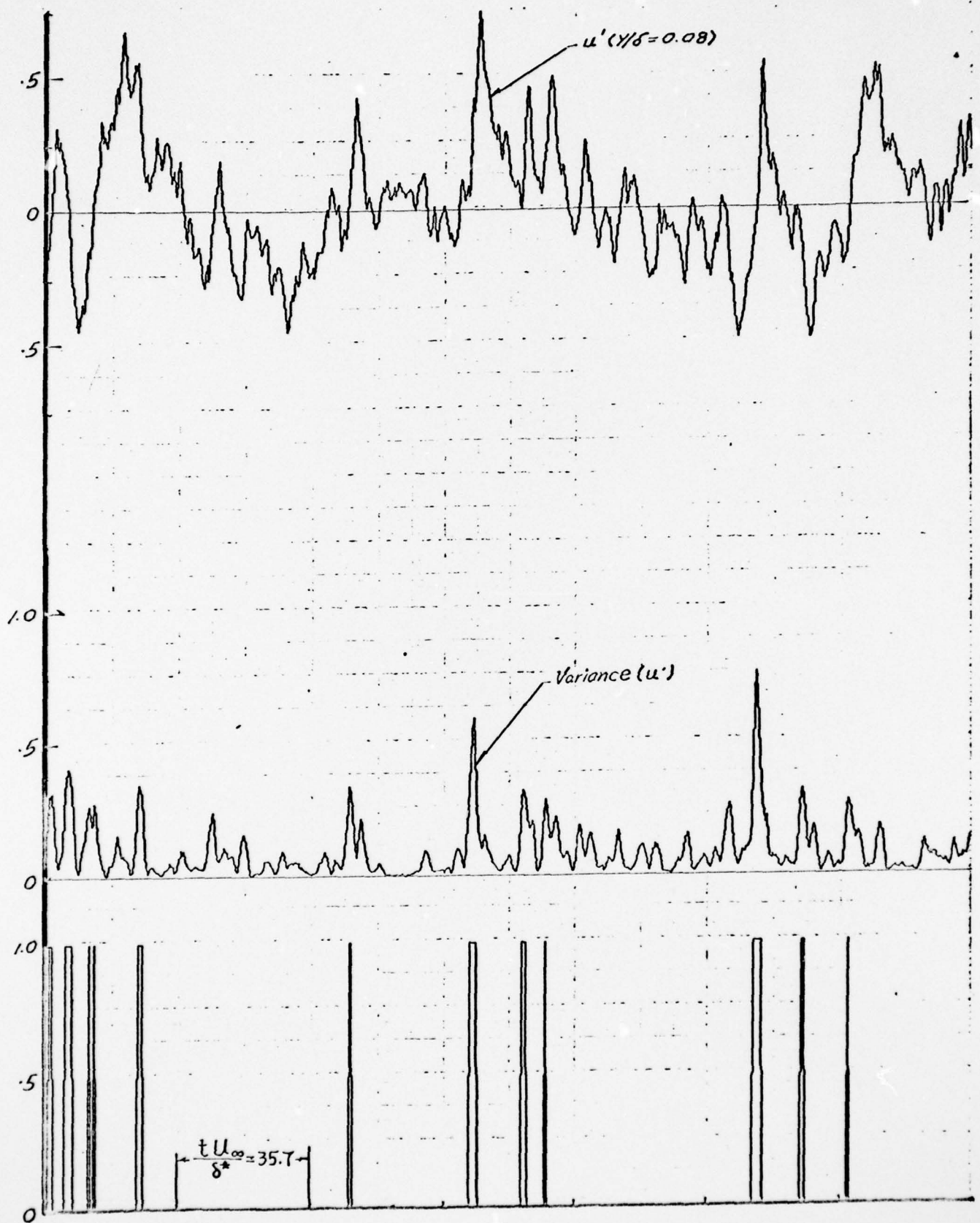$$(4955 < \frac{tU_\infty}{\delta^*} < 5205)$$

72<

Fig. 20g Output of Digital Processing Scheme Showing the Fluctuating Velocity at
$y/\delta = .14$, its VITA Variance, and the Associated Detector Function
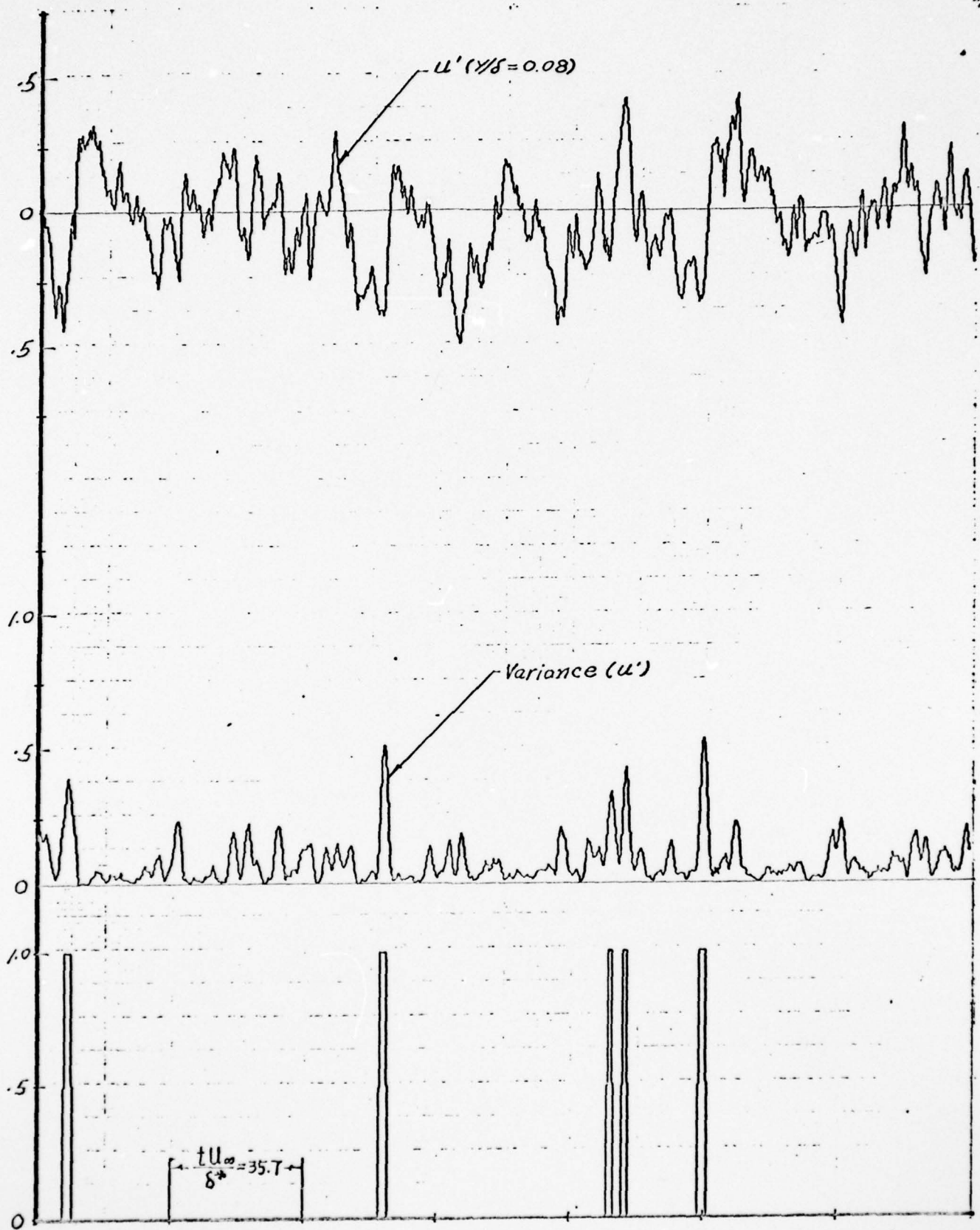$(5205 < \frac{tU_\infty}{\delta^*} < 5455)$

73<

Fig. 20h Output of Digital Processing Scheme Showing the Fluctuating Velocity at
$y/\delta = .14$, its VITA Variance, and the Associated Detector Function
$(5455 < \frac{tU_\infty}{\delta^*} < 5705)$

74<

Fig. 21a Output of Ditigal Processing Scheme Showing the Fluctuating Velocity at
$y/\delta = .08$, its VITA Variance, and the Associated Detector Function
$(5 < \frac{tU_\infty}{\delta^*} < 255)$

75<

Fig. 21b Output of Ditigal Processing Scheme Showing the Fluctuating Velocity at
$y/\delta = .08$, its VITA Variance, and the Associated Detector Function
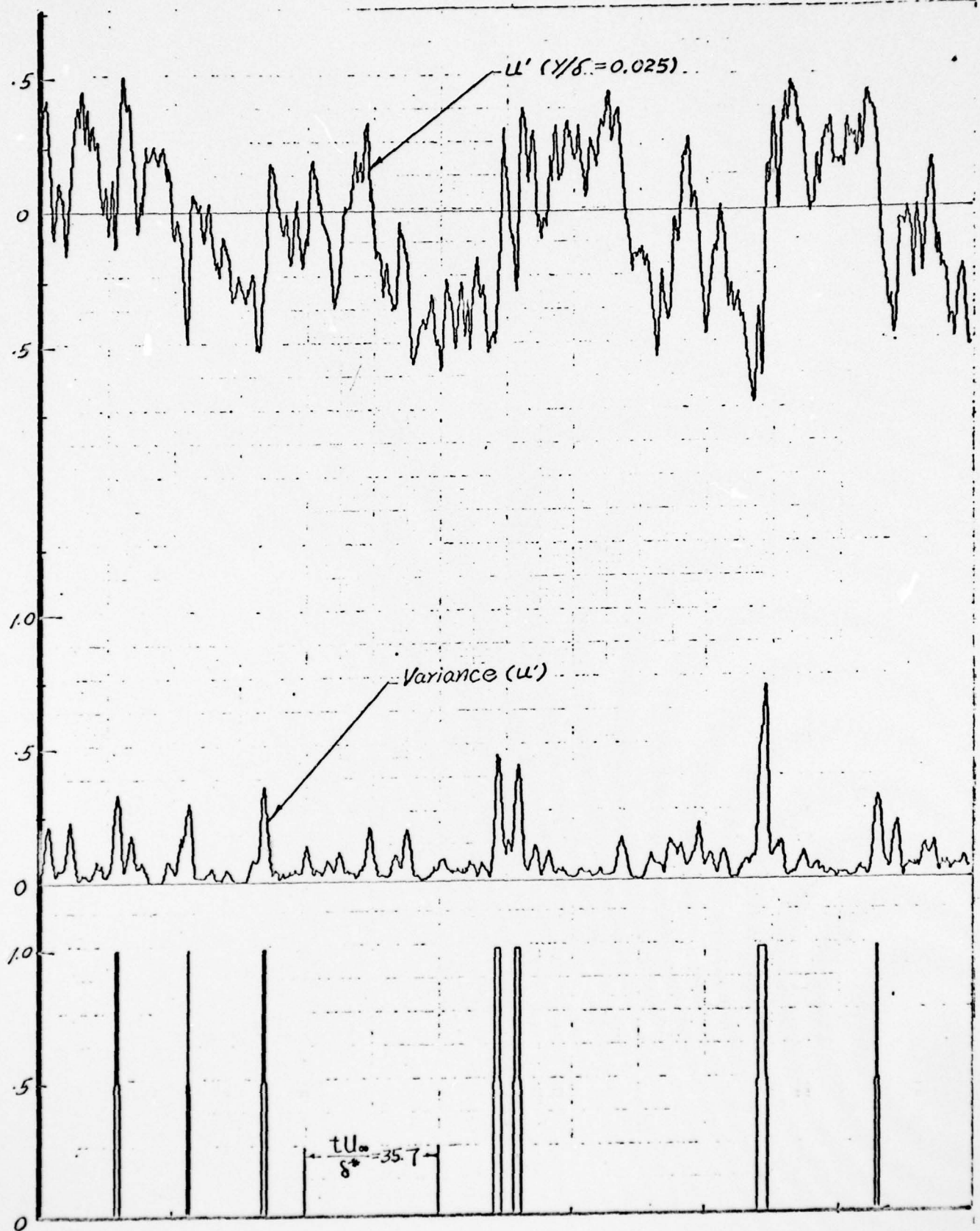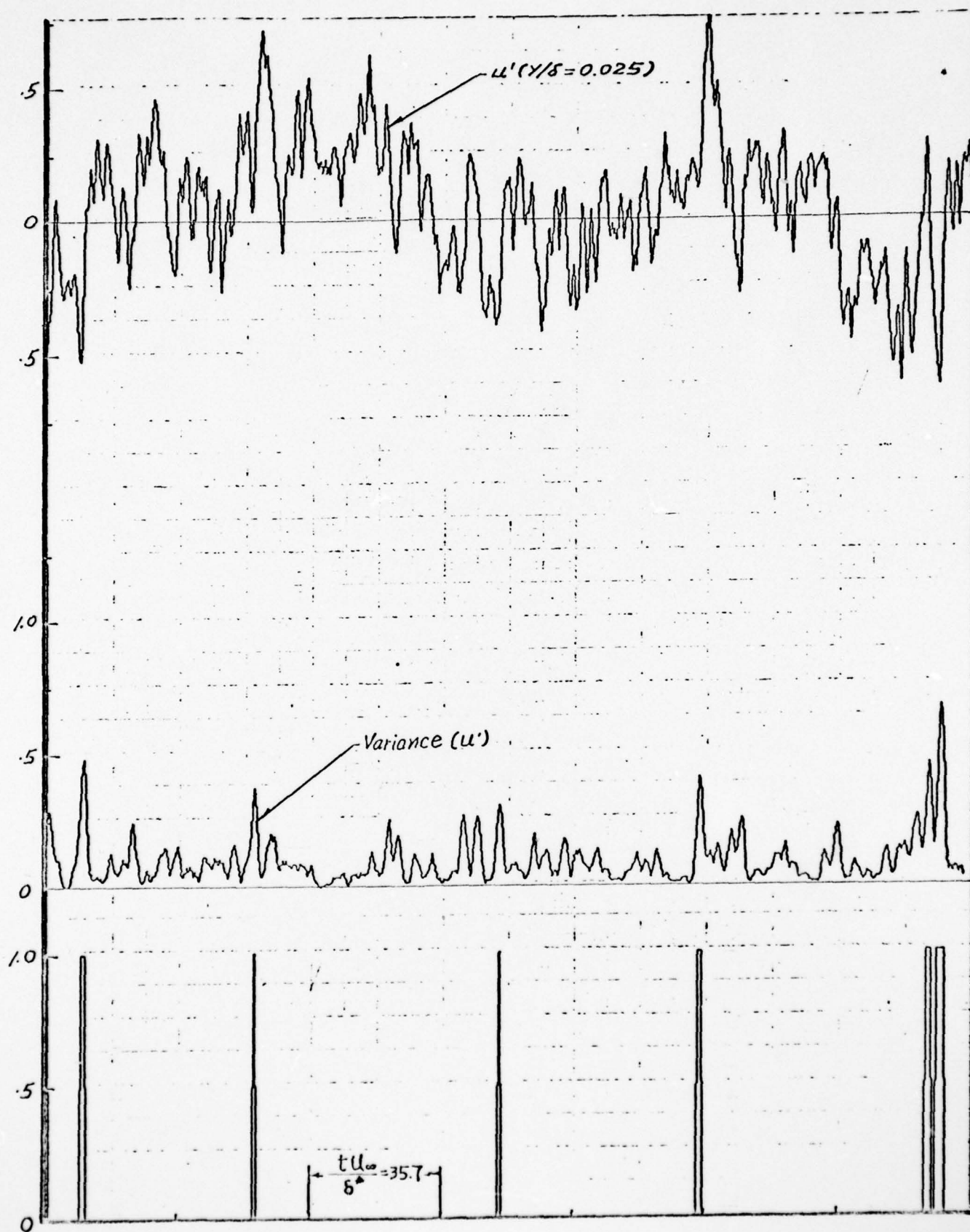$(255 < \frac{tU_\infty}{\delta^*} < 505)$

76<

Fig. 21c Output of Ditigal Processing Scheme Showing the Fluctuating Velocity at $y/\delta = .08$, its VITA Variance, and the Associated Detector Function $((505 < \frac{tU_\infty}{\delta^*} < 755)$

Fig. 21d Output of Ditigal Processing Scheme Showing the Fluctuating Velocity at
$y/\delta = .08$, its VITA Variance, and the Associated Detector Function
$(755 < \frac{tU_\infty}{\delta^*} < 1005)$

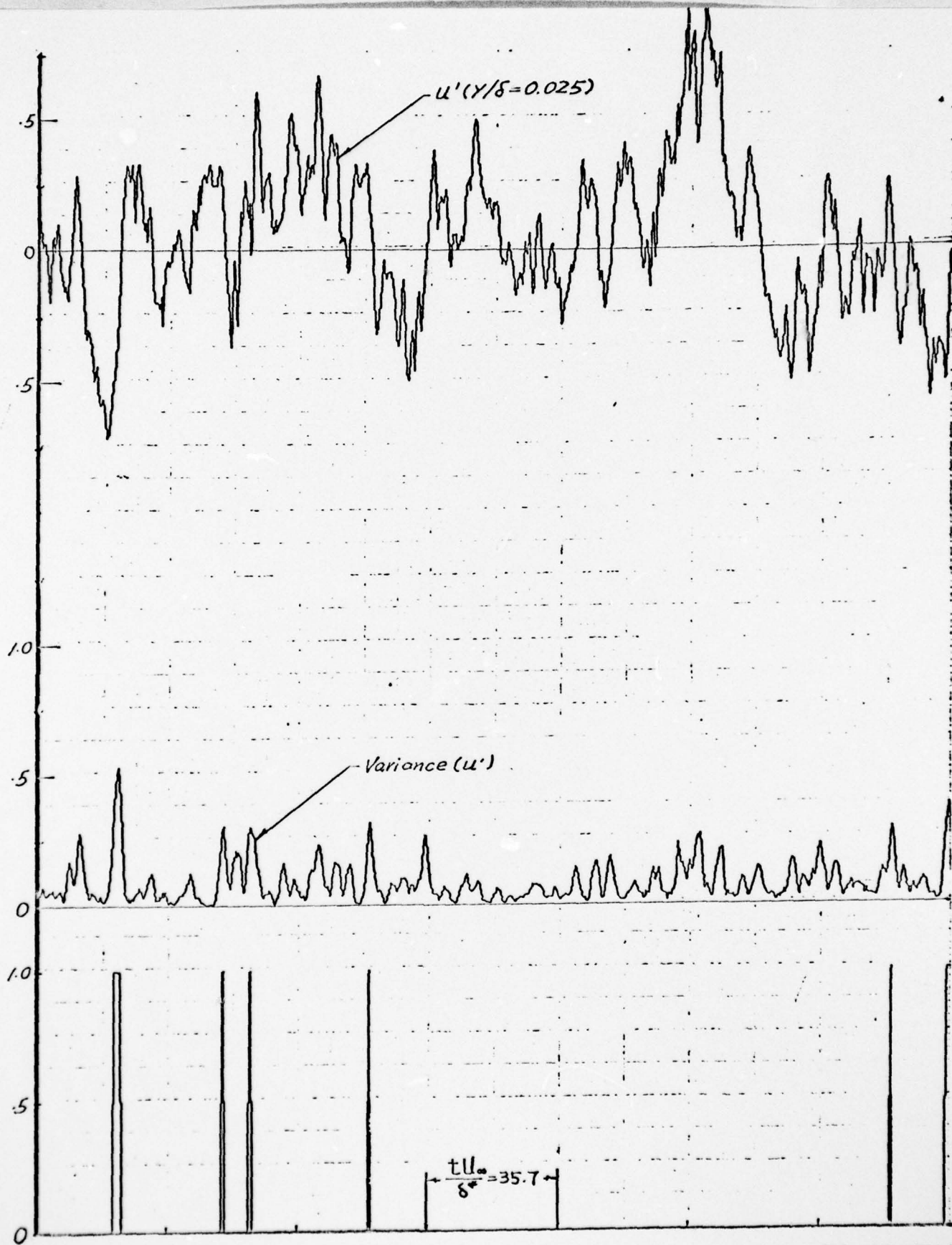Fig. 21e Output of Ditigal Processing Scheme Showing the Fluctuating Velocity at
$y/\delta = .08$, its VITA Variance, and the Associated Detector Function

$(4705 < \frac{tU_\infty}{\delta^*} < 4955)$

Fig. 21f Output of Ditigal Processing Scheme Showing the Fluctuating Velocity at
y/δ = .08, its VITA Variance, and the Associated Detector Function
$(4955 < \frac{tU_\infty}{\delta^*} < 5205)$

Fig. 21g Output of Ditigal Processing Scheme Showing the Fluctuating Velocity at $y/\delta = .08$, its VITA Variance, and the Associated Detector Function $(5205 < \frac{tU_\infty}{\delta^*} < 5455)$
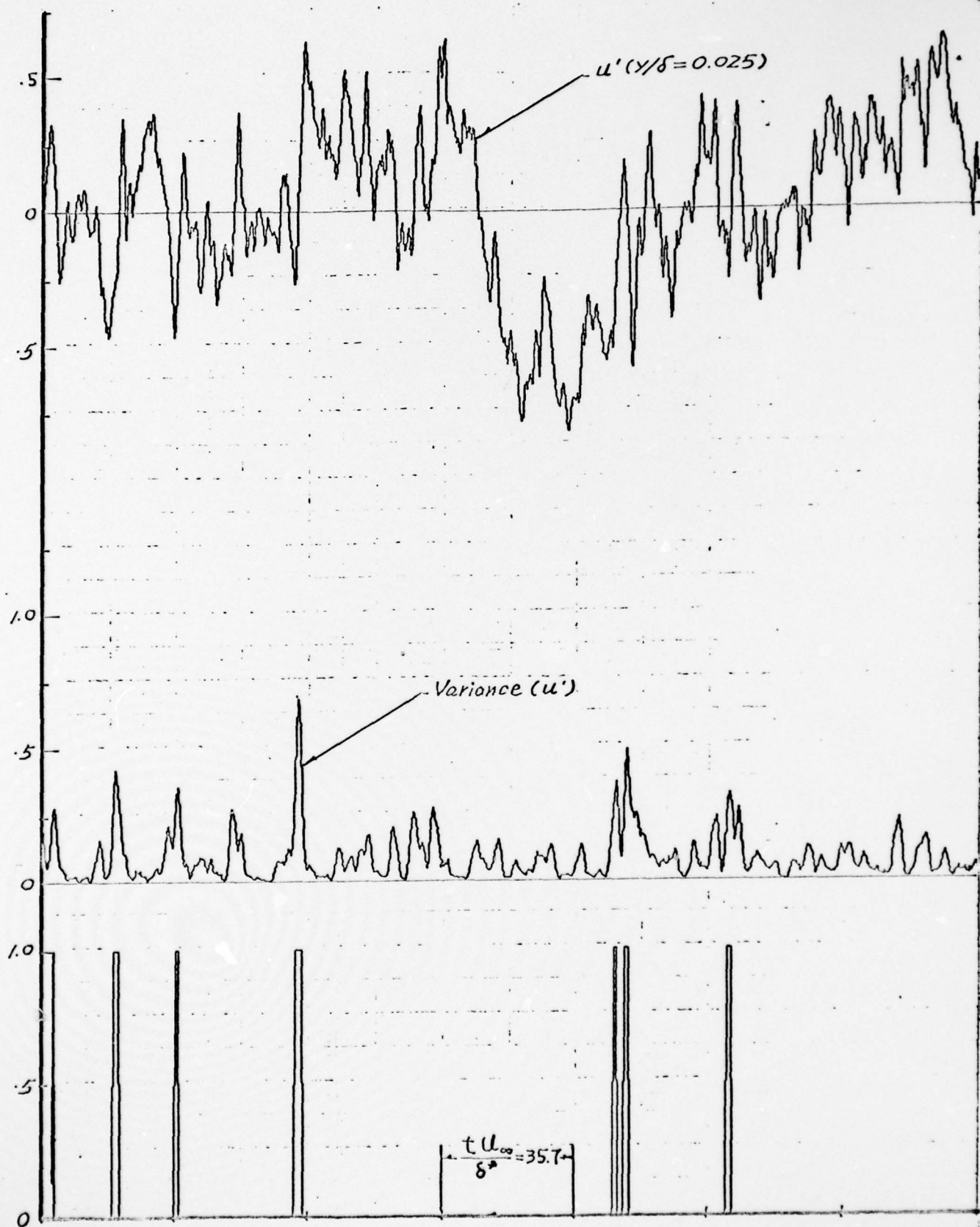
81<

Fig. 2lh Output of Ditigal Processing Scheme Showing the Fluctuating Velocity at
y/δ = .08, its VITA Variance, and the Associated Detector Function
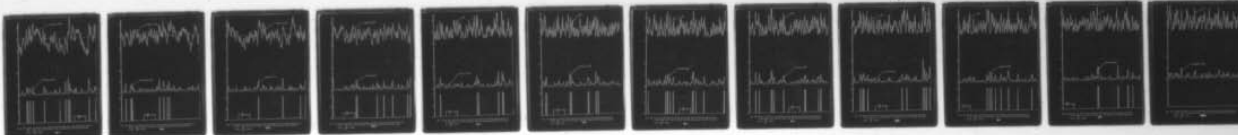$(5455 < \frac{tU_\infty}{\delta^*} < 5705)$

82<

Fig. 22a Output of Digital Processing Scheme Showing the Fluctuating Velocity at
y/δ = .025, its VITA Variance, and the Associated Detector Function
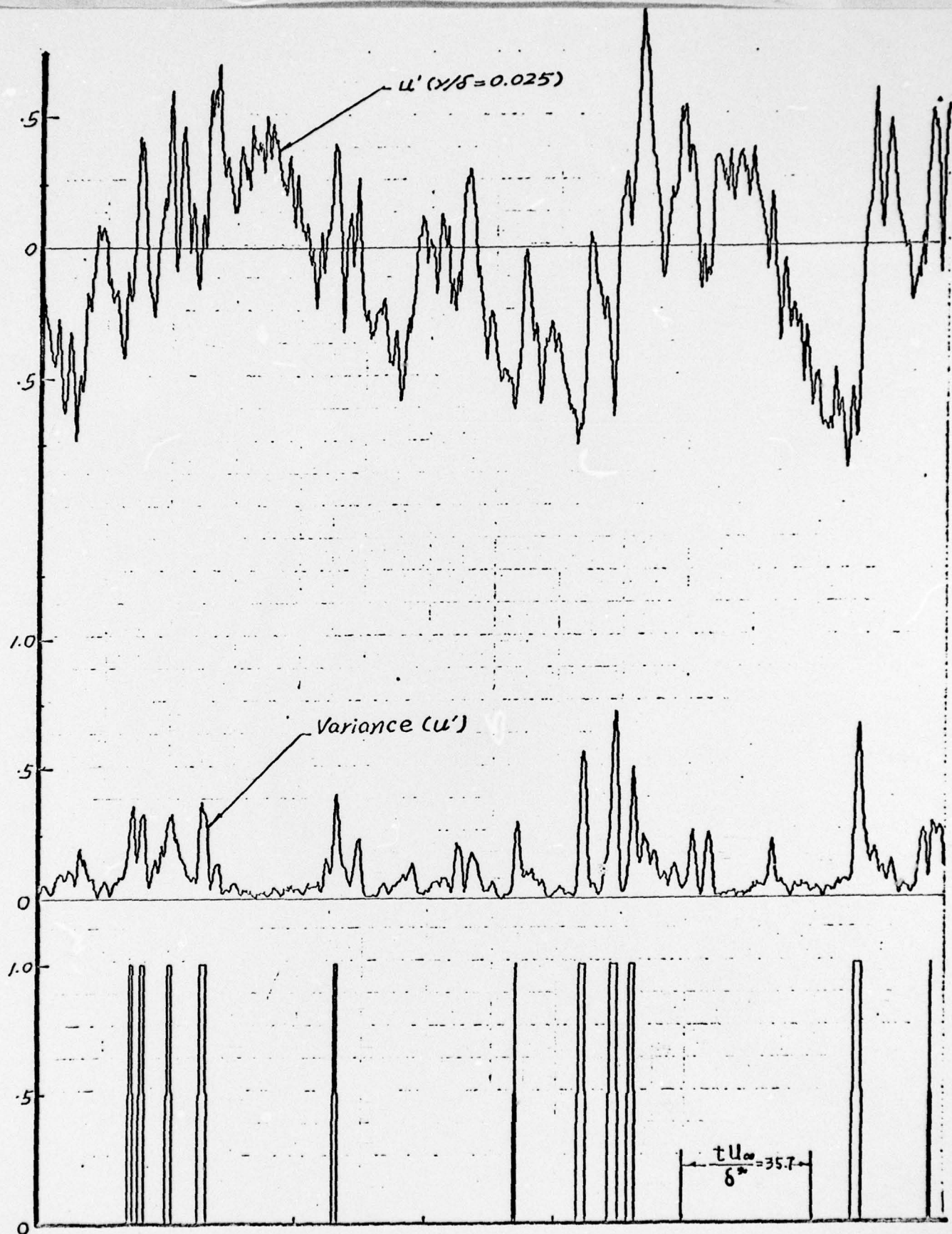
$(5 < \frac{tU_\infty}{\delta^*} < 255)$

83

Fig. 22 Output of Digital Processing Scheme Showing the Fluctuating Velocity at
y/δ = .025, its VITA Variance, and the Associated Detector Function
$(255 < \frac{tU_\infty}{\delta^*} < 505)$

84

Fig. 22c Output of Digital Processing Scheme Showing the Fluctuating Velocity at
y/δ = .025, its VITA Variance, and the Associated Detector Function
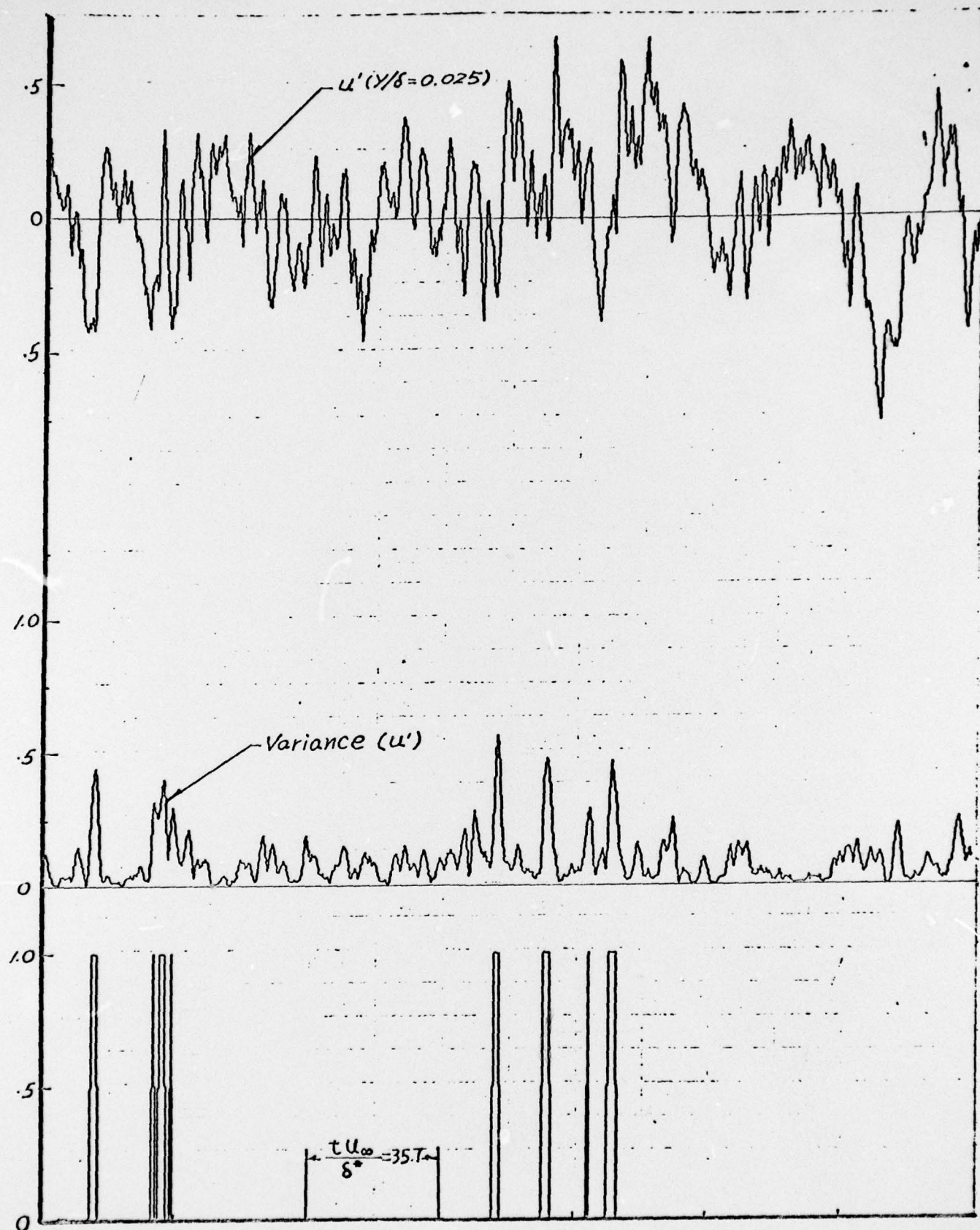
$(505 < \frac{tU_\infty}{\delta^*} < 755)$

Fig. 22d Output of Digital Processing Scheme Showing the Fluctuating Velocity at
$y/\delta = .025$, its VITA Variance, and the Associated Detector Function
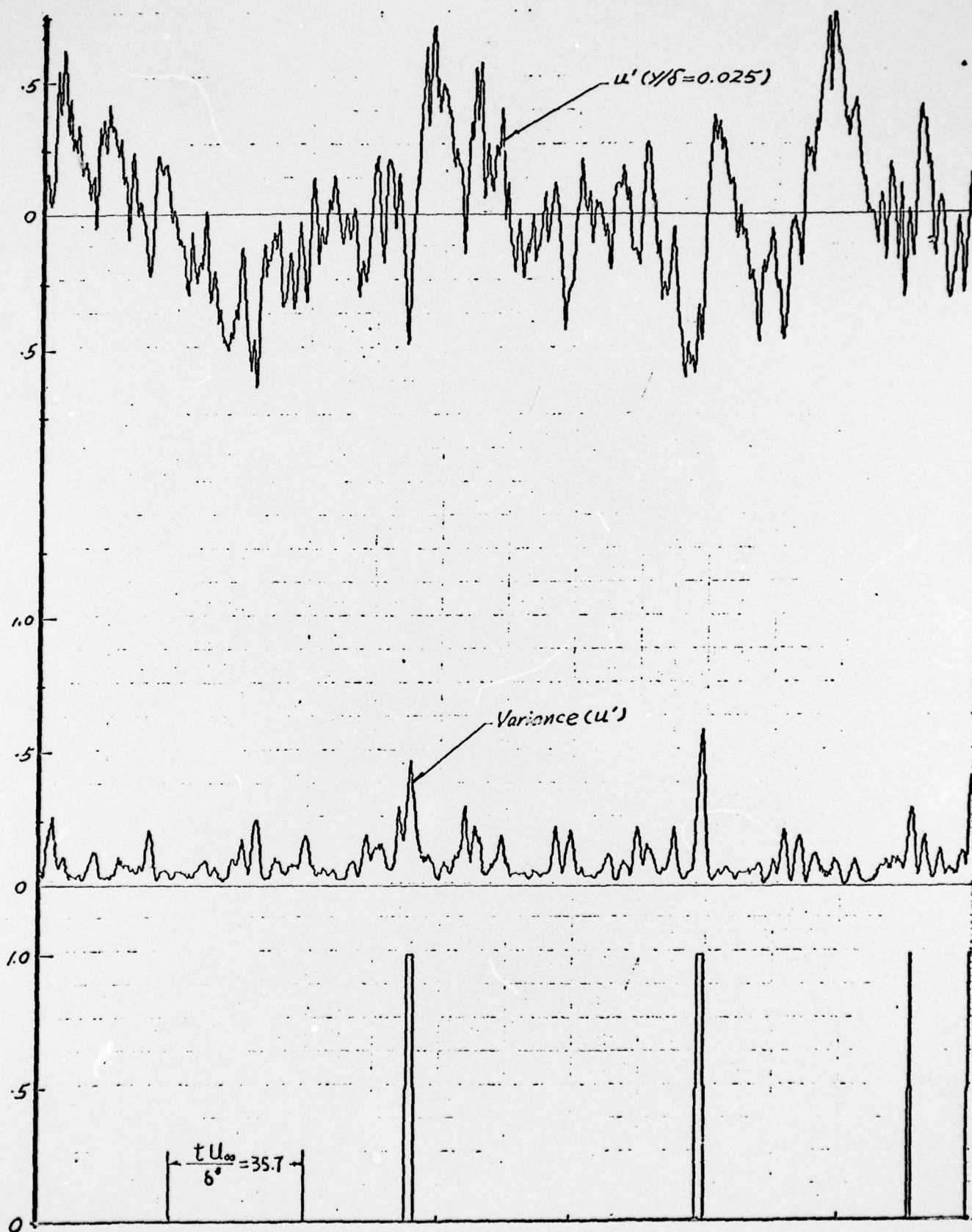$(755 < \frac{tU_\infty}{\delta^*} < 1005)$

Fig. 22e Output of Digital Processing Scheme Showing the Fluctuating Velocity at
$y/\delta = .025$, its VITA Variance, and the Associated Detector Function
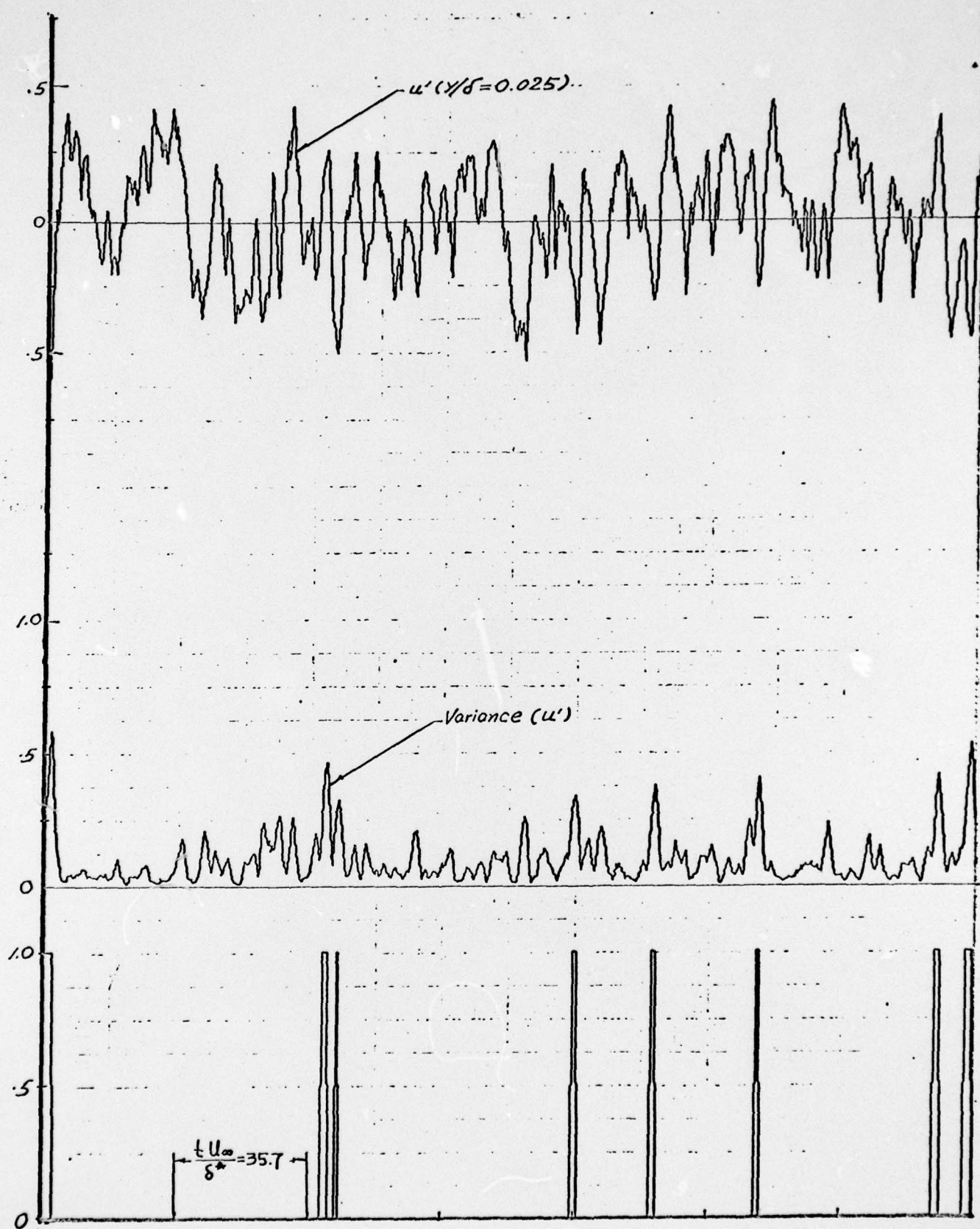$(4705 < \frac{tU_\infty}{\delta^*} < 4955)$

87<

Fig. 22f Output of Digital Processing Scheme Showing the Fluctuating Velocity at y/δ = .025, its VITA Variance, and the Associated Detector Function $(4955 < \frac{tU_\infty}{\delta^*} < 5205)$

Fig. 22g Output of Digital Processing Scheme Showing the Fluctuating Velocity at y/δ = .025, its VITA Variance, and the Associated Detector Function $(5205 < \frac{tU_\infty}{\delta^*} < 5455)$

Fig. 22h Output of Digital Processing Scheme Showing the Fluctuating Velocity at
y/δ = .025, its VITA Variance, and the Associated Detector Function
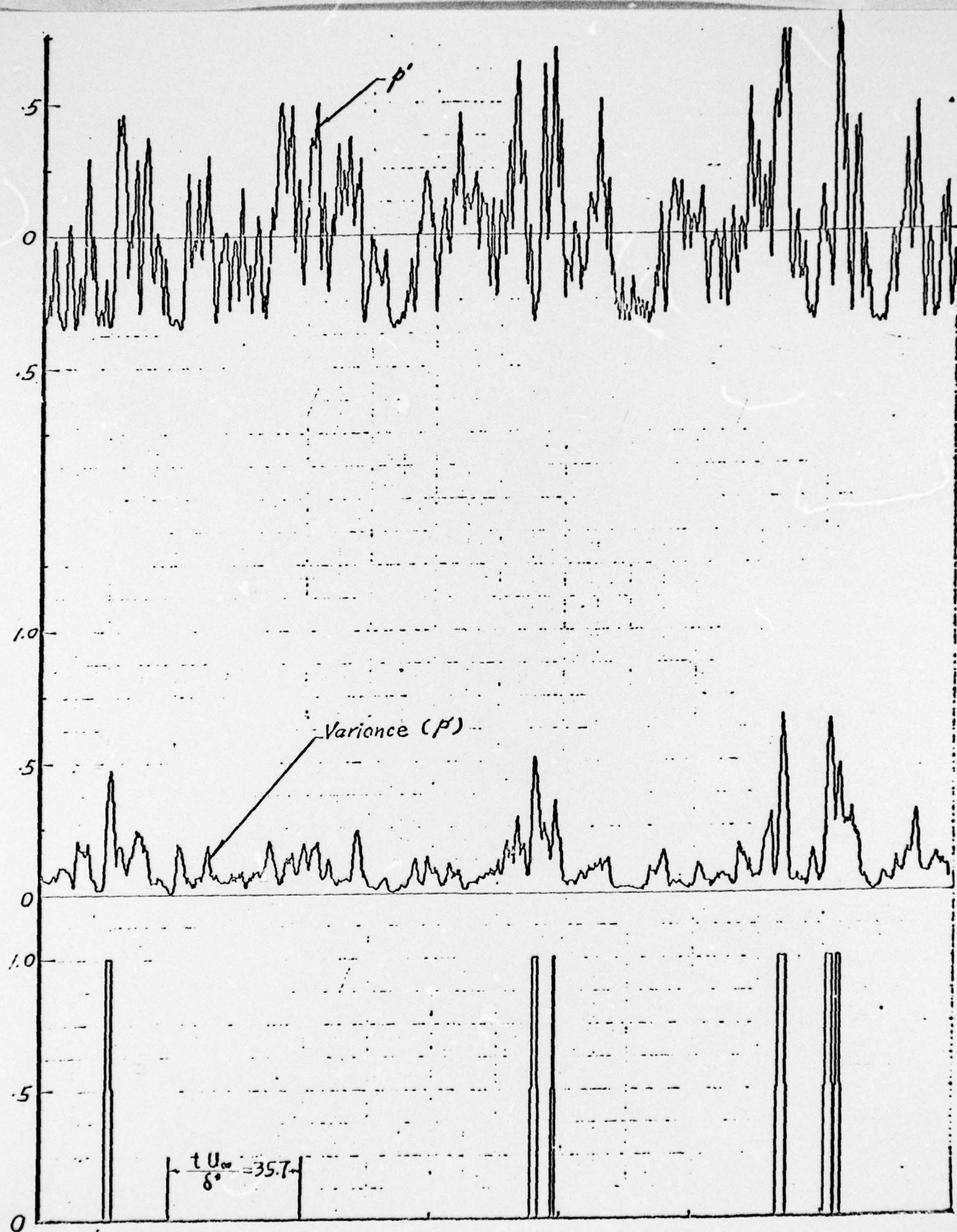
$(5455 < \frac{tU_\infty}{\delta^*} < 5705)$

Fig. 23a Output of Digital Processing Scheme Showing the Fluctuating Pressure at the Wall, its VITA Variance, and the Associated Detector Function $(5 < \frac{tU_\infty}{\delta^*} < 255)$
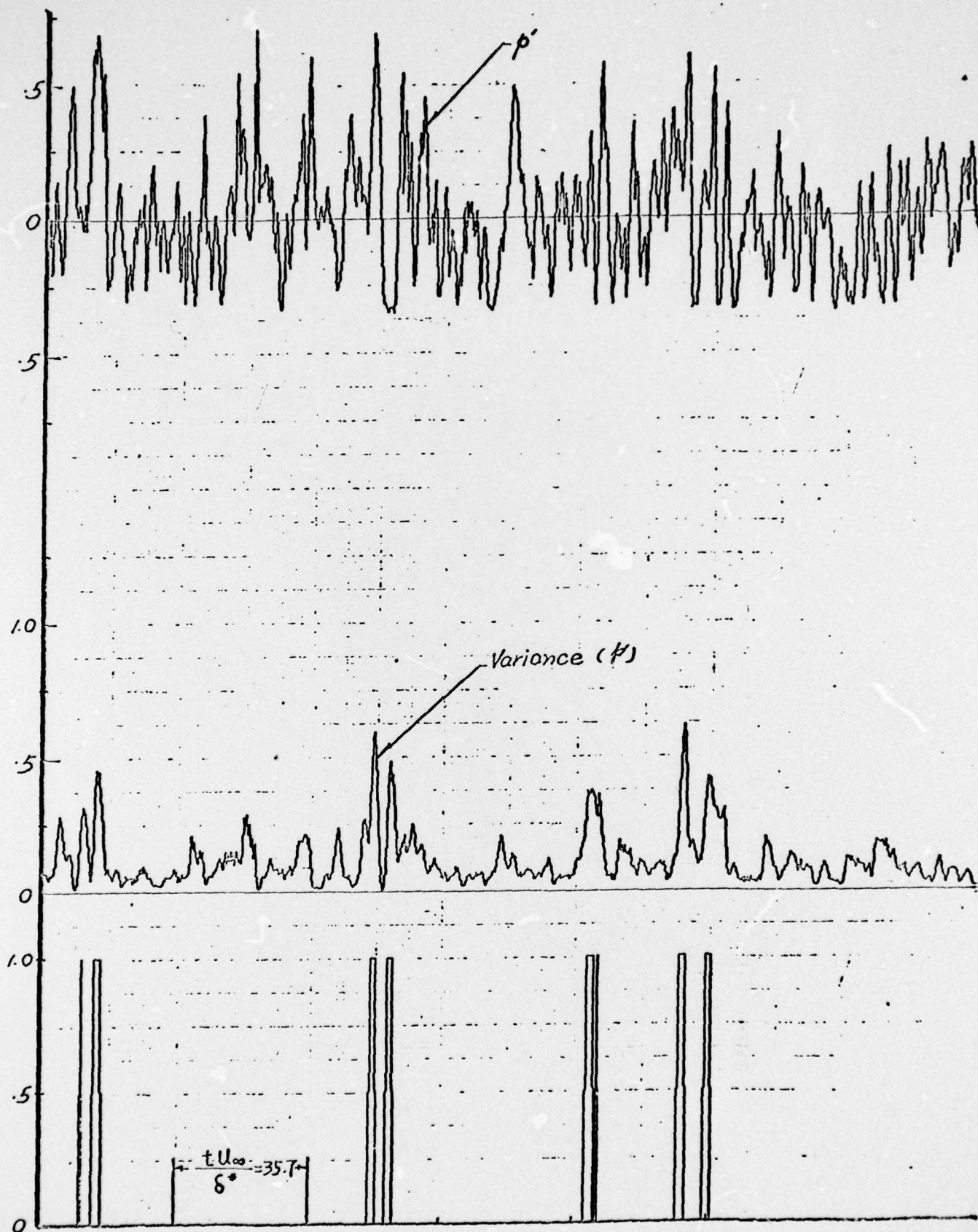
91<

Fig. 23b Output of Digital Processing Scheme Showing the Fluctuating Pressure at the Wall, its VITA Variance, and the Associated Detector Function $(255 < \frac{tU_\infty}{\delta^*} < 505)$
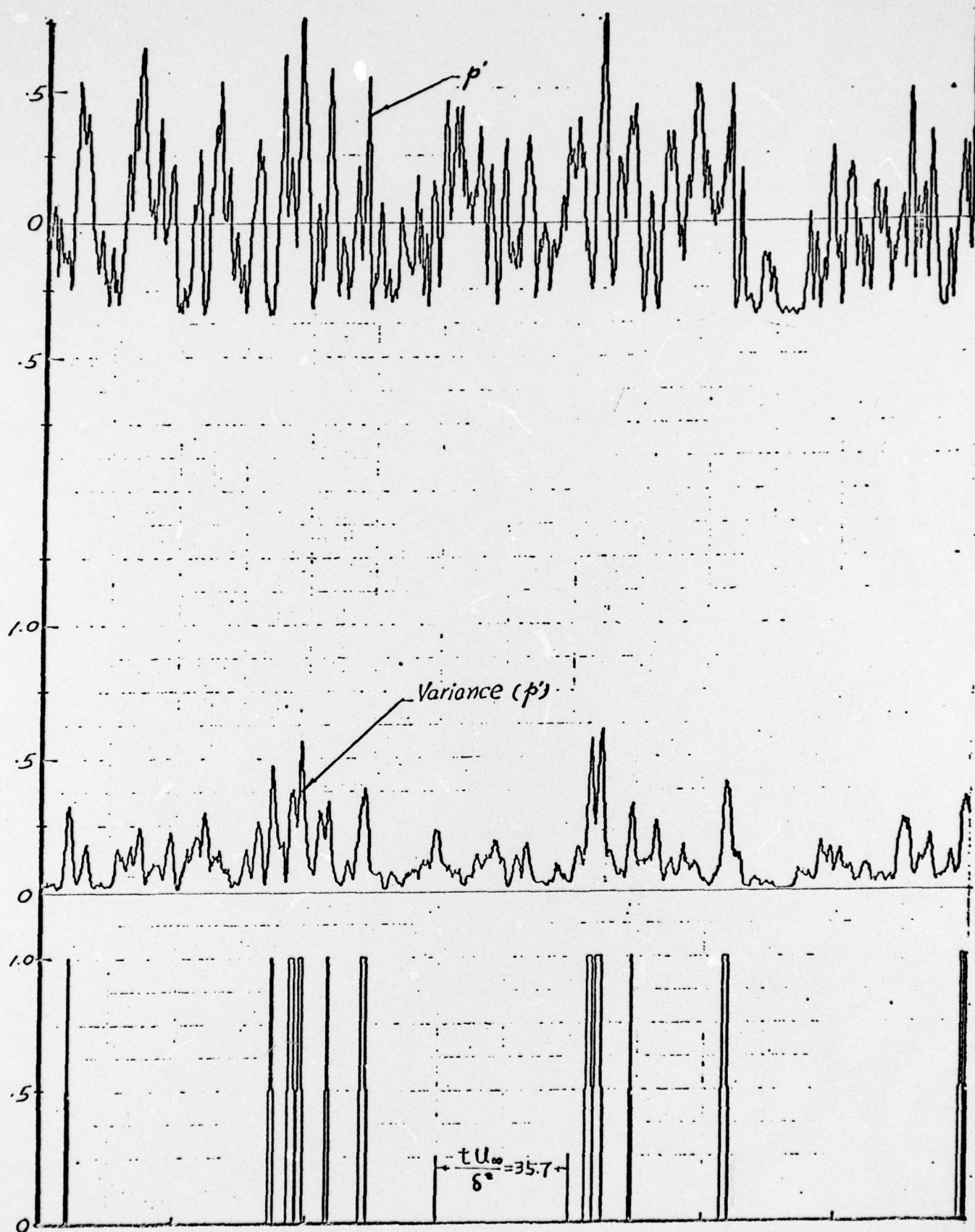
92<

Fig. 23c Output of Digital Processing Scheme Showing the Fluctuating Pressure
at the Wall, its VITA Variance, and the Associated Detector Function

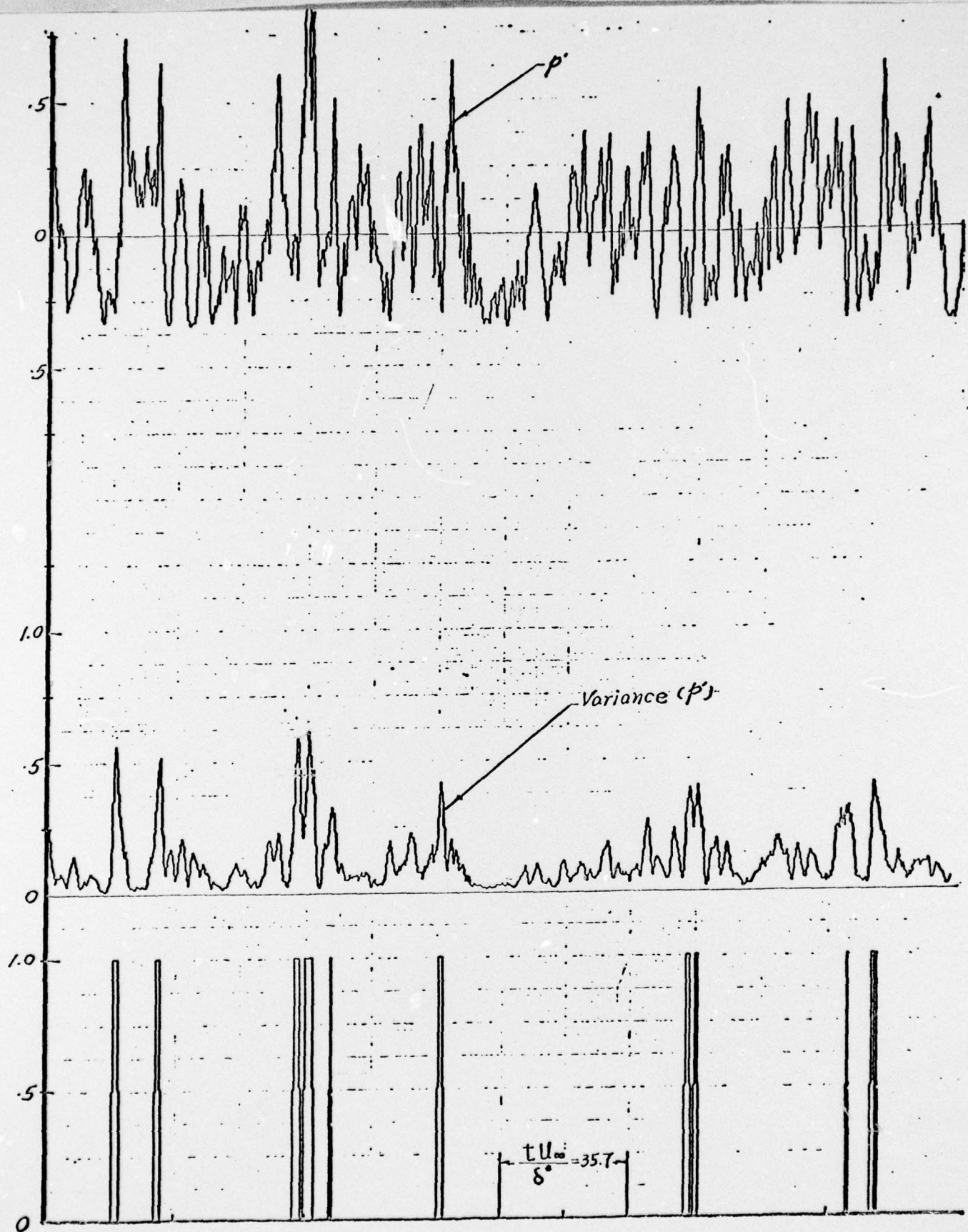$(505 < \frac{tU_\infty}{\delta^*} < 755)$

93

Fig. 23d Output of Digital Processing Scheme Showing the Fluctuating Pressure at the Wall, its VITA Variance, and the Associated Detector Function $(755 < \frac{tU_\infty}{\delta^*} < 1005)$

Fig. 23e Output of Digital Processing Scheme Showing the Fluctuating Pressure at the Wall, its VITA Variance, and the Associated Detector Function

$(4705 < \frac{tU_\infty}{\delta^*} < 4955)$
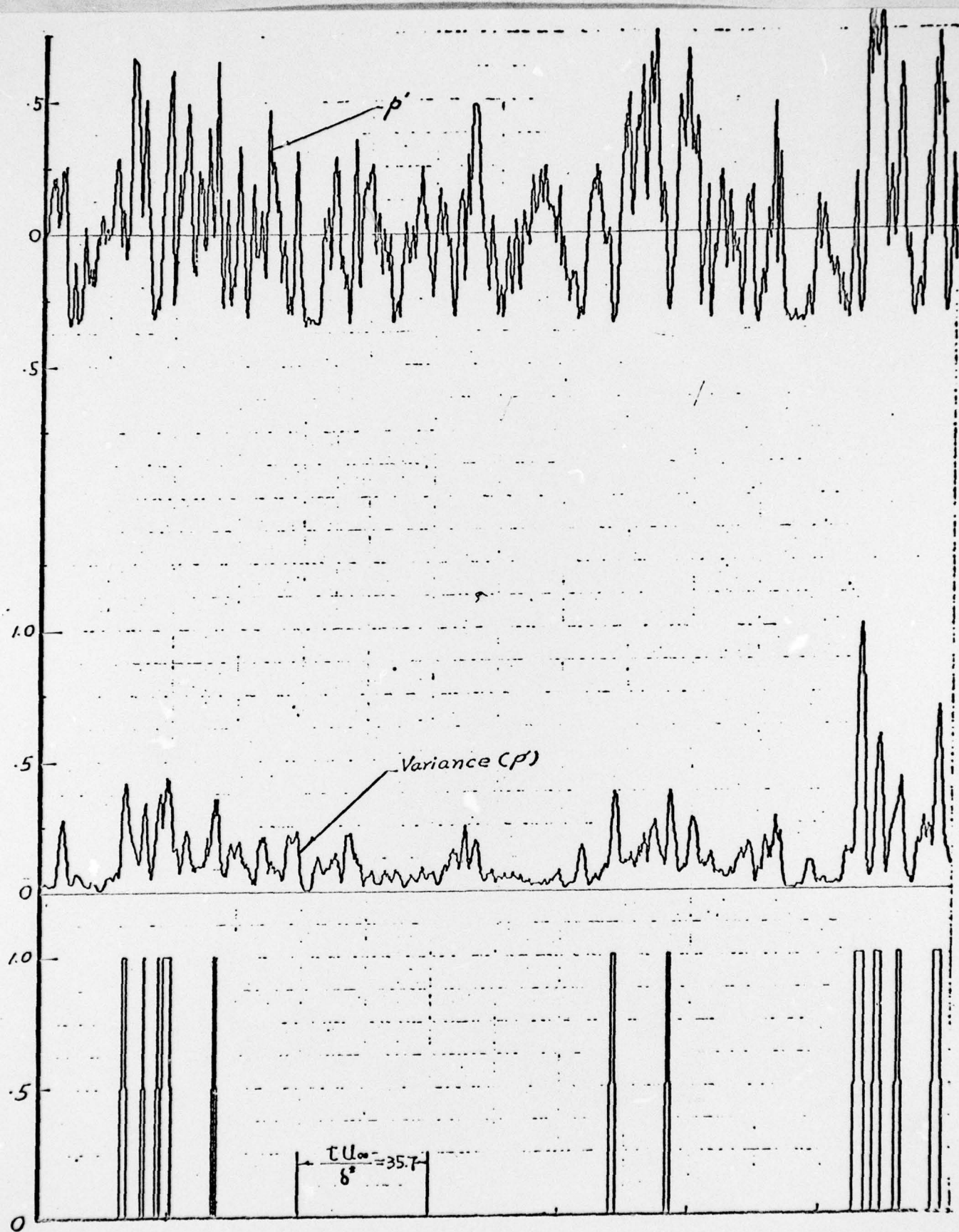
95

Fig. 23f Output of Digital Processing Scheme Showing the Fluctuating Pressure
at the Wall, its VITA Variance, and the Associated Detector Function
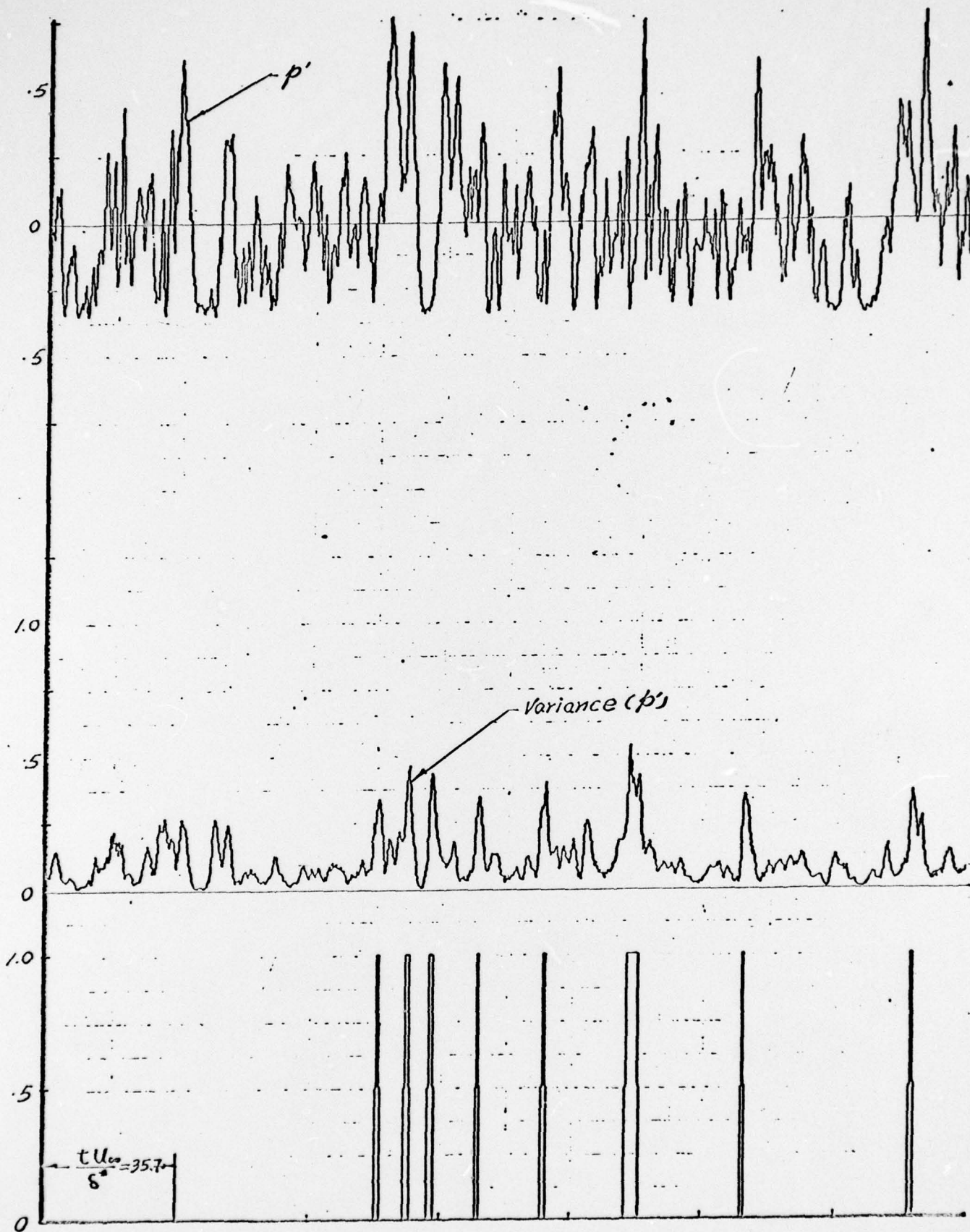$(4955 < \frac{tU_\infty}{\delta^*} < 5205)$

96

Fig. 23g Output of Digital Processing Scheme Showing the Fluctuating Pressure
at the Wall, its VITA Variance, and the Associated Detector Function

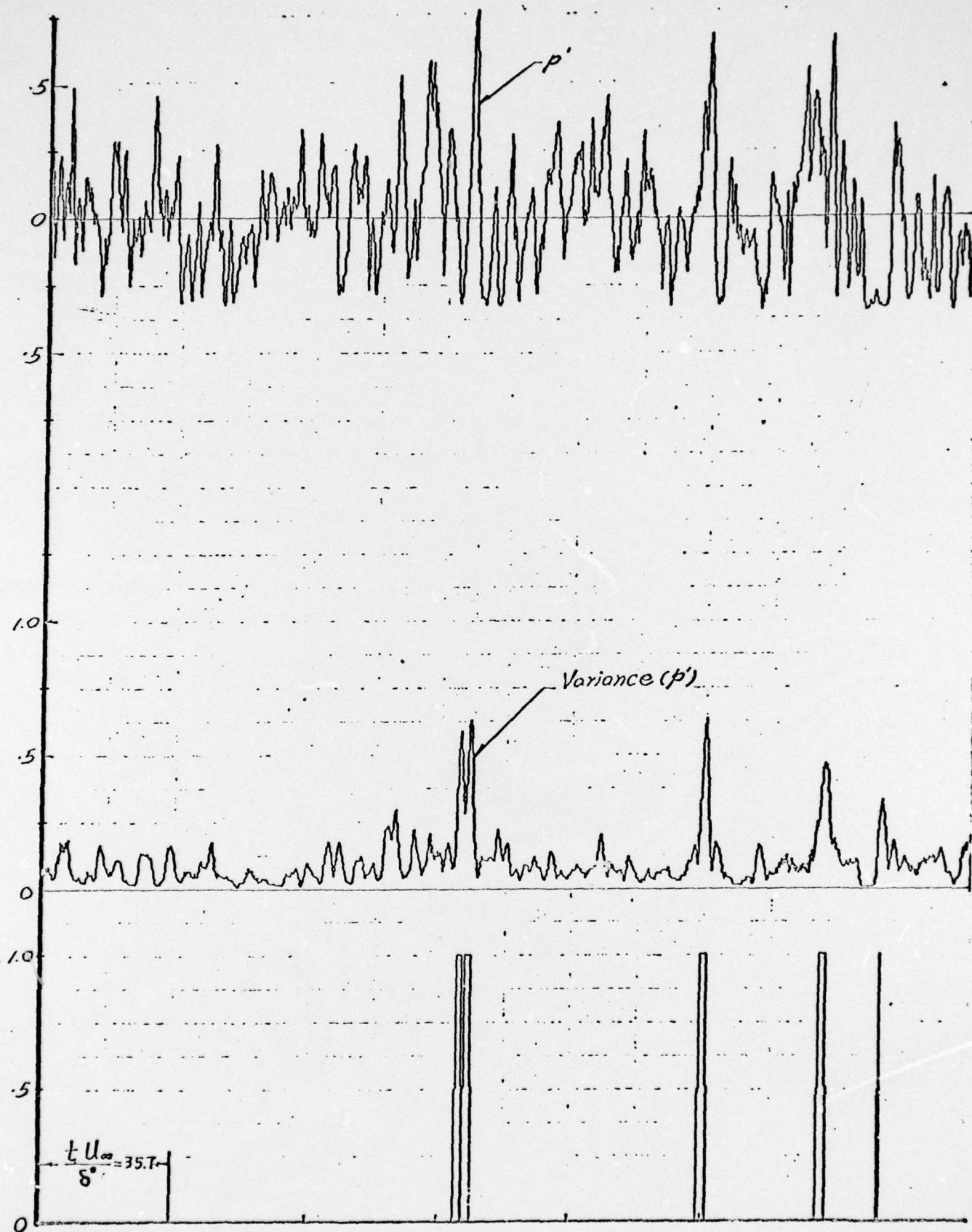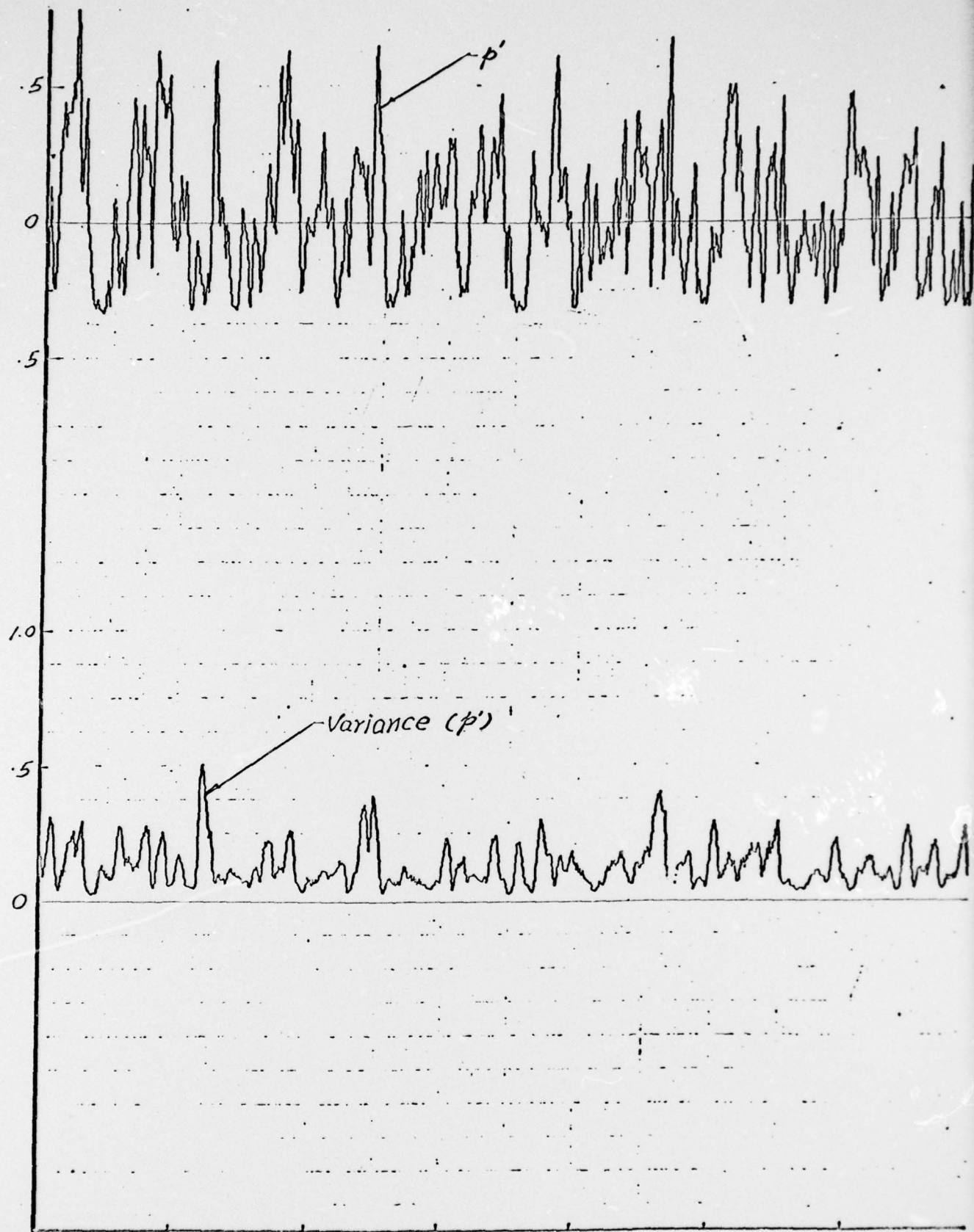$(5205 < \frac{tU_\infty}{\delta^*} < 5455)$ **97-**

Fig. 23h Output of Digital Processing Scheme Showing the Fluctuating Pressure at the Wall, its VITA Variance, and the Associated Detector Function

$$(5455 < \frac{tU_\infty}{\delta^*} < 5705)$$

REPORT DOCUMENTATION PAGE	READ INSTRUCTIONS BEFORE COMPLETING FORM

1. REPORT NUMBER AFOSR - TR- 77 - 0099	2. GOVT ACCESSION NO.	3. RECIPIENT'S CATALOG NUMBER

4. TITLE (and Subtitle) INVESTIGATION OF THE PROPAGATION MECHANISM OF PRESSURE FLUCTUATIONS IN TURBULENT FLOW	5. TYPE OF REPORT & PERIOD COVERED INTERIM 1 Sep 75 - 30 Sep 76
	6. PERFORMING ORG. REPORT NUMBER

7. AUTHOR(s) VICTOR ZAKKAY VINCENT BARRA CHI R WANG	8. CONTRACT OR GRANT NUMBER(s) AFOSR 76-2947

9. PERFORMING ORGANIZATION NAME AND ADDRESS NEW YORK UNIVERSITY/ AEROSPACE & ENERGETICS LAB MERRICK AND STEWART AVE WESTBURY L I, NY 11590	10. PROGRAM ELEMENT, PROJECT, TASK AREA & WORK UNIT NUMBERS 681307 2307A2 61102F

11. CONTROLLING OFFICE NAME AND ADDRESS Directorate of Aerospace Sciences /NA Building 410, Bolling AFB, D.C. 20332	12. REPORT DATE Dec 76
	13. NUMBER OF PAGES

14. MONITORING AGENCY NAME & ADDRESS(if different from Controlling Office)	15. SECURITY CLASS. (of this report) UNCLASSIFIED
	15a. DECLASSIFICATION/DOWNGRADING SCHEDULE

16. DISTRIBUTION STATEMENT (of this Report)

Approved for public release; distribution unlimited.

17. DISTRIBUTION STATEMENT (of the abstract entered in Block 20, if different from Report)

18. SUPPLEMENTARY NOTES

19. KEY WORDS (Continue on reverse side if necessary and identify by block number)

TURBULENCE
WALL PRESSURE FLUCTUATIONS
WAVE PROPAGATION
CONDITIONAL SAMPLING
TURBULENT BOUNDARY LAYER

20. ABSTRACT (Continue on reverse side if necessary and identify by block number)

A wind tunnel facility (M = 0.6 to 0.8) with extremely low noise levels (u'/u_∞ .08%) has been designed, constructed, and tested at the New York University Aerospace and Energetics Laboratory. The facility is to be used for the purpose of investigating the propagation mechanism of pressure fluctuations in turbulent boundary layers. The facility was designed as an induction tunnel in order to minimize the influence of the downstream region of the wind tunnel on the flow field in the test section. This report presents a description of the facility and the flow quality obtained, and a discussion of the instrumentation and

DD FORM 1473 1 JAN 73   EDITION OF 1 NOV 65 IS OBSOLETE   99   UNCLASSIFIED